Spectrum Sharing in White Spaces

Farzad Hessar

A dissertation
submitted in partial fulfillment of the
requirements for the degree of

Doctor of Philosophy

University of Washington

2015

Reading Committee:

Sumit Roy, Chair

John D. Sahr

Archis Vijay Ghate

Program Authorized to Offer Degree:
Electrical Engineering

University of Washington

Abstract

Spectrum Sharing in White Spaces

Farzad Hessar

Chair of the Supervisory Committee:
Professor Sumit Roy
Electrical Engineering

Demand for wireless Internet traffic has been increasing exponentially over the last decade, due to widespread usage of smart-phones along with new multimedia applications. The need for higher wireless network throughput has been pushing engineers to expand network capacities in order to keep pace with growing user demands. The improvement has been multi-dimensional, including optimizations in MAC/Physical layer for boosting spectral efficiency, expanding network infrastructure with reduced cell sizes, and utilizing additional RF spectrum. Nevertheless, traffic demand has been increasing at a much faster pace than network throughput and our current networks will not be able to handle customer needs in near future.

While assigning additional spectrum for cellular communication has been a major element of network capacity increase, the natural scarcity of RF spectrum limits the extend of this solution. On the other hand, researchers have shown that licensed spectrum that is owned and held by a primary user is heavily underutilized. Examples are TV channels in the VHF/UHF band as well as radar spectrum in the SHF band. Hence, a more efficient use of this spectrum is to permit unlicensed users to coexist with the primary owner, i.e. to share the same spectrum if it is not utilized at the current time/location.

Spectrum sharing has received considerable attention in recent years for its potential in improving network capacities. Especially, with formal opening of TV-band frequencies by FCC to unlicensed operation as well as proposals for radar-bands to be opened in near

future, wireless industry is also showing a great deal of interest in these unlicensed bands. The main challenge behind spectrum sharing is detection of spectrum opportunities, known as white spaces, by the secondaries. Classic methods are based on spectrum sensing which requires highly sensitive receivers. Newer methods, that are currently proposed by FCC for TV white space spectrum, are the so-called DBA approach in which a centralized database determines availability of shared spectrum at any location and time. This work is focused on the latter method.

In this work, we have focused on major challenges in spectrum sharing in the white space spectrum. *First*, the available capacity that is opened through TV white space spectrum is not clearly understood. We define a mathematical framework to evaluate achievable white space capacity in the TV band as a function of location, FCC regulation and secondary network parameters. We use this framework to simulate available TV white space channels and capacity over the entire United States and explore its dependency on various parameters.

Second, unlike licensed spectrum, available TV white space spectrum is significantly location-dependent. The number of channels as well as their quality (noise and interference floor) can severely change from place to place. Therefore, designing a cellular network that is based on spectrum sharing requires special channel allocation algorithms to consider these variations in to account. We define the problem of channel allocation in a spectrum sharing scenarios and explore various solutions.

Third, spectrum sharing rules in dynamic scenarios such as radar bands are not defined. Due to rotation of radar antennas, the available spectrum is time-dependent and coexistence scenario depends on how much information about the time-varying primary user (radar transmitter) is available to the secondary user. We introduce a spectrum sharing paradigm with rotating radar transmitters that models radar target detection operation as well as random distribution of secondary WiFi transmitters in the environment. We use this model to calculate protection region for the radar as well as achievable throughput.

Fourth, the lack of suitable SDR hardware has made evaluation and prototyping of available white space spectrum very challenging. We develop a SDR platform for operation

of WiFi devices in the UHF spectrum from 300-MHz to 3.8-GHz band. This platform is then utilized for development of fully functional WiFi-like networks in UW campuses to evaluate white space opportunities in the UHF spectrum and to provide Internet connectivity to end users.

TABLE OF CONTENTS

Page

LIST OF FIGURES

LIST OF TABLES

GLOSSARY

AGC: Automatic Gain Control

AWGN: Additive White Gaussian Noise

AP: Access Point

CR: Cognitive Radio

CDBS: Consolidated Database System

CMRS: Commercial Mobile Radio Services

CSMA/CA: Carrier Sense Multiple Access with Collision Avoidance

CTS: Clear To Send

CW: Contention Window

DBA: Database Administrator

DCF: Distributed Coordination Function

DIFS: DCF Interframe Space

DL: Down Link

EIFS: Extended Interframe Space

FCC: Federal Communications Commission

FDMA: Frequency Division Multiplexing

GPS: Global Positioning System

HAAT: Height Above Average Terrain

HETNET: Heterogeneous Network

INR: Interference to Noise Ratio

IP: Internet Protocol or Integer Programming

ISM: Industrial Scientific Medical

LR: Longley-Rice

LRC: Long Retry Counter

LTE: Long Term Evolution

MAC: Medium Access Control

MIMO: Multiple Input Multiple Output

MPDU: MAC Protocol Data Unit

MSDU: MAC Service Data Unit

PCF: Point Coordination Function

PHY: Physical layer

PIFS: PCF Interframe Space

PLCP: Physical Layer Convergence Procedure

PLMRS: Private Land Mobile Radio Services

PMD: Physical Medium Dependent

PPDU: PLCP Protocol Data Unit

PSDU: PLCP Service Data Unit

PU: Primary User

RF: Radio Frequency

RTS: Request to Send

SDR: Software Defined Radio

SIFS: Short Interframe Space

SINR: Signal to Interference and Noise Ratio

SNR: Signal to Noise Ratio

SPECOBS: Spectrum Observatory

SRC: Short Retry Counter

SU: Secondary User

TVBD: TV Based Device

TVWS: TV White Space

UE: User Equipment

UHF: Ultra High Frequency

UL: Up Link

VHF: Very High Frequency

WIFI: Wireless Fidelity

WLAN: Wireless Local Area Network

WS: White Space

ACKNOWLEDGMENTS

The author wishes to express sincere appreciation to colleagues, friends, and family, without whom this dissertation might not have been possible, and to whom I am greatly indebted.

I thank my PhD adviser, Prof. Sumit Roy, for his guidance and support throughout my graduate studies at University of Washington. His continuous encouragements for research and his invaluable advice has been an inspiration for my work.

I thank my committee members, Prof. John Sahr and Prof. Archis Ghate for their advice and suggestions, which have definitely improved the quality of this dissertation. Furthermore, I would like to thank Prof. Thomas Henderson for his insightful comments about the thesis.

Many thanks and appreciation to Prof. Payman Arabshahi for being an incredible friend and for always helping me generously at the time of need. I cannot say thank you enough.

I would like to thank my colleagues at Fundamentals of Networking Laboratory and fellow graduate students for the insightful discussions and for the quality time we spent together. This work is accomplished with the help of Joshua Stahl, Chang Wook Kim, Xuhang Ying, Benjamin Boyle, Mehrdad Hessar, Bowen Xue, Patrick Ma, and Jiaming Chen, in development of SpecObs and CampusLink projects; to whom I am very grateful. A very special thanks goes to Dirk Sommer for generously providing us access to his WLAN IP core and patiently answering our questions.

Lastly, my deepest gratitude and thanks goes to my parents and my love Maryam for their endless support and encouragement. They have always been my source of enthusiasm and inspiration throughout my life and I cannot express my appreciation in words.

DEDICATION

To my parents and my wife for their love and support

Chapter 1

INTRODUCTION

> *"Demand for spectrum is rapidly outstripping supply. The networks we have today won't be able to handle consumer and business needs."*
>
> — Julius Genachowski, *past FCC Chair, Mar. 2011 [10]*

The proliferation and relentless penetration of new generation of mobile devices (smartphones, tablets, and eReaders) along with new multimedia applications running on all these mobile devices has increased the demand for broadband wireless Internet access exponentially, figure 1.1, and is predicted to outstrip the capacity of 4G (LTE/LTE-A) networks. The total number of mobile subscribers is predicted to be 9.3 billion (far more than global population) by 2019 with 8 billion mobile broadband subscriptions [11]; the number of smartphone devices will be tripled and mobile data traffic driven by video will be ten times larger. Therefore, improving capacity of cellular network effectively is a serious matter concern for network operators. Few solutions have been proposed to fill this gap between supply and demand for wireless Internet access which can be summarize as follows:

- **Additional Licensed Spectrum**: Providing additional spectrum for wireless Internet access will obviously increase the capacity of current cellular networks as Shannon capacity scales linearly with bandwidth. However, spectrum is a scarce resource, enormously expensive and typically fragmented. Releasing more licensed spectrum is always challenging particularly in developed countries where major parts of the spectrum is already licensed for various commercial and military applications. Utilizing frequencies beyond 60 GHz is not feasible yet and it will need a significant improvement in current RF devices and network structure to adapt. For example, PHY and MAC layers must be re-designed for the changes in channel characteristics including higher path loss, multipath and fading variations. Therefore, relying ONLY on

new spectrum cannot be an effective strategy; mechanisms to more efficiently (re) use current licensed spectrum must be a part of the discussion.

- **Higher Spectral Efficiency**: The idea is to transmit as many bits as possible for a given bandwidth to maximize spectral efficiency (bps/Hz) of the radio link. This requires improvements in both PHY and MAC layers to keep the practical throughput close to Shannon theoretical limit [12]. Advanced MIMO techniques with large number of antennas that enables transmission of multiple stream of data over the same channel (multiplexing) as well as more efficient time/frequency division scheduling of users are employed in this area. These techniques are currently considered as main components of cellular standards. Spectral efficiency for LTE-A has increased from 16 bps/Hz in release 8.0 to 30 bps/Hz in release 10.0 with supporting up to 8×8 MIMO for DL and 4×4 for UL. The amount of capacity gain from further improvement in this aspect is expected to be marginal as the current practical performances are very close to theoretical limits [13].

- **Smaller Cell Size**: Every cell in the network is served with one base station and each base station has access to the same amount of bandwidth (typically). This spectrum must be shared among all the users in the cell. Therefore, smaller cell sizes results in larger bandwidth-to-user ratio. This metric is defined as the area spectral efficiency (bps/Hz/m^2). Since performance of a single link is not expected to increase significantly, it will be beneficial to increase the number of links between base stations and users by increasing cell density. The capacity of cellular networks has increased by a gain of one million since 1957, out of which an impressive 1600-fold gain is due to smaller cell sizes [13].

  However, there are challenges in reducing cell size indefinitely. Considering infrastructure and operational cost, deploying more cells are expensive for the network operators. Backhaul must be provided to each base station, deployment is slow and faces site limitations, especially in dense urban environments where most data demand is generated. For these reasons, deploying more small/micro cells is not a desirable

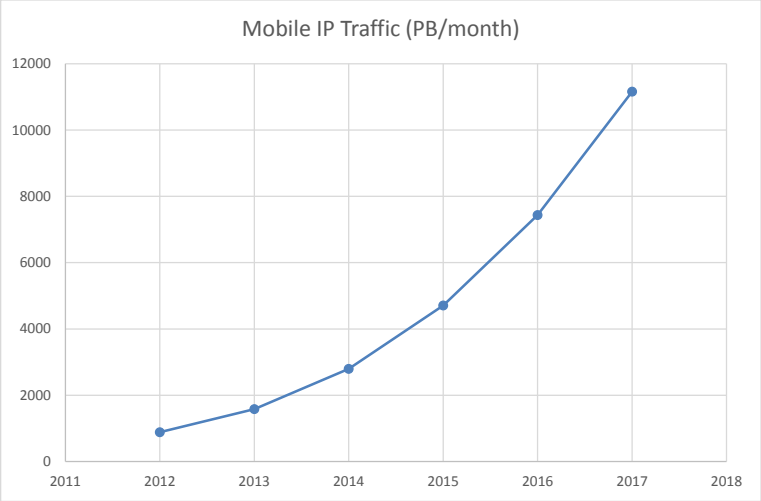

Figure 1.1: Mobile IP traffic prediction [2]

choice for network operators [14].

- **Unlicensed Spectrum Access**: Despite the scarcity of spectrum as a limited resource, various studies have shown that licensed spectrum is in fact highly underutilized [15, 16]. Licensed devotion of spectrum to users in the past has resulted in inefficient usage of spectrum with large gaps between channels and low spectral efficiency. While unlicensed frequency bands such as ISM (2.4 GHz) are highly saturated with large number of users, licensed bands such as TV (V/UHF) and radar are significantly underutilized. This situation has motivated the idea of sharing licensed spectrum with unlicensed users assuming no harmful interference is caused to licensed devices. Further discussion about this idea is followed in the next section.

1.1 Unlicensed Spectrum Sharing

Cognitive Radio (CR) devices have been introduced on the notion of reusing licensed spectrum by a secondary user (SU) without interfering with primary user (PU). Therefore, SU devices must coexist with PU devices on a lower priority paradigm. The operation of SU must be fully transparent to PU and usually no cooperation is made by the PU. This sce-

nario places specific requirements to be considered in the design process for the CR-based network as following:

1. The SU must detect the available part of the RF spectrum, i.e. frequency bands that are not currently utilized by any licensed user and operation of the SU will not interfere with normal operation of licensed receiver.

2. The SU transmitter and receiver should tune to a free channel to setup physical link connection.

3. The SU should periodically detect PU activity in the selected channel and repeat steps 1 through 2 if PU is active.

The most challenging task for CR network is the first task, *detecting free channels*. This is non-trivial for the following reasons. First, there is no universal definition for channel activity as *idle* v.s. *busy*. In reality, channel status is better classified as gray - i.e. even in the presence of an active primary, simultaneous secondary transmissions on the same spectrum may be allowed, depending on the primary receiver characteristics. For example, a high level of interference can be acceptable for a TV receiver while the same level can be severely intolerable for a sensitive radar receiver.

Second, primary user activity model is unknown in some cases. This is important for the SU to know how frequently it should detect PU activity. For example a TV broadcaster that is continuously active is easily detectable because there is no changes in activity of TV signal over time. On the other hand, a radar PU is very hard to detect because while the transmitter is active, the generated signal is a very narrow pulse that shows up in random (from SU point of view) times. Therefore, scheduling a detection mechanism for the latter case is significantly more challenging that the former.

Third, many of licensed spectrum bands are used for military operations and technical information about primary networks are not publicly available. Having technical specification of PU transmitter, receiver and network structure is extremely helpful in managing coexistence between secondary and primary devices. For example, location of primary

transmitter/receiver (mobility model), signal power and receiver sensitivity can be used to estimate the coverage area for the transmitted signal and protect all the receiver inside that area. However, for security reasons, these information are not made available to SU networks.

Different methods have been considered for detecting available spectrum for cognitive radio which can be categorized in two broad groups:

- *Spectrum Sensing based*: All methods in this category are based on measuring RF spectrum or a variant metric of that and thresholding the results to classify each channel as idle or busy. The accuracy of the decision made by these methods depends on sensitivity of the sensing device (SU), duration of sensing[1] and computational capabilities[2] of the sensor. The hidden terminal problem, signal shadowing and fading and spread spectrum users are some of the known technical problems in this category. However, the main issue is the hardware requirement for supporting current sensing algorithms which needs high sampling rate, large dynamic range analog to digital converter and fast processors.

- *PU Modeling based*: In this category, technical information about the primary transmitter such as transmission power, antenna height, receiver sensitivity, etc. are used at a central database, called database administrator (DBA), to model the coverage area for each specific primary user. The resulting coverage areas, combined with various regulations that are defined by corresponding entities (FCC in USA, OfCom in UK) determines what parts of spectrum is available for unlicensed operation at each particular location. Modeling based methods are computationally extensive and needs careful attention to underlying rules governing secondary access. Therefore, implementing this operation in a DBA is a reasonable practical choice to ensure all secondary units have an identical understanding of the rules. In this paradigm, each secondary unit provides its location to DBA and queries for available spectrum. After

[1]Longer sensing time increases the chance of detecting lower power signals

[2]Complex signal processing algorithms are introduced in the literature to improve accuracy of sensing results with the cost of higher computational requirement for the SU.

receiving a list of available channels, SU can setup its communication link by selecting one of the available channels. The limitation of this approach is that PU cannot be highly dynamic which requires DBA to frequently update its analytical models and inform SU. This technique has been regulated by FCC for TV channels and the resulting available channels are called TV White Space (TVWS) spectrum.

In this thesis, we consider spectrum sharing (coexistence) based on PU modeling approach in different frequency bands. Our focus is on TV channels and radar spectrum as two categories of primary users.

1.2 Overview of Contributions

The contributions of this thesis can be summarized in following categories:

- First, we focus on unlicensed spectrum access in TV band, a.k.a. TV white spaces by quantifying available white space spectrum in the USA after considering various FCC rules and technical details. We define a mathematical framework to analyze performance of WS-based secondary networks in terms of *how much capacity is achievable in the network?* Various network design trade-offs are studied and spatial variations of network capacity due to irregularity of primary network is explored.

- Second, the problem of resource allocation to secondary cellular networks in TVWS is considered and multiple solutions are provided. This problem is particularly important because of spatial variations in number of available channels. We consider a cellular network for the secondary users and define resource allocation problem correspondingly to optimize overall throughput of this network from different viewpoints.

- Third, we consider the problem of coexistence between SU and PU in other frequency bands with a focus on radar bands. Here we find available spectrum for unlicensed devices with full/partial information about primary user (radar TX/RX) and quantify available capacity. This problem has received significant attentions recently for following reasons. First, the behavior of radar transmitter is considerably different from most

of regular communication systems (very narrow and high power pulses with constant changes in direction of antenna). The instantaneous variation in radar's transmitted power complicates detection of white space opportunities. Second, a major part of the spectrum (1.7 GHz from 225 MHz to 3.7 GHz [17]) involves radar or radio-navigation infrastructure. Therefore, there is a significant white space opportunity in coexistence between SU and radar transmitters.

- Fourth, we design and implement an SDR platform for unlicensed wireless operation in the UHF band. This SDR provides full WiFi connectivity in the 300-3800 MHz band with maximum configurability of network parameters. Implementation covers PHY and MAC layers of IEEE 802.11 using a combination of hardware (FPGA) and low-level software. This work is the first step toward constructing a campus-wide secondary network for providing Internet access based on TVWS (and future unlicensed) spectrum. Portable secondary devices will be designed that can be used with any personal computer as an external network card providing connection in the unlicensed band. This network platform will be equipped with a centralized network planner software for controlling channel access to each device, gathering spectrum sensing data from each device and monitoring link throughput.

1.3 Thesis Organization

This dissertation is based on three structural pieces. The DBA for TV white space spectrum, as an intelligent database and the natural point of integration, is discussed in chapter 2. Various algorithms and analysis corresponding to spectrum sharing in TV and radar white spaces are provided in chapters 3, 4 and 5. The requirements for hardware support in the white spaces as well as our SDR platform is presented in chapter 6.

In details, the rest of this thesis is organized as follows. In chapter 2, we introduce a software platform, called *SpecObs*, for analysis and simulation of TVWS availability in the United States based on FCC regulations, technical information of TV broadcasters, secondary devices characteristics and real terrain information. This platform is used in chapter 3 along with a mathematical framework to define available capacity in TV band

for secondary operation. Various Trade-offs have been studied between available network capacity for SU against design parameters such as cell size, antenna height, transmission power, etc.

Chapter 4, discusses the problem of resource allocation (channel assignment) to secondary devices in TVWS. Spatial variation of channels is considered in the problem formulation and various optimal/sub-optimal solutions are discussed with corresponding numerical results.

Chapter 5 is focused on spectrum sharing between a rotating radar (PU) and WLAN networks (SU). Maximum tolerable interference by the radar is calculated as a function of radar parameters and it is used for defining radar protection region. Spatial distribution of secondary users is considered in spectrum sharing scenario and different paradigms are evaluated based on the extent of available information about PU.

Chapter 6, describes design and implementation of an SDR platform for wireless operation in the white space spectrum. Characteristics of PHY and MAC layers that are based on IEEE 802.11 are presented and various challenges are discussed. And finally, chapter 7 introduces future directions in these areas.

Chapter 2

SPECOBS FRAMEWORK

2.1 Introduction

In this chapter we explore design and implementation of a cloud-based software platform, called *SpecObs*[1], that is developed at University of Washington as part of this dissertation for analyzing available spectrum in TV band (currently) and other bands (future work).

Let's start with exploring the role and responsibilities of a DBA as defined by FCC [18–20] to determine various components and modules that are required for its functionality. The main role of DBA in TVWS is to enable secondary access to TV spectrum without requiring SU to perform spectrum sensing or computationally expensive algorithms. Therefore, DBA is obligated to manage coexistence between SU and PU.

The structure of a secondary network based on TVWS is comprised of a central node, known as DBA, and several secondary devices, called TVBD. Each TVBD could be an AP for a small home/office WLAN network. All TVBDs are divided in two groups:

- **Master**: A master TVBD is equipped with a geo-location device and is aware of its location. This device can directly contact DBA by providing its location information.
- **Slave**: A slave device is not aware of its location and therefore cannot directly contact DBA. Each slave TVBD is obligated to use TVWS channels under control of a master device.

For a small home/office network, it is sufficient to equip the AP with GPS for location awareness and place every user device (UE) in slave mode. AP queries DBA by sending its location and receiving a set of available channels, allowed transmission power, etc. for that

[1]This software platform considers all FCC regulations for operation of TVBD in TVWS to find available spectrum. The results provided by this service is compatible with other certified FCC DBAs. The software is completely designed and implemented at Fundamentals of Networking Lab, by TVWS team, and is publicly available at following address: http://specobs.ee.washington.edu

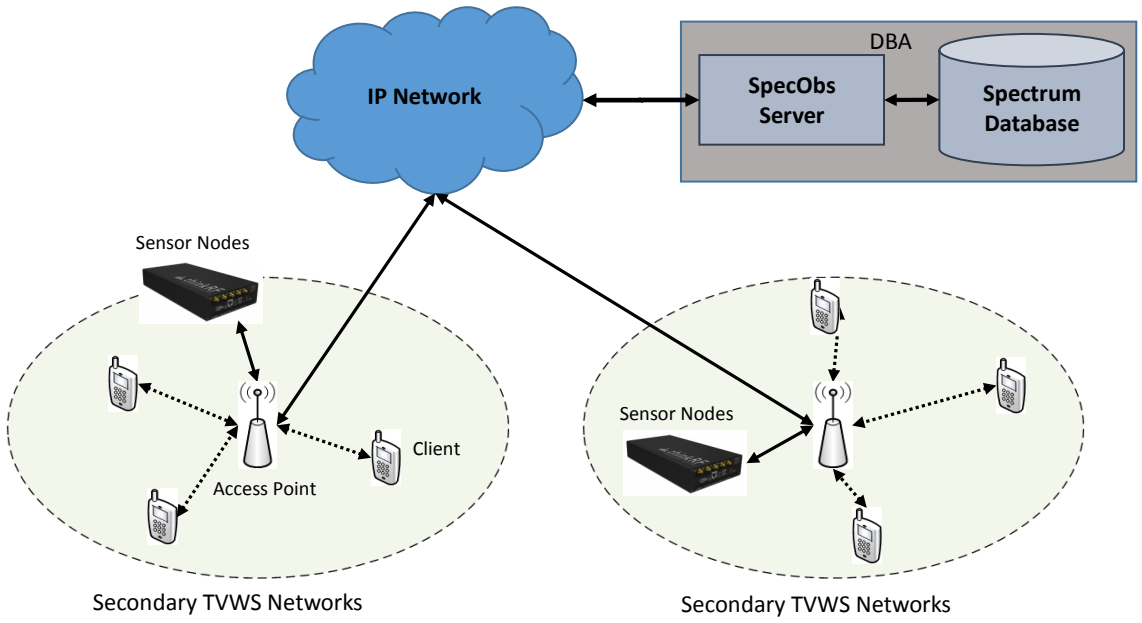

Figure 2.1: System architecture including TVWS local networks, spectrum sensors and DBA

particular location as shown in Fig. 2.1. According to the set of available channels and quality of each channel (reported by DBA optionally) each AP sets up the network connection with participating clients. Connection between master device and DBA is through Internet (IP network). Hence, master device must already have a network connection (either wired or wireless) to access DBA.

The architecture in Fig. 2.1 presents additional features than what is considered by FCC for TVWS networks. For example, each AP in this figure can be optionally equipped with spectrum sensing capabilities. Also, dedicated spectrum sensors can be considered in the network for constant monitoring of spectrum usage to discover additional WS opportunities or manage coexistence. Therefore, measurements obtained by either method is sent to DBA (SpecObs server) through IP network for further processing.

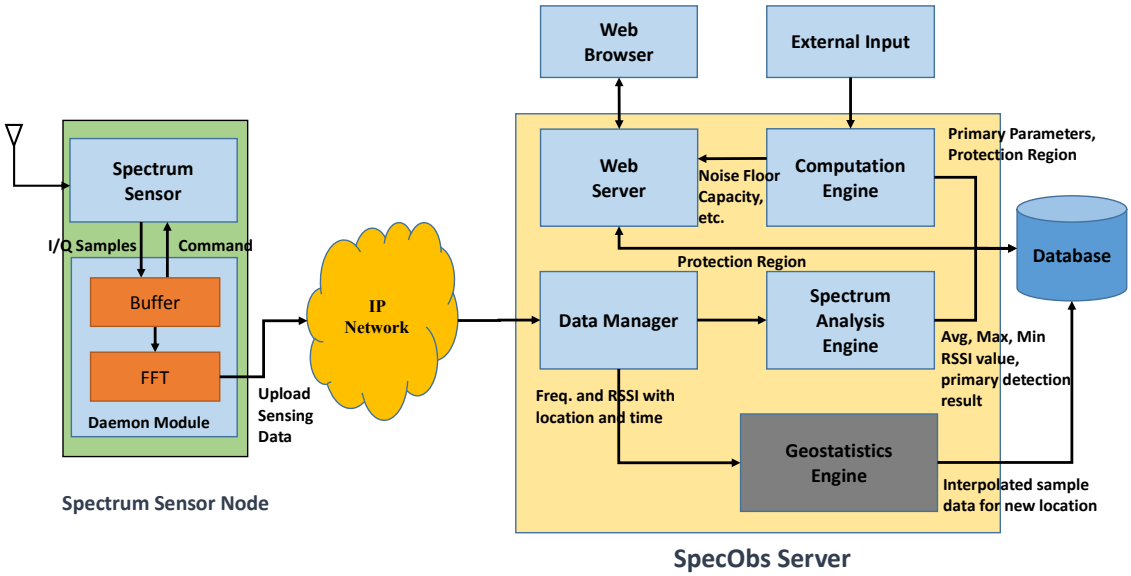

Figure 2.2: Main components of SpecObs system

2.2 SpecObs Architecture

DBA's main responsibility is replying to client queries (accompanied by their location information) with a list of available channels (white space) together with technical information for using the channel (such as antenna height and transmission power). We enable SpecObs with more features for improved management of TVWS networks (reducing cross-interference between SU networks). One extra feature is the support for collection of spectrum sensing data from clients and corresponding signal processing techniques to reduce intra-network interference.

Fig. 2.2 shows the main components that we have considered in SpecObs for implementation of various features. In this figure, a spectrum sensor node is connected to SpecObs server through IP which periodically senses broadband spectrum and computes FFT to produce power spectral density. The results are uploaded to database server along with other information such as location and time of sensing. A number of sensor nodes can be deployed in various locations for scaling to a wide area.

The internal components of the SpecObs server and their interactions is described in

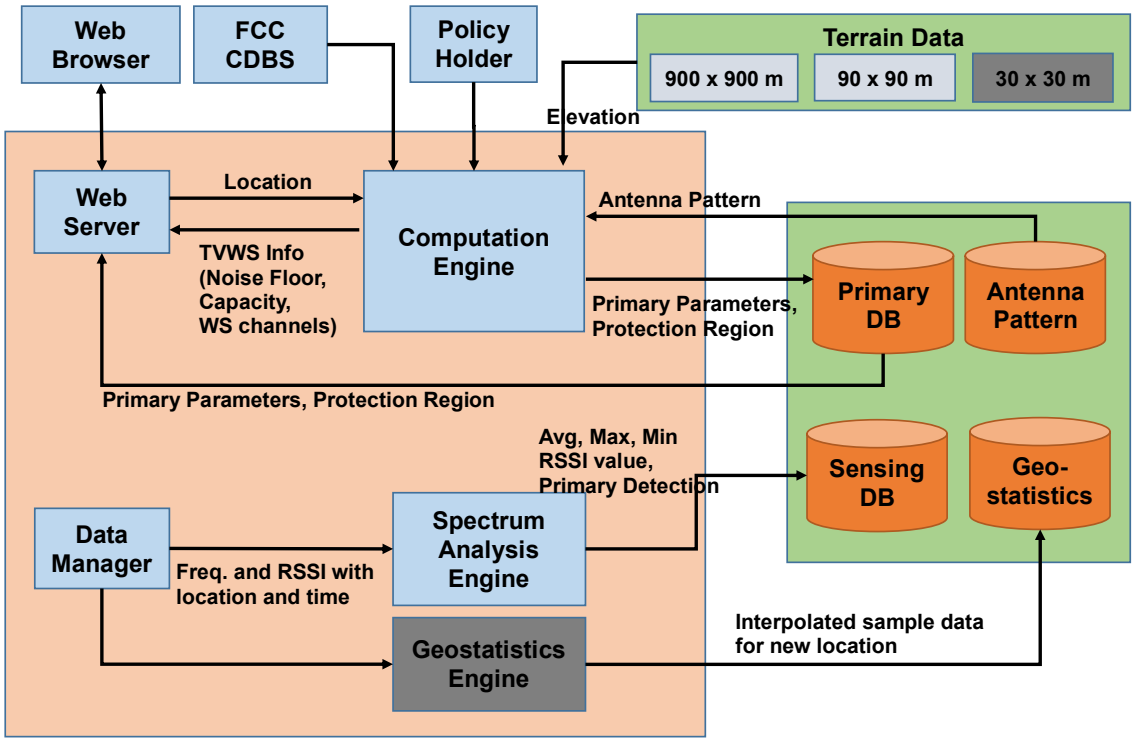

Figure 2.3: Main components of SpecObs system

Fig. 2.3. Each component in the server has been implemented in order to perform its own independent function. The database is divided into four sub-databases to store different types of data. Terrain database contains elevation data versus latitude and longitude over the globe with various resolutions. In the following sections we discuss each component separately.

2.2.1 FCC CDBS

FCC CDBS is a database that contains technical information about all active transmitters in the TV band (VHF/UHF). It includes both TV broadcasters and non-TV transmitters that are licensed to operate in this band. This information includes:

- Location (latitude, longitude) of the transmitter
- Channel Number which defines center frequency; the signal spectrum is 6-MHz wide

around the center frequency.

- Service Type: which defines characteristics of transmitting signal
- Transmission power
- Antenna height above average mean sea level (AMSL), above ground level (AGL), above average terrain (HAAT)
- Antenna pattern

SpecObs server downloads CDBS from FCC server, processes all the information provided and then places them into our local database 'Primary DB' and 'Antenna Pattern' in Fig. 2.3. This update procedure is performed on a daily basis automatically to ensure our data is in sync with FCC's list.

2.2.2 Policy Holder

Availability of WS spectrum at any location depends (among other parameters) on local spectrum policies that are defined by authorities such as FCC in the United States and Ofcom in the United Kingdom. Therefore, DBAs such as SpecObs must be aware of local regulation for the location that is queried by the user. The policy holder contains detailed rules imposed by corresponding agencies and provides the data to computation engine to calculate protection regions and estimate available white space spectrum.

2.2.3 Terrain Data

There are few terrain databases available publicly with different resolutions (number of sample points per arc-degree in latitude and longitude). Some of these are local (NED for US) and some are global (Globe 30 arc-sec database also known as Gtopo30). We consider three sets of data with 30, 90 and 900 meters resolution in latitude and longitude. Terrain data are used by the computation engine to estimate path loss between a pair of transmitter-receiver for the purpose of calculating coverage area (will be discussed later).

2.2.4 Computation Engine

There are two main tasks for computation engine as follows:

1. **Protection Region Calculation**: For each primary TV transmitter, FCC defines an area called protected region in which primary receivers are able to receive the signal successfully. Therefore, this area should be protected from any source of external interference. Computation engine imports all technical information for each primary transmitter that is obtained from FCC CDBS database to calculate the coverage area of that specific transmitter. This block also needs terrain data for estimating coverage area. Currently we support three path-loss models known as 'Longley-Rice Point-to-Point', 'Longley-Rice Area' and 'FCC Propagation Curve' for calculation of coverage. The latter is the official FCC-sponsored model for path loss calculation. The resulting calculated coverage is stored in the 'Primary DB', an example of which is presented in Fig. 2.4.

2. **TVWS Estimation**: Once a user queries for TVWS information, the web server receives HTTP request including queried location from the user. The web server calls the computation engine by passing location (latitude and longitude). The computation engine calculates available WS channels, predicts noise floor (dBm) and capacity (Mbps) for each available channel in real-time and provides the results to web-server.

2.2.5 Data Manager

The data manager block is the interface between SpecObs server and spectrum sensor nodes. It is responsible for receiving sensing data packets from sensor nodes, reformat the data for internal compatibility and provide the information to spectrum analysis engine and Geo-statistics engine. For example, the sensor nodes can save sensing data in CSV file format and upload to the server. Data manager periodically checks for new files, once received it parses the data and passes them to spectrum analysis engine.

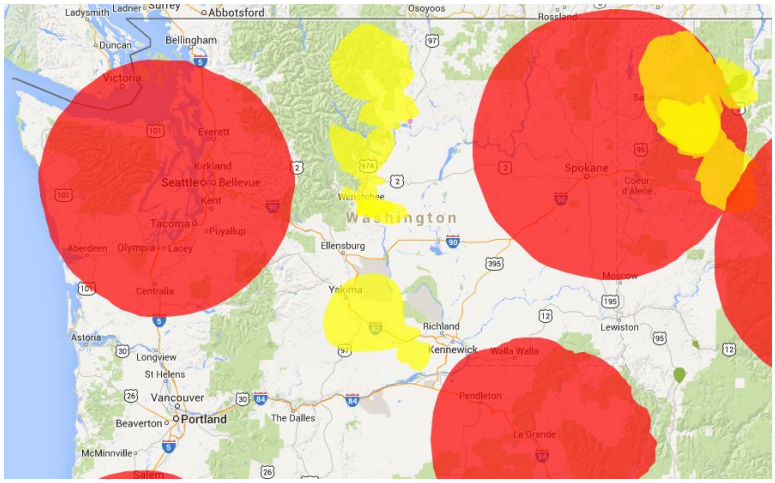

Figure 2.4: Sample protection regions calculated by SpecObs for WA state using 'FCC Propagation Curve' as path loss model. Different colors correspond to different types of TV transmitters.

2.2.6 Spectrum Analysis Engine

The engine calculates statistical information of received sensing data (such as average, minimum and maximum RSSI) for different frequencies within the broadband spectrum and tags them with location and time. For TV bands, the engine calculates average, minimum, maximum, and total RSSI for each 6-MHz TV channel. Furthermore, it performs a DTV pilot detector algorithm to search for presence of digital TV waveforms and it differentiates between TV/non-TV signals that are active in this band.

2.2.7 Geo-statistics Engine

One major limitation of spectrum sensing methods is the lack of sensing data for every location and time. Clearly, deployment of many spectrum sensors in the environment is not a practical choice. The geo-statistics engine is considered to cover for places with no real measurement data. It utilizes Kriging techniques to model spatial correlation of signals in the environment and then interpolates them for unknown locations. Our improvements on the geo-statistics model is an ongoing efforts in which we use real measurement data obtained for TV bands in the New Jersey area.

Table 2.1: Protected TV Services Considered by SpecObs

DB Key	Service	Type
TX	TV Translator/LPTV	Analog
LD	Digital TV Translator or LPTV	Digital
CA	Class A TV	Analog
DT	Digital TV	Digital
DC	Digital Class A TV	Digital
DD	DTV Distributed Transmission System (DTS)	Digital
TV	Canadian and Mexican Border Stations	—
DX	Digital Auxiliary (backup) Facilities	Digital
DTS	Distributed Television Service stations	Digital

2.3 Computational Architecture of SpecObs

There are various types of entities that share TV spectrum and are protected by FCC rules. This includes TV transmitters, Private Land Mobile Radio Services (PLMRS), Commercial Mobile Radio Services (CMRS), etc. Protection rules are highly dependent on the type of service. Table 2.1 shows TV services that are considered for protection in SpecObs (and other DBAs). The main difference between these services is minimum signal strength for defining the edge of protection region and maximum acceptable interference from SU devices (which determines the minimum separation distance).

Table 2.2 shows some of non-TV protected entities in TV bands that are considered by DBAs.

2.3.1 Path-Loss Calculation

As it was explained before, computation engine calculates protection region for each licensed entity. Each region is defined in terms of the maximum distance at which signal strength is above a certain threshold. Estimating signal strength at each location needs calculation of path-loss between PU transmitter and desired location.

There are many path loss models in the literature that are defined for various spectrum bands and various applications. For TV services, we need a path loss model that basically considers many physical parameters related to transmitter and receiver antennas and it

Table 2.2: Other Protected Entities in TV Band

Name	Service Description
PLMRS/CMRS	Also known as T-band devices, are active in channels 14 to 20 in eleven metropolitan areas across US.
Wireless-Mic	Specific channels are reserved for wireless microphones. In addition, individuals can register their device for further number of channels as required.
Radio Astronomy Sites	Passive sites that are used for radio astronomy operations. No SU operations is allowed within 2.4 km from the location of these sites.
Offshore Radio Services	Active in channels 15 to 18 at four areas across US and are protected from SU interference.

has a wide range for input parameters (for example antenna height in TV applications can vary from 30 meters to several hundred meters above average surrounding terrain). A suitable path loss model that is specifically designed for this matter is Longley-Rice model. FCC however mandates a weaker version of this model for use by DBAs known as 'FCC Propagation Curves'.

- **Longley Rice Model**: which is defined for two operational modes:

  1. LR Area Mode
  2. LR Point to Point Mode

  The basic difference between these two modes is the way terrain information is utilized. In summary, LR Area uses average information about terrain heights relative to TX/RX height and does not use detailed information about height across any specific path connecting TX/RX. On the other hand, LR P2P uses detailed height data across a line connecting TX to RX to estimate path loss along that specific path. Common parameters in both modes are listed below:

  – Frequency: Similar to most of other path loss models, frequency has a major effect on calculated path loss.

- Polarization: Antenna polarization is also a factor that can affect path loss.
- Time/Location/Confidence (TLC) Percentage (.01 to .99): These three factors introduce statistics into path loss models. For example, time percentage defines the fraction of time in which path loss is less than this value. So is the location percentage for the fraction of location. These parameters significantly affect the final result.
- SGM Conductivity: Conductivity of ground in S/m, with a default value of 0.005
- Surface refractivity (N-unit); default value is 301.0
- Epsilon Dielectric: Dielectric constant of ground; default value in ITM application is 15.0;
- Radio Climate: for which following options are possible
  - Equatorial
  - Continental Subtropical
  - Maritime Tropical
  - Desert
  - Continental Temperate
  - Maritime Temperate, Over Land,
  - Maritime Temperate, Over Sea

1. **LR Area Mode**: The main intent of LR in Area mode is to provide a relatively accurate estimate of path loss that is circular around the transmitter (However, we modify it to a non-circular model). The main terrain parameters in this mode are:
   - *TX height above average terrain*: This parameters defines relative height of transmitter with respect to surrounding terrain. Originally this is meant to be measured around the transmitter in every direction as a single number but we calculate it separately in every direction with step of 1 degree to provide a non-circular pattern for path loss. Therefore, for every direction, we select points in 3.2km to 16.0km from the transmitter and find average terrain height.

- *RX height above average terrain*: Just like previous parameters, RX height above average terrain shows relative height of the receiver antenna w.r.t. surrounding area.
- *Terrain Roughness (or Irregularity)* ΔH: This parameter captures the characteristics of the path connecting TX to RX. According to FCC documents, it should be calculated in a range of 10 to 50 km from transmitter. The parameter is defined as the height difference between the 10% point to 90% point in the histogram of the heights along the path. Therefore, for a plain path, ΔH turns out as a small number and for a mountain like path it will be a large number. In our implementation, we calculate ΔH for every angle around TX to achieve a non-circular path-loss model. Therefore, ΔH and TX height are the factor we use for achieving a non-circular model.
- *Tx Site Criteria*: This parameter defines how transmitter site is set up. Possible values are 'Random', 'Careful', and 'Very Careful'.
- *Rx Site Criteria*: The same definition as above for receiver.

2. **LR Point to Point Mode**: LR P2P is originally defined as a non-circular path loss model that is calculated for a pair of TX, RX. The main terrain parameters in this model are:
   - *TX height above average terrain*: Just the same way as LR Area mode, this parameter defines transmitter height w.r.t. surrounding area for every angle.
   - *RX height above average terrain*
   - *Vector of (distance, height) pairs*: The main difference between LR P2P and LR Area is the usage of this vector. Unlike LR Area, terrain variations in P2P is not averaged out along the path connecting TX to RX. Instead, exact values of terrain height along this path are provided to the model as a vector of (distance, height) which defines terrain height at a particular distance from transmitter.

- **FCC Propagation Curve**: which is a simpler path loss model than Longley-Rice. This is the path-loss model that is suggested by FCC as the standard for all DBAs

and has following input parameters:

- Propagation Curve: Which has the following three options F(50, 50), F(50, 10), F(50, 90). The numbers in bracket represents location, time percentages respectively. This is equivalent to TLC percentages in LR model with less flexibility in possible values.
- Transmitter HAAT: Transmitter height above average terrain. Receiver height is considered a fixed number of 10.0 meters in the model and is not modifiable.

2.3.2 Capacity Calculation

Capacity in this context is equivalent to estimation of noise and interference floor. We define capacity as the maximum throughput that is possible for a single pair of secondary Tx-Rx based on Shannon theory. Therefore, we need to calculate total interference that is experienced by a secondary user at any specific location. This includes following sources of interference:

1. *Co-Channel Interference*: All transmitters that are active in the current channel for a distance of up to 300 km are considered for this interference. The received signal strength is calculated using any of the aforementioned path loss models and accumulated for all active TV broadcasters.

2. *Adjacent Channel Interference*: This source of interference is calculated by considering a specific transmission filter for TV broadcasters and calculating power leakage in physically adjacent channels (Note that some channels are not physically adjacent even though their channel number is adjacent, such as channel 13 and 14).

3. *Secondary to Secondary Interference*: For mutual interference of secondary transmitters, a more suitable model is HATA model which is specifically calibrated for urban, suburban, rural areas [21]. We use this model to estimate possible mutual interference between secondary users that are sharing the same channel.

Chapter 3

CAPACITY CONSIDERATION IN TV WHITE SPACE

The so-called 'TV white spaces' (TVWS) - representing unused TV channels in any given location as the result of the transition to digital broadcasting - is designated for unlicensed use [18, 19, 22] by U.S. Federal Communications Commission (FCC). This presents significant new opportunities within the context of emerging 4G networks for developing new wireless access technologies that meet the goals of the US National Broadband Plan [23] (notably true broadband access for an increasing fraction of the population). There are multiple challenges in realizing this goal; the most fundamental being the fact that the available WS capacity is currently not accurately known, since it depends on a multiplicity of factors - including system parameters of existing incumbents (broadcasters), propagation characteristics of local terrain as well as FCC rules. In this chapter, we explore the capacity of white space networks by developing a detailed model that includes all the major variables, and is cognizant of FCC regulations that provide constraints on incumbent protection. Real terrain information and propagation models for the primary broadcaster and adjacent channel interference from TV transmitters are included to estimate their impact on achievable WS capacity. The model is later used to explore various trade-offs between network capacity and system parameters and suggests possible amendments to FCC's incumbent protection rules in the favor of furthering white space capacity.

3.1 Introduction

Next generation of cellular data networks will face an exponential growth of wireless data traffic resulting from the boom in multimedia applications running on smart phones, tablets, and other wireless devices [24]. Available 4G (licensed) spectrum will clearly be insufficient to meet this demand, leading to cellular operators searching for novel mechanisms to achieving operational efficiencies that enhance network capacity. Obviously, an essential response

to this increasing demand is the opening of new spectrum - both licensed, and recently, *unlicensed*. Resulting from the transition to digital TV broadcasting[1] and the consequent freeing up of VHF/UHF spectrum (between 50-700 MHz), FCC took the unprecedented step of allocating significant portions for unlicensed use, intended for providing enhanced wireless broadband access [18,19]. These bands - collectively denoted as TV White Spaces (TVWS) - are juxtaposed with the 4G 700-MHz *licensed* bands[2] and will allow secondary (unlicensed) users to opportunistically access them as long as *interference protection guarantees* to the neighboring primary (licensed) networks are ensured. A strategy for *coordinated use of both licensed and unlicensed 700 MHz spectrum* is the likely answer for 4G cellular operators, just as offloading to 802.11 WLAN hotspot networks has proved to be a boon for 3G network providers. TVWS (sometimes subbed as 'super Wi-Fi') may potentially provide even more significant offload/spectrum aggregation opportunities, considering other proximal government-held spectrum that are also being explored for de-regulation [25–29].

Clearly, the most critical task for a Dynamic Spectrum Access (DSA)-based cognitive user is finding spectrum 'holes' efficiently [30], i.e., spectrum resources in *time-frequency-spatial* dimensions at any location that are currently available, which can be then used for unlicensed operation. Current FCC rules of operation for unlicensed users in TVWS require them to register with and obtain recommendations from a list of approved Database Administrators (DBA) - such as a list of available TVWS channels - for their operation, so as to ensure interference protection to the incumbents. The DBA is responsible for complying with FCC regulations [19] in modeling all primary users status, as a basis of providing the necessary recommendations to the secondary users requesting access.

In this work, we explore a fundamental issue pertaining to WS usage by secondary networks, which may be succinctly captured by the question *How much WS network capacity actually exists per FCC rules*?. Clearly, the answer to this question is of paramount importance to 4G network operators as they consider new infrastructure for unlicensed WS access as part of their operations. We show that it depends on multiple factors:

---

[1]In the U.S. this was completed by June 2009.

[2]For example, portions of 698-806 MHz were auctioned off by 2008 in the U.S. to provide for 4G mobile broadband services.

- ◇ Primary Network Parameters (transmit power and signal masks, modulation/coding)
- ◇ FCC rules for protection of primary users/networks by limiting secondary operation (protection regions, adjacent TV channels, primary receiver design and sensitivity)
- ◇ Propagation Characteristics (location dependent terrain models, heights etc.)
- ◇ Secondary network parameters (transmit power and signal masks, modulation/coding, multiple access schemes)

Prior works on this topic, notably [31–35] do not provide a sufficiently nuanced exploration of this question (available secondary network capacity) as a function of *all* the parameters above. Notably, the *structure of the spatial variations* in secondary capacity has not been adequately captured, in our opinion. Further, FCC regulations have evolved significantly since the first release of TVWS [19, 22] as well as the primary network (TV broadcasters) which in turn impact TVWS capacity analysis. Mutual effects of secondary and primary networks, such as co-channel and adjacent-channel interference, are not considered. Furthermore, realistic and empirical path loss models that are based on actual terrain information have not been previously used.

We develop a *spatial description of WS capacity* via a model that captures both primary and secondary network aspects as well as channel and environmental characteristics. An important side benefit of our analysis is the spotlight it shines on *whether the current incumbent protection rules proposed by the FCC may need amending in the interests of promoting more WS availability.* Our analysis thus provides fundamental insights into aspects of coexistence between secondary users and primary transmitters as a function of FCC regulations [18, 19]. The rest of the chapter is organized as follows. Section 3.2 defines the network structure for coexistence of secondary and primary users. Section 3.3 formulates capacity of each secondary cell. The problem of channel availability determination is discussed in section 3.4 which includes current FCC rules, primary protection region definition as well as selection of propagation (path loss) model along with underlying physical environmental parameters. Section 3.5 introduces interference models. Numerical calculations

in section 3.6 provides high level results on available secondary capacity whereas section 3.7 explores multiple trade-offs that arise. Finally, section 3.8 concludes the chapter and some supplementary details are provided in the appendix.

3.2 Secondary Network Architecture

In practice, secondary networks can be deployed arbitrarily as an ad-hoc network. However, the outcome of such ad-hoc networks will be increased mutual interference and degradation of throughput (this is what has already been observed in chaotic WiFi deployments in 2.4 GHz). Therefore, cellular planning is a smarter choice; a very good use case are Small Cells that are deployed outdoors (stadiums, halls etc. for events) under control of the network operator. In this section, we consider secondary cellular networks that coexist with primary network.

Cellular communication systems are based on the notion of *frequency reuse* which allows a channel to be spatially re-used by different users, as long as the co-channel interference is within acceptable bounds. However, for TVWS applications, the cellular layout of the secondary cells (SC) is further restricted by the primary protection regions, as shown in Fig. 3.1. This figure presents TV towers as an *irregular* primary network, where each primary cell corresponds to the coverage area of the associated tower extended by an additional distance for protection of PUs on the edge. Here, r_i is the maximum distance at which the received TV signal is above the detection threshold [19, 36, 37]. The regions outside the primary transmitter coverage area constitute the white/gray space [17] that can be utilized by secondary networks; secondary cells are naturally much smaller than primary cells, due to power and antenna height limitations.

Characterizing the white spaces and the primary-to-secondary interference requires knowledge of deployment of TV towers (primary transmitters) and their parameters, which is available from the FCC database [38]. Comparing the examples of TV channels 13 (see Fig. 3.6) and 5 (see Fig. 3.7) indicates that the patterns of spatial reuse for primary (TV channels) are irregular (across channels). As a result, the availability of WS shows significant spatial variations, which we explore in more details later.

Let's define the set of available white space channels in a secondary cell A (according to

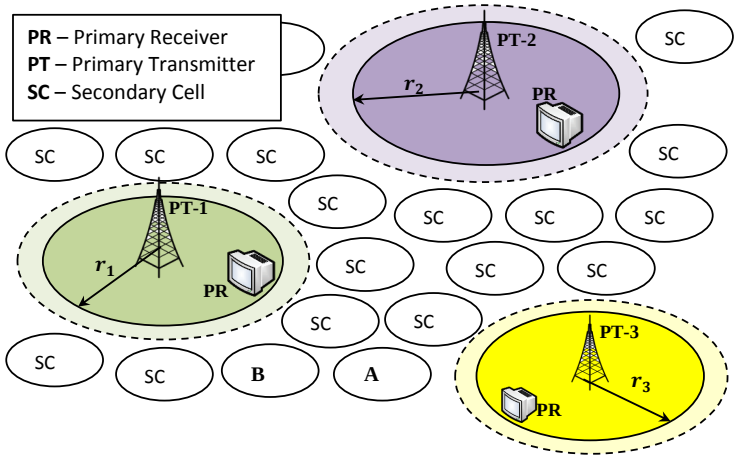

Figure 3.1: Coexistence of primary and secondary cellular networks

FCC rules for protection of *primary users*) as:

$$\Upsilon(A, \Gamma_A) = \{c_i : \text{ Channel } c_i \text{ is available at cell A with parameter } \Gamma_A\} \tag{3.1}$$

where Γ_A represents all relevant network parameters that can affect channel availability, including transmission power, antenna height above average terrain, out of band emission, etc. Note that $\Upsilon(B, \Gamma_B)$ represents a different list of available channels. In order to protect secondary users from secondary interference, only a subset of available channels are assigned to each secondary cell which is considered in section 3.5.

3.3 Secondary Link Capacity

We begin developments by computing the Shannon capacity of a (hypothetical) secondary transmitter-receiver pair located at a point, i.e. the capacity of an infinitesimal cell with one active link where the separation between the source and receiver is negligible. At this point, we assume that the secondary users are allocated one of the available channels $c_i \in \Upsilon(A, \Gamma_A)$ at any secondary cell A (this assumption will later be generalized by summing over all possible channels); the capacity is a function of the usual parameters - *signal to*

noise + interference ratio and *available bandwidth*

$$C_{cell} = W_0 \log_2(1 + \text{SINR}) \tag{3.2}$$

where $W_0 = 6$ MHz (for TV channels in USA) represents the bandwidth of an NTSC TV channel. Since the allocated channel c_i is not available at every location, a more appropriate measure of available capacity is an *area average*. To do this, we introduce a Bernoulli random process for the availability of any secondary WS channel, as follows:

$$W(Q_T, \Gamma) = \begin{cases} W_0 & Q_T \notin \Omega \text{ and } \Gamma \vdash \text{FCC rules} \\ 0 & Q_T \in \Omega \text{ or } \Gamma \nvdash \text{FCC rules} \end{cases} \tag{3.3}$$

where Q_T is the transmitter location, Ω is the set of all protection regions for the channel currently under exploration. Γ, as defined before, is the set of network parameters that must comply with FCC requirements ($\vdash$) for incumbent protection. Using this, let's define the *channel availability probability* $p(\Gamma) = Pr[Q_T \notin \Omega]$ as the normalized average of $W(Q_T, \Gamma)$ over an area $\mathcal{A}$

$$p(\Gamma) = \frac{1}{\mathcal{A}} \int_{\mathcal{A}} \frac{W(Q_T, \Gamma)}{W_0} dQ_T \tag{3.4}$$

The capacity averaged over transmitter and receiver locations is thus

$$\overline{C_{cell}}(\Gamma) = \int_{\mathcal{A}} \int_{\mathcal{A}} \frac{W(Q_T, \Gamma) \log_2(1 + \text{SINR}(Q_R))}{\mathcal{A}^2} dQ_R dQ_T \tag{3.5}$$

where the SINR depends on (secondary) receiver's location Q_R. Eq. (3.5) can be calculated for every channel separately and the overall capacity of a cell that is exploiting all available channels is obtained by summing over all channels

$$\overline{C_{cell,total}}(\Gamma) = \sum_{c_i \in \Upsilon(cell, \Gamma_{cell})} \int_{\mathcal{A}} \int_{\mathcal{A}} \frac{W(Q_T, \Gamma) \log_2(1 + \text{SINR}(Q_R, c_i))}{\mathcal{A}^2} dQ_R dQ_T \tag{3.6}$$

3.4 Channel Availability Determination

Availability of every permissible TV channel $c_i \in \{2:51\}$ is mainly a function of location and secondary user transmission characteristics. FCC defines various rules for secondary TV band devices (or TVBDs, subsequently) to protect primary receivers [18,19] that affect the probability of channel availability. A brief summary of the relevant FCC regulations follows:

- ◇ **Permissible Channels**: A fixed TVBD may operate on any channel in $\{2:51\} \setminus \{3,4,37\}$ subject to conditions below [18,19]. Further, personal/portable devices may only transmit on available channels above channel 20, $\{21:51\} \setminus \{37\}$ subject to following requirements.

- ◇ **Power limit**: For fixed TVBD, the maximum power delivered to antenna may not exceed 1 watt in 6 MHz with a maximum of 6-dBi gain for antenna (maximum 36-dBm of EIRP[3]). For personal/portable TVBD, the maximum EIRP shall not exceed 20dBm per 6 MHz. If portable TVBD is transmitting in an adjacent channel to a primary transmitter, then maximum EIRP is limited to 16-dBm.

- ◇ **Antenna height**: The transmit antenna for fixed devices may not be more than 30 meters above the ground. In addition, fixed devices may not be located at sites where the antenna height above average terrain is more than 250 meters. Portable device antenna is assumed to be less than 3 meters above the ground.

- ◇ **Interference protection**: TVBD must protect digital and analog TV services within the contours defined in Table 3.6 for various types of TV services. Fixed and portable TVBD are not allowed to transmit within a minimum separation distance from the border of protected contour that is defined in [19] based on secondary transmitter class and height above average terrain (HAAT). Fixed devices must be outside protection regions of co-channel and adjacent channel stations. Portable devices are allowed to transmit within adjacent channel contours with a maximum power of 40 mW.

[3]Effective Isotropic Radiated Power

- ◇ **PLMRS/CMRS**: In 13 major metropolitan areas that are specified by FCC, some of the channels between 14 to 21 are reserved for PLMRS/CMRS. Therefore, TVBD may not operate at distances less than 134-km for co-channel operation and 131-km for adjacent channel operation from the center of those designated areas.

- ◇ **Radio Astronomy Sites**: TVBDs are not allowed to operate at any TV channel within 2.4 km from registered radio astronomy sites in FCC database.

- ◇ **Microphone Reserved**: The first available TV channel above and below channel 37 are reserved for wireless microphones. If no channel is available above(below) channel 37 then the two channels below(above) are reserved. TVBDs are not permitted to operate on these reserved channels.

The aggregate effect of FCC rules is modeled through defining protection regions for primary users, as discussed below, where no secondary is allowed to transmit. Note that protection region includes protection contour as well as minimum separation distance. Therefore, channel availability probability represents the ratio of the area where channel is considered free (according to regulations above) to the total area of discussion.

3.4.1 Primary Protection Region

Considering a permissible WS channel c_i at any location and an area $\mathcal{A}$ with N co-channel secondary and M adjacent-channel (either channels $c_i - 1$ or $c_i + 1$) primary users. For every licensed device, a protected contour [18], defined by FCC for different types of stations, is considered that represents the coverage area of that transmitter. This grade B contour for TV broadcasters, is a function of following parameters:

- ◇ P_t: Primary transmitter effective power (EIRP)

- ◇ Δ: Minimum required signal for primary receiver, defined in Table 3.6

- ◇ f: Frequency

◇ h_t/h_r: Tx/Rx Antenna height above average terrain (HAAT)

◇ ΔH: Terrain irregularity parameter which distinguishes plains versus mountains.

◇ Service type: FCC regulates different rules for various services in TV band, such as PLMRS/CMRS[4] versus low power auxiliary services including wireless microphones.

◇ Environmental effects that change propagation path loss, such as radio climate, conductivity of ground, surface refractivity, etc.

The overall protection region is an area of radius $r_p = r_{PC} + d_{MS}$ where r_{PC} is the protected contour radius and d_{MS} is an additional minimum separation distance as shown in Fig. 3.2. Detailed description of protection region calculation is provided in Appendix 3.A. We define this area as the primary network cell shown in Fig. 3.1. The secondary cells can exist in any region beyond these primary protected cells. Therefore, the channel availability probability, using an area average, is approximated as

$$p(\Gamma) = 1 - \frac{\sum_{j=1}^{N} \mathcal{A}_{p,co}(j) + \sum_{k=1}^{M} \mathcal{A}_{p,adj}(k) - \sum_i \sum_j \mathcal{A}_p(i,j)}{\mathcal{A}} \tag{3.7}$$

where $\mathcal{A}_{p,co}(j)$ is the co-channel protection area for transmitter $j \in \{1:N\}$ and $\mathcal{A}_{p,adj}(k)$ is adjacent-channel protection area for transmitter $k \in \{1:M\}$. In most cases, as our simulation reveals, there are significant overlaps between co-channel and adjacent channel areas which is considered in $\mathcal{A}_p(i,j)$. Dependency of $\mathcal{A}_{p,co}$, $\mathcal{A}_{p,adj}$ on Γ is removed for notational simplicity.

We remark that the protection region in reality is generally an irregular area that is non-circular, largely due to varying terrain heights as a function of azimuth angles as seen at a primary transmitter location.

---

[4]Personal Land/Commercial Mobile Radio Services

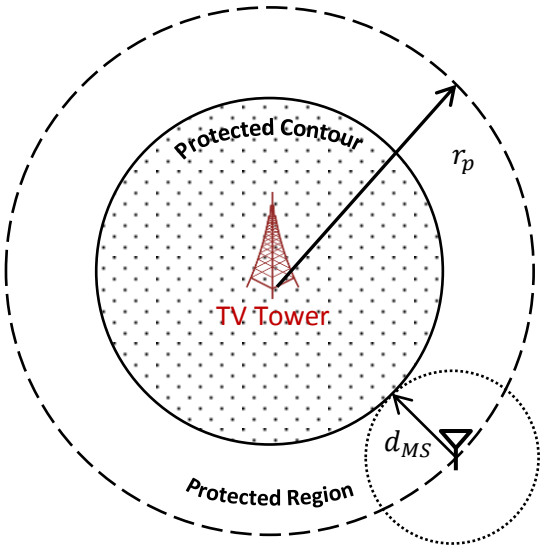

Figure 3.2: Protected contour v.s. protection region defined by FCC

3.4.2 Path Loss Model

Choosing an appropriate path loss model is very important in TVWS capacity analysis because it directly affects all subsequent results and choice of secondary parameters. There are various path loss models in the literature that has been adopted for different applications, frequency range and environments [21, 37, 39–42]. Except for free space model that is derived from pure theory, most useful path loss models are based on experimental measurements; this includes the well-known *HATA* model family for different terrain categories such as urban, suburban and rural areas [21] that has been widely used in cellular network planning. However, such path loss models are significantly limited in terms of accuracy in their range of parameters such as transmitter/receiver antenna height, coverage distance and frequency. Therefore, for TV tower specifications including very high altitude (as high as 700 meters) and broad coverage area (upto 100 km), more general models are required that incorporate real terrain information. We thus settle on the Longley-Rice (ITM) model that is measurement-driven and covers a wide range of input parameters, appropriate for TV coverage estimation [36]. A computer implementation of this model is provided by NTIA [41] called ITM, and is described here.

Irregular Terrain Methodology (ITM) estimates radio propagation losses for frequencies between 20-MHz and 20-GHz as a function of distance and the variability of the signal in time and space. It is an improved version of the Longley-Rice Model [43], which gives an algorithm developed for computer applications. The model is based on electromagnetic theory and signal loss variability expressions derived from extensive sets of measurements [40, 44]. It is applicable to point-to-area calculations with *point* being the location of a broadcast station or a base station for mobile service and *area* refers to locations of broadcast receivers or mobile stations. The area is described by the terrain roughness factor (irregularity parameter) Δh, which is defined as the interdecile value computed from the range of all terrain elevations for the area, calculated separately in every direction.

Based on Longley-Rice methodology, calculation of coverage is as follows. For analog TV, computation is made inside the conventional Grade B contour defined in Section 73.683 of the FCC rules, with the exception that the defining field for UHF channels is modified by subtracting a dipole factor. The same adjustment is needed for digital TV calculations. Modified signal strength tables for analog and digital TV are shown in Table 3.7.

ITM - Input Parameters

The following input parameters are required for a proper description of the communication link. The main parameters affecting this model are:

- f: frequency, 20 MHz to 20 GHz.
- d: Distance between the two terminals, 1 km to 2000 km.
- h_{g1}, h_{g2}: Antenna structural heights, 0.5 m to 3000 m.
- *pol*: Horizontal or Vertical polarization.
- Δh: Terrain irregularity parameter. This is the main parameter that captures the effect of terrain elevation on path loss calculation.

Note that antenna heights are calculated relative to average terrain height surrounding TV transmitter. This in fact changes in different angles and results in non-circular path loss patterns just as terrain roughness parameter Δh creates angle dependency.

3.5 Interference Model

SINR is by definition the ratio of received power at receiver location to noise and interference:

$$\mathrm{SINR}(Q_R) = \frac{P_{sec,RX}(Q_R)}{N_0 W_0 + I(Q_R)} \tag{3.8}$$

There are two sources of interference in TV white space networks:

3.5.1 Primary-to-Secondary

Although primary users are protected from undesired interferences from unlicensed devices, they introduce a significant source of interference to secondary users working in the same or adjacent bands. The level of interference at every location depends on the distance from the secondary receiver to nearby TV broadcasters, as shown in Fig. 3.3, as well as other physical parameters such as antenna height.

TV transmitters introduce both co-channel and adj-channel interference to secondary users, due to signal leakage from each channel to lower/upper bands. The aggregate interference for the receiver location Q_R is:

$$I_{P2S}(Q_R) = \sum_{i=1}^{N} (1-\eta) \frac{P_i G_i}{L_{TV}(d_i)} G_r + \sum_{j=1}^{M} \eta \frac{P_j G_j}{L_{TV}(d_j)} G_r \tag{3.9}$$

where P_i/G_i is the transmitter power and antenna gain, $L_{TV}(.)$ is path loss function from TV broadcaster, G_r is the receiver antenna gain and N/M is number of co-channel/adj-channel surrounding TV towers (we consider TV transmitters up to a distance of 300 km in numerical calculation section). η is the leakage factor for TV transmitters defined as the ratio of power transmitted in upper/lower band to total power and d_i is distance to primary transmitter i. Note that, location dependency, $I_{P2S}(Q_R)$ is hidden inside distance factor d_i.

In order to consider adjacent channel interference in simulation, we consider a practical

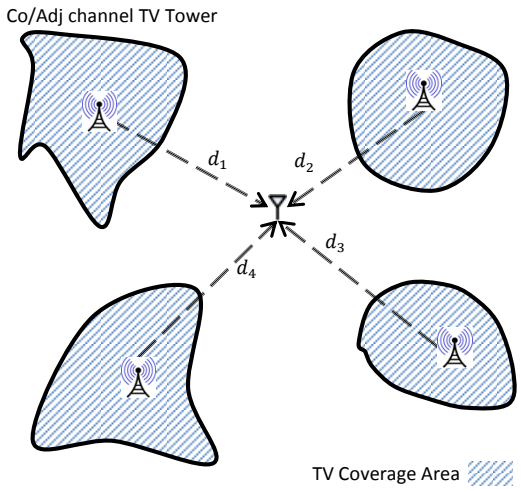

Figure 3.3: Primary-to-Secondary interference

transmission mask, introduced for 8-VSB standard [45], shown in Fig. 3.4 for full service digital TV transmitters. It defines maximum power leakage to upper and lower channels for a maximum of two channel distance. Similar masks are defined for TV translators and low power TV broadcasters [45]. Full service transmitter mask is defined as below:

- ◇ In the range between Channel Edge and 500 kHz from the Channel Edge: $Emission \leq -47dB_{DTV}$[5]
- ◇ More than 6 MHz from Channel Edge: $Emission \leq -110dB_{DTV}$
- ◇ At any frequency between 500kHz and 6 MHz from the Channel Edge: $Emission \leq -(11.5(|\Delta f|-0.5)+47)dB_{DTV}$, with Δf being the frequency difference in MHz from the Channel Edge.

By defining the emission mask function $E(f)$ as above for full service DTV, the overall

[5] dB_{DTV} is the relative power with respect to *total power in the transmitter's 6 MHz Channel including the pilot*

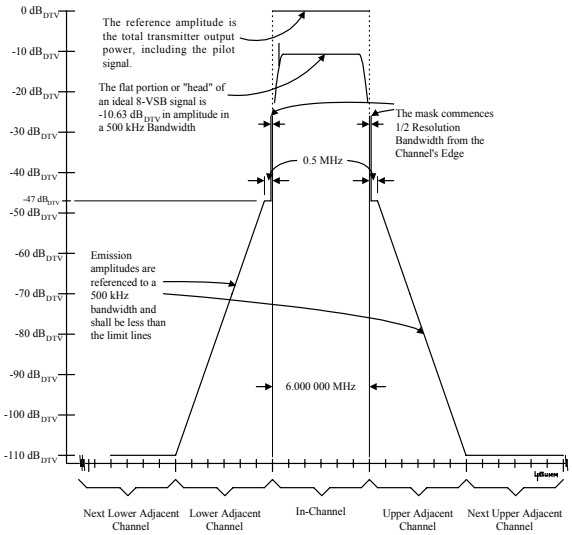

Figure 3.4: 8-VSB Full Service Transmitter Emission Limits [3].

leakage to adjacent channels with respect to total power is:

$$\eta_{\pm 1}(DTV) = \int_0^6 10^{E(f)/10} df = 1.75 * 10^{-5}$$
$$\eta_{\pm 2}(DTV) = \int_0^6 10^{-110/10} df \approx 0$$

Following the same procedure for LPTV DTV or translator services results in:

$$\eta_{\pm 1}(LPTV) = \int_{0.5}^3 10^{-(1.15(f-0.5)+4.7)} df$$
$$+ 5 * 10^{-5.7} + 3 * 10^{-7.6} = 1.76 * 10^{-5}$$
$$\eta_{\pm 2}(LPTV) = \int_0^6 10^{-76/10} df = 1.51 * 10^{-7}$$

3.5.2 Secondary-to-Secondary

The interference that is experienced by a white space receiver from *other* TVBD users has severe impacts on its performance. As discussed before, the area $\mathcal{A}$ is divided to multiple cells and each channel is used several times in non-adjacent cells. The minimum distance

that allows the same frequency to be reused will depend on many factors, such as the number of co-channel cells in vicinity of the center cell, the type of geographic terrain contour, antenna height, and transmitted power at each cell site, [46].

The frequency reuse distance D can be determined from

$$D = \sqrt{3K} r_{cell} \tag{3.10}$$

where K is the frequency reuse pattern, defined by shift parameters $K = i^2 + ij + j^2$. In theory, increasing D will reduce the chance of co-channel interference and is desired. On the other hand, spectrum inefficiency will also increase as the ratio of $q = \frac{D}{r_{cell}}$ increases. The goal is to obtain the smallest K that maximizes efficiency and still meets the protection requirements on incumbents. This involves estimating co-channel interference and selecting the minimum frequency reuse distance D feasible.

Here, we assume that secondary cell size is fixed and is determined by the coverage area corresponding to the secondary transmit power [46]. For a homogeneous secondary network with fixed cell size, the co-channel interference is *independent* of the transmitted power of each cell, i.e. the receiver threshold at a mobile secondary receiver is adjusted to the size of the cell. The received carrier-to-interference ratio at the desired mobile receiver is [46]

$$\frac{C}{I_{S2S}} = \frac{C}{K_I \sum_{i,j \in [0,1,...]} I_{i,j}} \tag{3.11}$$

where K_I is the number of interferer at each tier and $I_{i,j}$ is the interference of the co-channel cell shifted by i, j. In a fully equipped hexagonal-shaped cellular system, $K_I = 6$ and $I_{i,j} = P_{sec,TX} G_{sec}^2 L_{sec}(D_{i,j})$ where $D_{i,j}$ is the distance from (i, j)'s interfering cell and $D_{i,j} = \sqrt{i^2 + ij + j^2} D$. G_{sec} is secondary antenna gain and $L_{sec}(.)$ is path loss function between secondary users. The overall experienced secondary-to-secondary interference is

$$I_{S2S} = P_{sec,TX} G_{sec}^2 K_I \sum_{i=0}^{\infty} \sum_{j=i, j \neq 0}^{\infty} L_{sec}(D_{i,j}) \tag{3.12}$$

In practice, the closest cells are the prominent interferers and the sum above is practically limited to $i, j = 2$ instead of infinity. Note that I_{S2S} depends on precise location of the

receiver inside the cell. However, we consider an uplink-only scenario in which interference is calculated at the center of the cell site. The resulting SINR is

$$\mathrm{SINR}(Q_R) = \frac{P_{sec}/L_{sec}(r_{cell})}{N_0 W_0 + I_{P2S}(Q_R) + I_{S2S}} \tag{3.13}$$

Using (3.5), (3.7) and (3.8), the average capacity per cell for each individual TVWS channel is

$$\overline{C_{cell}}(\Gamma) = \int_{\mathcal{A}} \int_{Q_R} \frac{W(Q_T, \Gamma)}{K\mathcal{A}^2} \log_2 \left(1 + \frac{P_{sec}/L_{sec}}{N_0 W_0 + I_{P2S}(Q_R) + I_{S2S}}\right) dQ_R dQ_T \tag{3.14}$$

3.6 Numerical Calculations

In this section, numerical results are provided for evaluation of the analysis in previous sections. The main focus is to explore dependency of network capacity on various parameters and subsequent optimization of parameter choices. All simulations are performed on a TVWS simulation platform developed at University of Washington, a snapshot of which is shown in Fig. 3.5. This platform models protection regions for all primary transmitters registered in the FCC database [38], and applies all FCC regulations to determine available channels to secondary devices. It also estimates interference level and achievable capacity at any location inside the United States. High resolution terrain elevation[6] is used for accurate computation of path loss function. Population data are obtained from [49] which is based on Census 2010 publication and provides high-resolution spatial distribution of US population especially in urban areas. Statistical results are based on Monte-Carlo simulation over 20,000 locations in contiguous United States which are carefully chosen to cover various population densities from unpopulated (<10) to overpopulated (>10000) regions[7].

We use particular path loss models for different parts of the analysis. Specifically, we use Longley-Rice in area mode to calculate protected regions of TV broadcasters. For

[6]Terrain data, obtained from [47] and [48], are used in calculation of transmitter height above average terrain (HAAT), terrain irregularity ΔH in Longley-Rice area-mode path loss model, and for terrain-specific Longley-Rice point-to-point model.

[7]This simulator considers all FCC regulations as specified in [20] and is publicly available at http://specobs.ee.washington.edu/

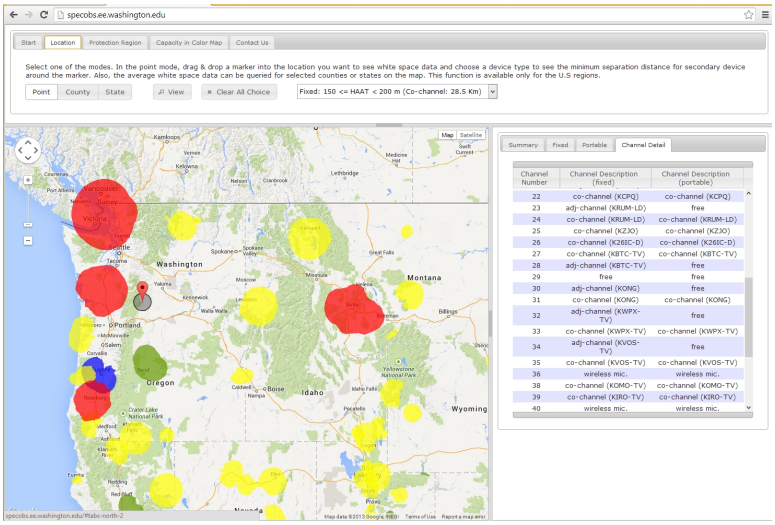

Figure 3.5: TVWS simulation engine, developed at University of Washington, a cloud based simulator for TVWS. Protection regions are shown for channel 19 across Washington state; List of available channels for fixed and mobile devices, as well as estimated interference level and capacity are shown for available channels [4]

primary to secondary interference, Longley-Rice in point to point mode is used that highly depends on the terrain profile between transmitter and receiver. This is a terrain-specific path loss model, well designed for calculation of path loss between two individual points. Finally, Hata model is used for secondary to secondary interference because it is particularly designed for mobile services in urban, suburban and rural areas.

Fig. 3.6 and 3.7 show calculated protection regions for TV transmitters on channel 13 and 5 across the continental US, using Longley-Rice methodology in area mode. The spatial distribution of transmitters as well as non-circularity of protections regions, as a result of terrain variations, are well highlighted in the figures. Note the general lack of structure in the distribution of TV transmitters, indicating the lack of any prior planning (as in cellular layout) for TV broadcast.

3.6.1 Channel Availability Statistics

FCC regulation restricts TVBD in many aspects from maximum power and antenna height to not using adjacent channel to active TV stations. In this section, we provide some

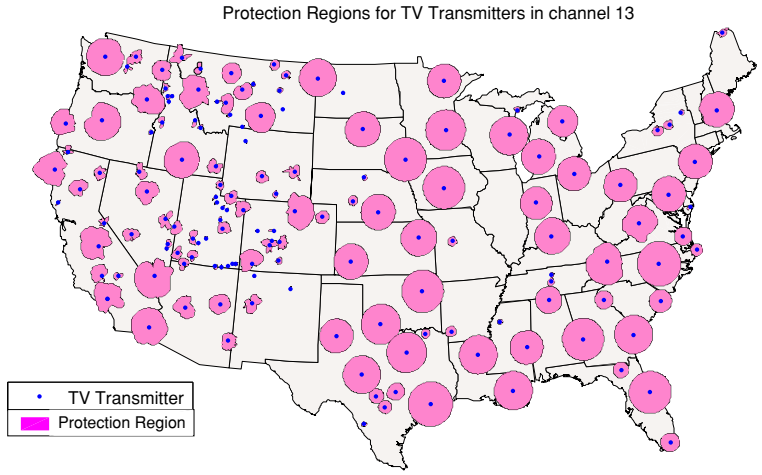

Figure 3.6: Protection region for TV transmitters broadcasting on channel 13; Using Longley Rice model in area mode

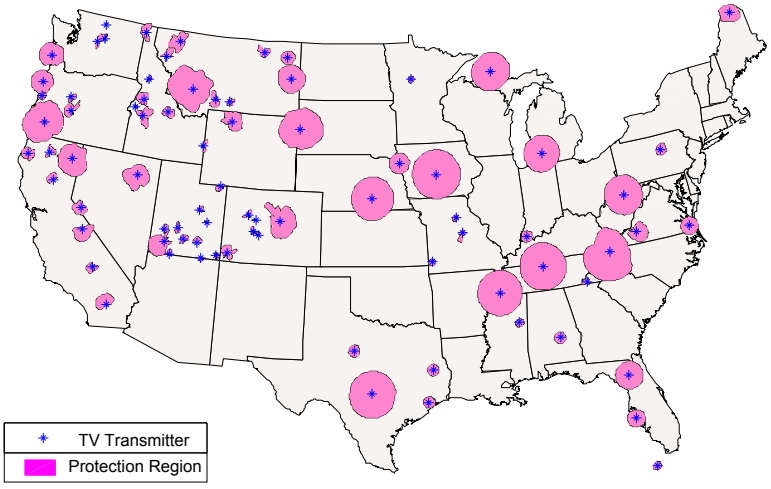

Figure 3.7: Protection region for TV transmitters broadcasting on channel 5; Using Longley Rice model in area mode

statistical information about the overall effects of these rules on total number of available WS channels for *fixed* and *portable* devices.

Table 3.1 shows the average number of available channels for *fixed* and *portable* TVBD in various frequency bands. In addition, the number of channels that are used by TV

Table 3.1: Average number of available channels for different TVBD classes

Device Type	LVHF(2:6)	HVHF(7:13)	UHF(14:51\37)	Total
Total Available	1.65	1.17	11.38	14.20
Fixed Devices	1.65	1.17	4.85	7.68
Portable/Personal	0	0	10.24	10.24
non-TV Services	0	0	4.2	4.2
Busy Channels by TV	1.04	3.65	19.34	24.03
Unused Channels	2.31	2.18	6.28	10.76
Channel Utilization Factor	53.8%	68.9%	83%	78%

transmitters (Busy[8] channels) as well as the total number of channels that are not released for unlicensed operation (Unused[9] channels) are provided. At the bottom of the table is the final utilization factor that is achieved by permitting unlicensed operation and it is defined as $CUF = 1 - \frac{\text{Unused Channels}}{\text{Total TV Channels}}$. As the table suggests, an average of 10.76 channels are still left unused even with operation of TVWS devices, which is $\approx 22\%$ of all channels. By repeating this simulation for two separate categories of locations, urban versus rural areas, interesting results are observed. As shown in Table 3.2 and Table 3.3, the number of available WS channels is highly dependent on population density. The total number of channels in rural areas are twice as many as in the urban areas, mainly because of significant reduction in the number of active TV transmitters; however, the number of unused channels is approximately the same in both.

The variation of the average number of channels versus population density is also of interest. Fig. 3.8 shows the total number of available channels, sub-divided into those for fixed and portables devices. There is a noticeable big reduction in TVWS channels as population density approaches 1000 per sq. mile (representing transition from rural to semi-urban areas) and thereafter, the changes are slower. The number of unused channels does not change significantly with population density, as noted in Tables 3.2 and 3.3. Fig.

[8]We consider a channel as busy if target location is inside the service contour for that transmitter.

[9]Any channel that is not used by TV services (outside service contour) and not released for TVWS operations. Thus, it includes channels reserved for wireless microphone, PLMRS/CMRS, and radio astronomy sites.

Table 3.2: Average number of available channels for urban areas; A minimum population density of 1000 person per squared miles is considered as urban areas.

Device Type	LVHF(2:6)	HVHF(7:13)	UHF(14:51\37)	Total
Total Available	1.60	1.10	10.66	13.35
Fixed Devices	1.60	1.10	4.23	6.93
Portable/Personal	0.00	0.00	9.63	9.63
non-TV Services	0.00	0.00	4.31	4.31
Busy Channels by TV	1.09	3.75	20.00	24.83
Unused Channels	2.31	2.16	6.34	10.81
Channel Utilization Factor	53.8%	69%	82.8%	78%

Table 3.3: Average number of available channels for Rural areas; With population density less than 1000 person per squared miles

Device Type	LVHF(2:6)	HVHF(7:13)	UHF(14:51\37)	Total
Total Available	2.38	2.17	21.30	25.84
Fixed Devices	2.38	2.17	13.34	17.89
Portable/Personal	0.00	0.00	18.54	18.54
non-TV Services	0.00	0.00	2.64	2.64
Busy Channels by TV	0.39	2.40	10.26	13.04
Unused Channels	2.24	2.43	5.45	10.11
Channel Utilization Factor	55%	65%	85%	79%

Table 3.4: Average number of available, busy, and unused channels for selected markets in United States

Device Type	NY	Houston	Chicago	Seattle	Miami	Denver
Total	1.43	5.16	10.21	17.18	1.00	7.42
Fixed	0.02	2.13	4.16	6.77	0	1.91
Portable	1.41	3.04	6.05	11.37	1.00	6.42
non-TV	5.06	3.93	5.00	2.0	4.00	2.00
Busy TV	36.70	31.25	28.71	22.22	39.00	33.12
Unused	10.88	11.58	10.08	9.60	9.00	8.46
CUF	78%	76%	79%	80%	82%	83%

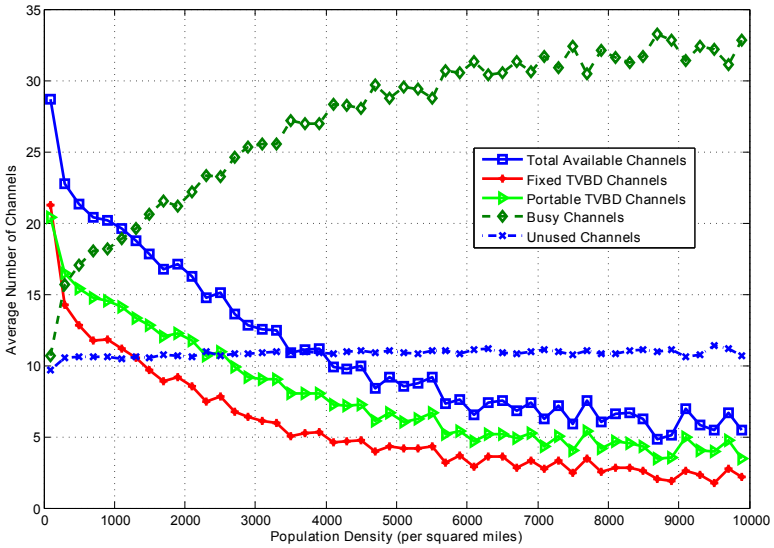

Figure 3.8: Average number of available channels vs. population density, calculated over the contiguous United States.

3.9 illustrates cumulative density function (CDF) for total number of available channels as well as number of available channels for fixed and portable devices, in urban and rural areas, defined as:

$$CDF(x) = Pr[\text{Number of channels } \leq x] \tag{3.15}$$

The rural CDF is shifted by approximately 10 channels, relative to urban CDF which again highlights further availability of TVWS in rural places.

3.6.2 Primary to Secondary Interference

Primary transmitters are usually of very high power with a poor transmission mask, as shown in Fig. 3.4. Therefore, they have considerable out-of-band emissions up to two adjacent channels, which significantly reduces secondary user's SINR. As a result, TV *white space* is in fact *gray space* with different levels of pollution in different channels. Fig. 3.10 illustrates noise and interference levels in all free channels (outside protection contour for primary transmitter) for *fixed* and *portable* devices. The figure also shows maximum and

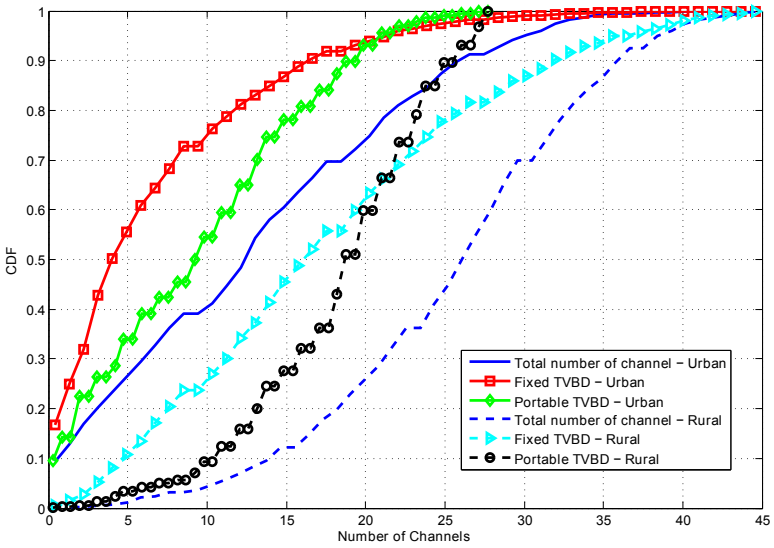

Figure 3.9: Cumulative density function of number of available channels for different TVBD classes. Statistics are provided for the contiguous United States.

minimum interference level for both device types. The minimum interference is practically the same as thermal noise floor -106 dBm. On the other hand, the maximum noise level can be as large as -30 dBm which is significantly high and can severely affect the performance of secondary network.

The level of interference to *fixed* devices is generally larger than *portables*. This is due to higher antennas that are used for *fixed* transmitters (up to 30 meters is allowed according to FCC regulation [19]) while *portable* transmitter antenna is supposed to be less than 3 meters high. The extend of this difference depends on specific location of the receiver and can be as large 15∼20 dB.

While it is expected to receive higher noise level at lower frequencies, the Fig. 3.10 does not reveal any specific pattern for noise level. This is mainly because the number of TV transmitters in each channel and their corresponding transmission power and antenna height is different. Here, we have considered TV transmitters in a range of 300-km from the receiver's location.

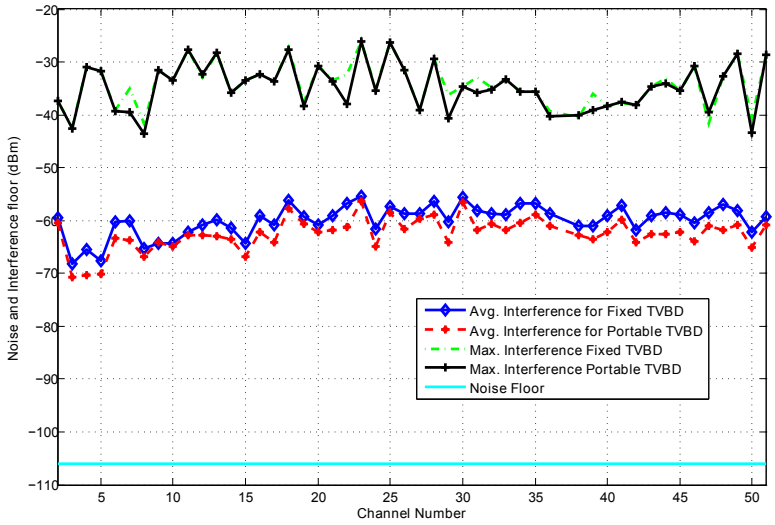

Figure 3.10: Noise and interference floor for *fixed* and portable TVBD, (3.9).

3.7 Practical Trade-Offs in Secondary Network Design

3.7.1 Link Capacity vs. TVBD Power

Suggested by (3.14), link capacity is a function of available bandwidth $W(Q_T, \Gamma)$ and SINR $= \frac{P_{sec}/L_{sec}}{N_0 W_0 + I}$. For the fixed bandwidth of TV channels, increasing link capacity should be through secondary power P_{sec}. In contrast to regular communication systems, higher power in TVWS has a negative effect on link capacity since it expands protection region of TV transmitters. As a result, channel availability probability $p(\Gamma)$ in (3.7) and average number of WS channels decreases which diminishes link capacity. The natural question is of course *what is the optimum secondary power?*

Latest FCC regulations [19] has set a maximum transmission power of 4.0 Watt for fixed and 100/40 mWatt for portable devices. Therefore, as long as P_{sec} is below the limit it does not affect available TV white space and any transmission power above the limit translates to zero white space availability. This is a severely quantized version of previous FCC rules [22] and it is not suitable for evaluation of capacity-power trade-off. Hence, for this section we use FCC rules in [22] (denoted as FCC2008[10]) as well as latest FCC regulation (FCC 2012).

[10]In which white space availability decision is based on the ratio of desired to undesired signal for fixed

Optimum transmission power that maximizes available white space depends on spatial distribution of TV transmitters. Therefore, it can change significantly from one market to the other. Fig. 3.11 and 3.12 present two different markets in states of Washington and Colorado. Each figure shows the number of available channels as well as capacity as a function of secondary power. For FCC2012, average number of channels is fixed as long as $P_{sec} \leq 4.0$ Watts and average capacity increases linearly because number of channels is not affected by power increase. However, after crossing the threshold of 4.0 watt, there is zero capacity available with the current ruling. On the other hand, using FCC2008, the number of available channels decreases monotonically by increasing secondary power because the ratio of desired to undesired signal decreases. Available capacity shows the trade-off between SINR improvement (which is dominant initially) and reduction in number of available channels that is dominant at higher power levels. Therefore, capacity increases up to a maximum point and then drops rapidly.

Comparing the two cases for FCC regulations, we notice that there are significant white space capacity for $P_{sec} \geq 4.0$ that is lost in the current FCC rules. Interference-based calculation of TVWS provides a more accurate measure of channel availability and opens further flexibility for secondary network design. These results show possible amendments to current FCC rules in favor of enabling more white space capacity particularly in rural areas[11] (as back-haul) where distances are larger and networks are power-limited.

3.7.2 Link Capacity vs. TVBD Antenna Height

The height of the secondary user's antenna is also affecting network capacity by changing path loss for TVBD transmitter. Increasing antenna height has following effects on network capacity:

- ◇ Secondary to secondary path loss decreases, higher capacity.
- ◇ Minimum distance increases, hence $p(\Gamma)$ reduces and results in lower capacity.

TVBDs

[11]Simulation points in this section are carefully chosen to represent both urban and rural areas.

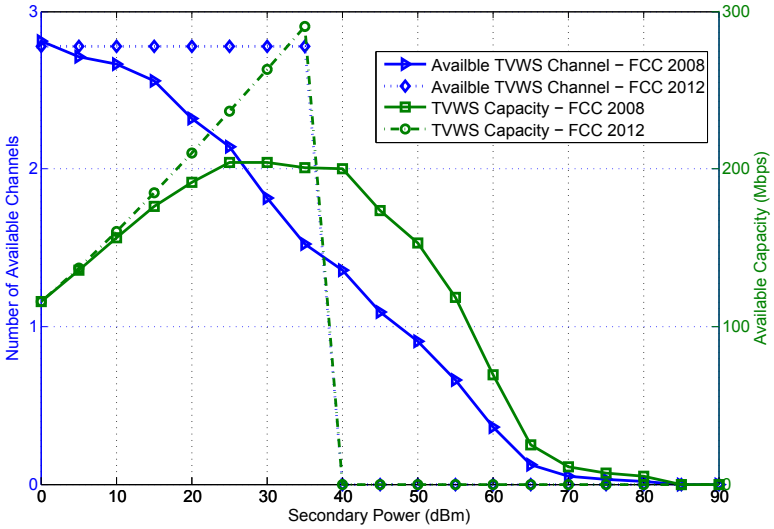

Figure 3.11: Average number of available TV white space channels and capacity for Denver market in state of Colorado. Capacity is calculated for a point to point link of fixed TVBDs, with 500 m distance. FCC2012/FCC2008 represents current/former FCC regulations. Antenna height is fixed to 20.0 meters.

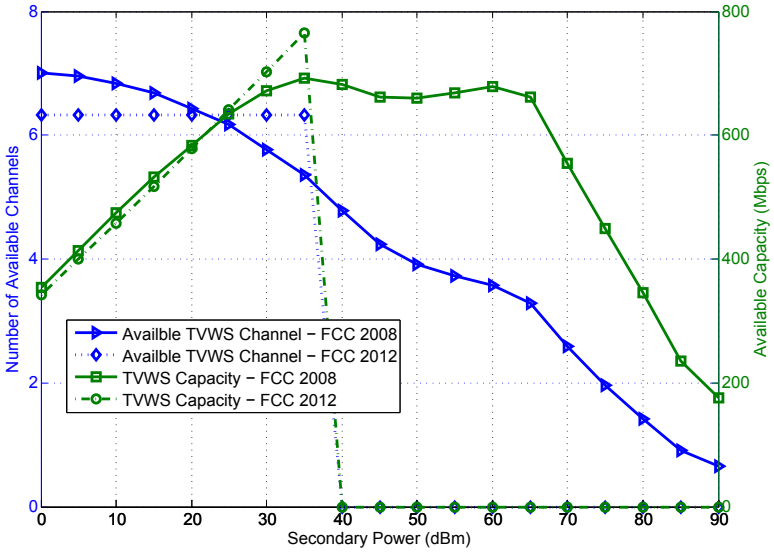

Figure 3.12: Average number of available TV white space channels and capacity for Seattle market in state of Washington. Capacity is calculated for a point to point link of fixed TVBDs, with 500 m distance. FCC2012/FCC2008 represents current/former FCC regulations. Antenna height is fixed to 20.0 meters.

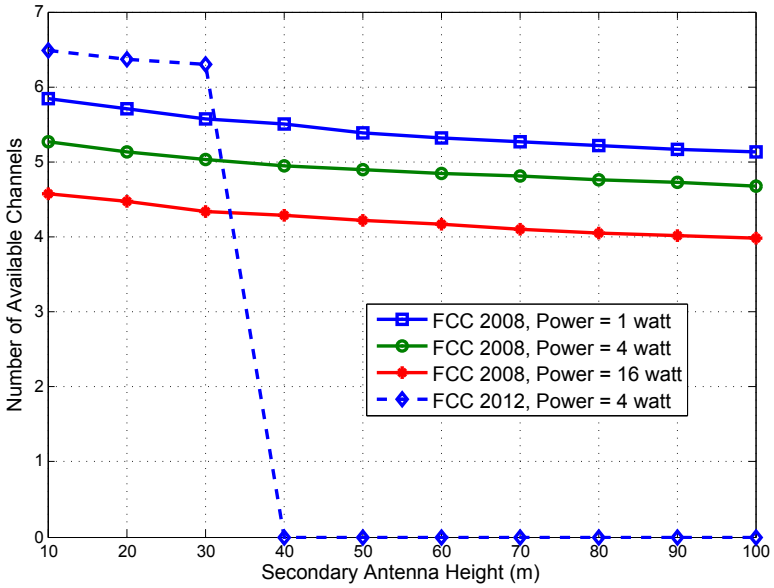

Figure 3.13: Average number of available TV white space channels for Seattle market in state of Washington. FCC2012/FCC2008 represents current/former FCC regulations.

◇ Primary to secondary interference increases, lower capacity.

The overall effect of increasing antenna height depends on transmitter power, link distance and other fundamental parameters in (3.5). But the trade-off is obvious that increasing height will not continuously enhance capacity and there should be a cutting point. This optimization rises from the counter effects of higher received power at the receiver against less channel availability and more interference. Fig. 3.13 shows dependency of average number of channels on TVBD antenna height for various transmission powers. Increasing antenna height monotonically reduces channel accessibility due to extended protection regions for TV transmitters.

Fig. 3.14 displays secondary network capacity as a function of TVBD antenna height for Seattle market. For lower power scenarios (EIRP$\leq$4W), increasing height will improve capacity even up to 100 meters. For higher power levels, there is an optimum height after which the reduced number of channels becomes dominant and capacity drops. In practice, secondary to secondary interference will also vary as antenna height changes, which depends on the frequency reuse distance. This is not considered here to avoid over complications.

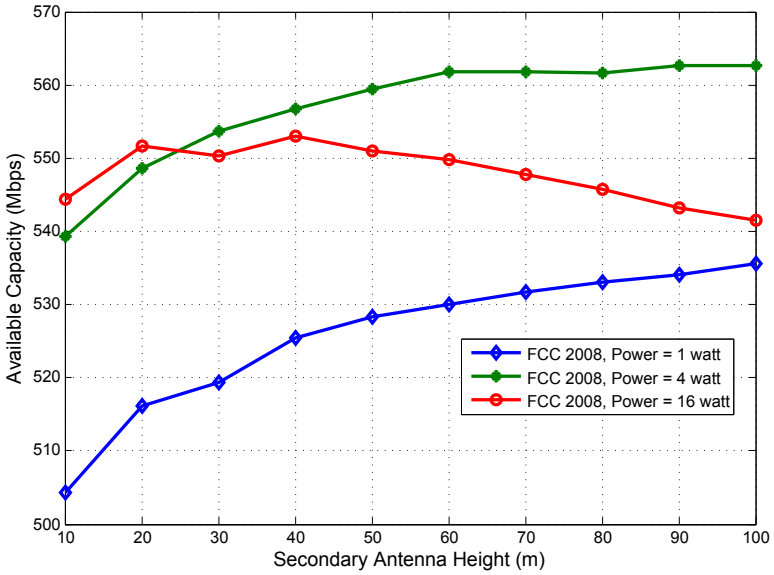

Figure 3.14: Average capacity of TV white space channels for Seattle market in state of Washington. Capacity is calculated for a point to point link of fixed TVBDs, with 500 m distance.

3.7.3 Link capacity vs. Terrain Irregularity

The characteristics of propagation environment is modeled through ΔH parameter in ITM model. It ranges from $\Delta H = 0$ for extremely flat to $\Delta H = 500$ for rugged mountainous-type area. In practice, ΔH should be calculated in every direction around TV transmitters (resulting in non-circular contour models) for computation of protection contour. The effect of this parameter on network capacity is through $p(\Gamma)$ in (3.7) which directly modifies the overall capacity (3.14). Precise evaluation of ΔH is very critical since it significantly affects ITM path loss model (and any other empirical model). Calculating the exact value of ΔH is very challenging mainly because available terrain information is sparse, for example Globe [48] provides terrain height for every 30 arc-seconds (or approximately every 1 *km* in latitude and longitude) which may easily miss localized tall buildings or skyscrapers. Therefore, it is necessary to understand how the value of ΔH affects $p(\Gamma)$.

Fig. 3.15 plots $p(\Gamma)$ versus ΔH for channel 14 and for different values of EIRP. Increasing ΔH translates to further irregularity of the area, larger values of path loss and eventually

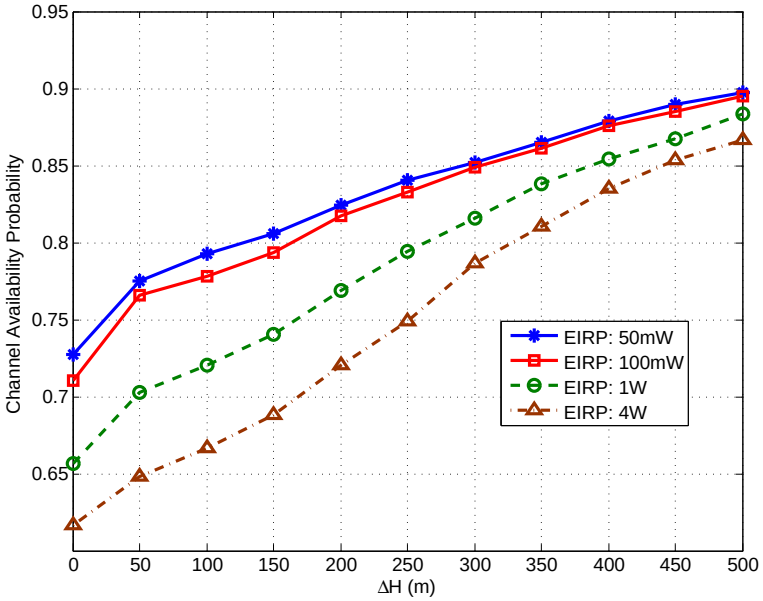

Figure 3.15: Channel 14 availability probability vs. terrain irregularity parameter ΔH. Results are averaged over the contiguous United States.

smaller protection regions. This will leave wider areas for unlicensed operation by TVBDs and therefore $p(\Gamma)$ increases. FCC has overlooked the use of this variable in calculating protection regions in [18–20,50]. This figure shows how significantly the value of $p(\Gamma)$ varies (from 60% to 90%) depending on the value of ΔH.

3.7.4 Cell Size

The throughput of each user in the secondary cellular network depends on the available capacity in that cell as well as the number of users U_R requesting service in the cell. By assuming a MAC layer with efficiency of η_{MAC}, capacity per user can be formulated as

$$C_{User} = \frac{\eta_{MAC}\overline{C_{cell}}}{U_R} \tag{3.16}$$

The number of service requests in a cell depends on population density and cell size, $U_R \propto \rho_{Pop} A_{cell}$. Thus $U_R = \alpha \rho_{Pop} \pi r_{cell}^2$ where α is proportionality constant. Therefore, capacity

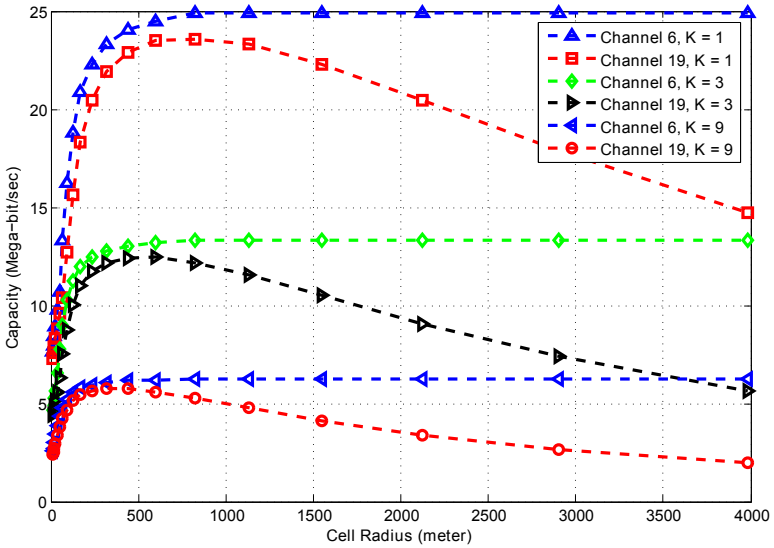

Figure 3.16: Cell capacity versus cell radius for static (non-mobile) user, for various values of K and channel number

per user can be rewritten as

$$C_{User} = \frac{\eta_{MAC}}{\alpha \rho_{Pop}} \frac{\overline{C_{cell}}}{\pi r_{cell}^2} \tag{3.17}$$

where the first factor is a constant and does not depend on network planning parameters. The second factor however is the normalized total capacity per area (bit/sec/m^2) and must be optimized to achieve the best throughput per user. The capacity per area (CPA) depends on the various parameters that we studied before as well as cell size. In the following, we will explore the behavior of CPA versus r_{cell} for which we employ (3.14) and evaluate it for various values of r_{cell}.

Fig. 3.16 shows capacity of a cell on different channels (channel 6 and 19) as a function of cell radius. The trade-off between the cell size and total capacity on each channel is clear for different frequency reuse patterns, $K = 1, 3, 9$ which is due to counter effect of higher received power and higher inter-cell interference. These results are averaged over different distances within the cell. The capacity per user, however, shows a different behavior versus cell size as shows in Fig. 3.17. Here, the capacity per area is presented which is proportional

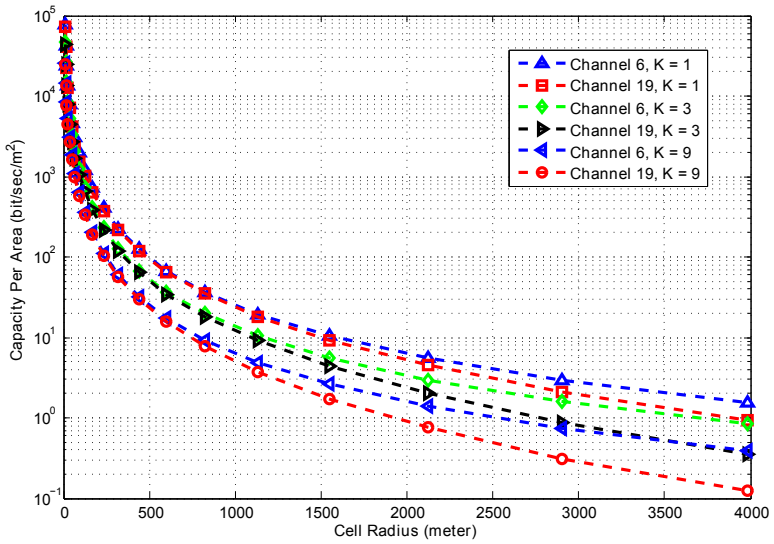

Figure 3.17: Average area capacity versus cell radius for static (non-mobile) user, for various values of K and channel number

to capacity per user as in (3.17). The results predict a uniform increase in capacity per user as cell radius decreases which is because the number of users in the cell decreases proportional to $\frac{1}{r_{cell}^2}$. This is an interesting effect because we can improve the capacity of each user by deploying more and more base stations with reduced coverage range. This conclusion however is valid only for stationary users that are not moving from cell to cell and therefore they do not incur additional overhead of being handed off from one cell to another.

For a mobile user that is moving from one cell to another cell, if the cell size is very small then the user has to be handed off very often. The hand-over process usually takes a certain delay overhead τ_{HO}, during which user data is not transmitted to base stations. Let's assume user is moving in a straight line with speed V m/s. During a duration of t, the number of times that the user must be handed off is proportional to $\frac{Vt}{r_{cell}}$. Therefore, the effective capacity that is experience by the mobile user is

$$C_{Mobile} = (1 - \frac{\beta \tau_{HO} V}{r_{cell}}) C_{User} \tag{3.18}$$

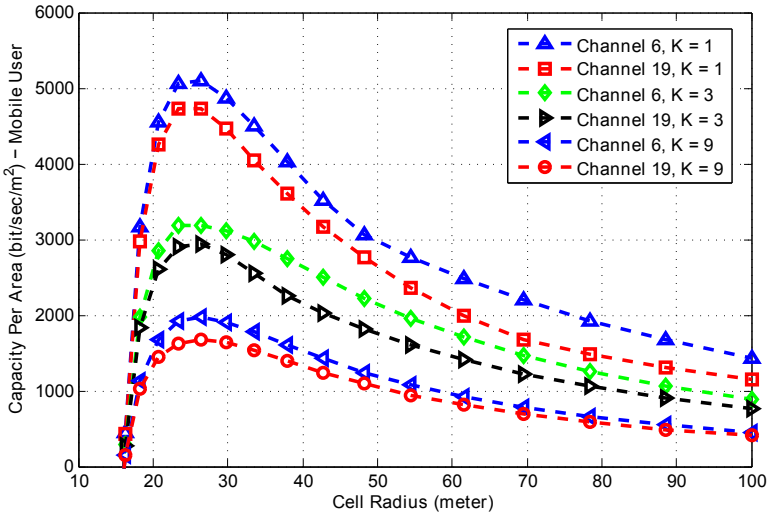

Figure 3.18: Average area capacity versus cell radius for mobile user with speed of 50 Km/h, for various values of K

with β being a proportionality constant. Fig. 3.18 shows the result for a mobile user of speed V=50 km/h and hand-over delay $\tau_{HO} = 1s$. As this figure suggests, the cell size cannot be less than 25 meters because the effective capacity drops fast.

3.8 Conclusion

In this chapter, we introduced a framework for analysis of secondary networks operating in the TV white space spectrum. There are two important factors which determine the overall performance of any secondary device in this band, *number of available channels* and *capacity of each available channel*. Both factors are spatially variable because of the irregular structure of the primary network (TV transmitters and other certified devices in TV band).

The number of available channels is defined through FCC regulations (which describes how primary services must be protected) and TVBD system parameters such as *power, antenna height, device type*. We studied white space availability for both fixed and portable devices over the contiguous United States by considering all FCC rules. Our simulation results revealed that there is a significant difference in total number of available channels

between rural (avg. of 25.84) and urban (avg. of 13.35) areas and the average number of available channels monotonically decreases as population density increases. Even in urban areas, there are significant variations between different markets; while no white space is available in Los Angeles, there are 17.18 channels available in Seattle.

The white space availability of a TV channel at any location is expected to be based on presence of active TV transmitters. However, our results showed that an average of $10 \sim 11$ channels are left unused[12] (neither by TV transmitters nor by TVBD) and this average number does not change significantly with population density. This is because current FCC rules are over protective, mainly due to poor design of TV receivers which cannot coexist with adjacent channel transmitters and a number of reserved channels for devices that may not necessarily use the channel at a given time/location. In addition, channels 3 and 4 are not opened for white space operation and therefore contribute to total unused channels.

We introduced a detailed model for secondary network capacity that includes the key parameters in both primary and secondary networks. The model includes two sources of interference for the secondary network, *primary transmitters* and *other secondary devices*. The information from current FCC database for TV broadcasters together with real terrain data and Longley Rice model were utilized to estimate co/adjacent channel noise floor at different channels (a standard transmission mask for TV broadcasters was considered that extends beyond the 6-MHz channel up to two adjacent channels). The results show that primary to secondary interference can be as large -30 dBm in certain locations. This is particularly important for network operators that are interested in using TV band as an off-loading mechanism for their services; high base stations can receive significant interference from TV broadcasters.

The proposed secondary network was arranged in a cellular layout inside the allowed regions for sharing WS channels between TVBDs. The cross interference between secondary devices were defined in the context of this cellular layout. We used this model to evaluate various trade-offs that exists between available capacity versus power, antenna height, cell size and path loss parameters to illustrate possible optimizations in future TVWS network

[12]This number includes the two channels that are reserved for wireless microphones as well as other non-TV services.

designs. We also explored the available capacity per user for both stationary and mobile user. The results showed a trade-off between average area capacity and cell radius for the case of mobile user.

APPENDIX

3.A Protection Radius Calculation

3.A.1 Protected Contour r_{PC}

For a given TV transmitter, protection contour r_{PC} is found by finding the maximum distance where signal strength (in dBu) or equivalently signal power (in dBm) drops to minimum threshold Δ, defined in Table 3.6. The received power P_r is defined in terms of transmitted power P_t as:

$$P_r = P_t + G_t - L_{TV}(r_{PC}) + G_r = \Delta \tag{3.19}$$

where G_t (G_r) is transmitter (receiver) antenna gain and $L_{TV}(.)$ is the path loss model for TV signals as a function of distance to transmitter. The range of protection contour highly depends on this path loss model:

$$r_{PC} = L_{TV}^{-1}(P_t + G_t + G_r - \Delta) \tag{3.20}$$

Note that protection contour is only a feature of TV transmitter and does not depend on secondary user parameters.

3.A.2 Protection Region r_p

Protection region is defined for every application of secondary users. For example for fixed TVBD, power limit is higher and it forces secondary users to be further away from TV transmitter than portable devices with much lower power limits. Let's assume γ is the desired interference ratio $\gamma = \frac{\text{Desired Signal Power}}{\text{Undesired Signal Power}}$, P_{sec} is the power of secondary user, and G_{sec} is the antenna gain of secondary transmitter. The minimum separation distance d_{MS} as shown in Fig. 3.2 should be such that resulting γ is at least equal to threshold γ_0

Table 3.5: Desired to undesired signal ratio defined by FCC for maximum tolerable interference in various TV applications

Type of Station	Protection ratios	
	Channel Separation	D/U ratio (dB)
Analog TV, Class A, LPTV, translator and booster	Co-channel	34
	Upper adjacent	-17
	Lower adjacent	-14
Digital TV and Class A	Co-channel	23
	Upper adjacent	-26
	Lower adjacent	-28

given by Table 3.5 for various TV channels and services.

$$P_{sec} + G_{sec} - L_{sec}(d_{MS}) + G_r \leq \Delta - \gamma_0 \tag{3.21}$$

where $L_{sec}(.)$ is the path loss model for secondary transmitter. Using this, r_p is found to be:

$$r_p = r_{PC} + L_{sec}^{-1}(P_{sec} + G_{sec} + G_r - \Delta + \gamma_0) \tag{3.22}$$

This equation shows how P_{sec} plays an important role in calculation of channel availability.

3.B ITM Path-Loss Model

The ITM path loss model in area mode is defined in terms of a reference attenuation A_{ref}. This is the *median* attenuation relative to a free space signal that should be observed on the set of all similar paths during times when the atmospheric conditions correspond to a standard, well-mixed, atmosphere. The reference attenuation is determined by three

Table 3.6: TV Station Protected Contours; Note that threshold values are in dBu and represents field strength rather than power

Type of Station	Protection contour		
	Channel	Contour (dBu)	Propagation curve
Analog: Class A, LPTV, translator and booster	Low VHF (2-6)	47	F(50,50)
	High VHF (7-13)	56	F(50,50)
	UHF (14-51)	64	F(50,50)
Digital: Full service TV, Class A TV, LPTV, translator and booster	Low VHF (2-6)	28	F(50,90)
	High VHF (7-13)	36	F(50,90)
	UHF (14-51)	41	F(50,90)

Table 3.7: Modified Field Strengths Defining the Area Subject to Calculation for Analog Stations

Channels	Defining Field Strengths, dBu, to be predicted using F(50, 50)
2 - 6	47
7 - 13	56
14 - 69	$64 - 20\log_{10}\left(\frac{615}{\text{channel mid frequency in MHz}}\right)$

piecewise equations as a function of distance:

$$A_{ref} = \begin{cases} \max[0, A_{el} + K_1 d + K_2 \ln(d/d_{Ls})], & d \leq d_{Ls} \\ A_{ed} + m_d d, & d_{Ls} \leq d \leq d_x \\ A_{es} + m_s d, & d_x \leq d \end{cases} \tag{3.23}$$

where the coefficients A_{el}, K_1, K_2, A_{ed}, m_d, A_{es}, m_s, and the distances d_{Ls} and d_x are calculated using ITM algorithms. The three intervals defined here are called line-of-sight, diffraction, and scatter regions. Dependency of path loss on frequency is not apparent in (3.23) but all the parameters are function of frequency[13]. The total path loss is the sum of A_{ref} and free space path loss which also depends on frequency:

$$L(d) = A_{ref} + 20 \log_{10} \left(\frac{4\pi df}{C} \right) \tag{3.24}$$

where C is the speed of light in vacuum. The irregularity parameter for an average terrain is $\Delta H = 90$; Using this, the reference attenuation for lowest/highest available frequency in TV band (channel 2 = 57 MHz, channel 51 = 695 MHz) are found as:

Channel 2:

$$A_{ref} = \begin{cases} \max[0, -7.1 + d \times 4.03e-4], & d \leq 94.1 \text{ km} \\ 5.87 + d \times 2.65e-4, & 94.1\text{km} \leq d \leq 159 \text{ km} \\ 38.58 + d \times 5.95e-5, & 159 \text{ km} \leq d \end{cases}$$

Channel 51:

$$A_{ref} = \begin{cases} \max[0, -17.94 + d \times 5.08e-4], & d \leq 94 \text{ km} \\ -17.2 + d \times 5.0e-4, & 94\text{km} \leq d \leq 136 \text{ km} \\ 42 + d \times 6.56e-5, & 136 \text{ km} \leq d \end{cases}$$

According to analysis in sec. 3.2 to sec. 3.5, determination of free channels as well as capacity calculations in TVWS highly depends on path loss model behavior. The more

[13]This dependency is not straightforward. They also depend on terrain irregularity parameter, Tx/Rx height, radio climate, polarization, etc.

precise the model the less spectrum resources are wasted and better protection is provided to TV receivers. In order to achieve some intuition about how coefficients in ITM model, (3.23)-(3.24), depend on fundamental parameters such as *frequency*, *antenna height* and *irregularity parameter*, a simplified version of ITM model that is more specific to TVWS system parameters is presented here. The original detailed ITM model can be found in [41].

$$A_{ref} = \begin{cases} \max[0, A_{el} + K_1 d + K_2 \ln(d/d_{Ls})], & d \le d_{Ls} \\ A_{ed} + m_d d, & d_{Ls} \le d \le d_x \\ A_{es} + m_s d, & d_x \le d \end{cases} \tag{3.25}$$

where line-of-sight distance d_{Ls} is defined as:

$$d_{Ls} = d_{Ls1} + d_{Ls2} = \sqrt{\frac{2h_{g,TX}}{\gamma_e}} + \sqrt{\frac{2h_{g,RX}}{\gamma_e}}$$

where $h_{g,TX}/h_{g,RX}$ are transmitter/receiver structural height and γ_e is the Earth's curvature constant. The diffraction range parameters are defined as:

$$m_d = \frac{A_{\text{diff}}(d_L + 4.3161X_{ae}) - A_{\text{diff}}(d_L + 1.3787X_{ae})}{2.7574X_{ae}}$$
$$A_{ed} = A_{\text{diff}}(d_L + 1.3787X_{ae}) - m_d * (d_L + 1.3787X_{ae})$$

with

$$d_L = \sqrt{\frac{2h_{g,TX}}{\gamma_e}} e^{-0.07\sqrt{\Delta h/h_{g,TX}}} + \sqrt{\frac{2h_{g,RX}}{\gamma_e}} e^{-0.07\sqrt{\Delta h/h_{g,RX}}}$$
$$X_{ae} = \left(\frac{2\pi}{\lambda}\gamma_e^2\right)^{-1/3}$$

illustrates dependency on antenna heights and terrain irregularity ΔH. The diffraction function $A_{\text{diff}}(s)$ is a complex function in terms of Fresnel integral [41]. The line-of-sight

coefficients in (3.25) are simplified to $K_2 = 0$,

$$K_1 = \begin{cases} \frac{A_{ed}+m_d d_{Ls}-A_{\text{los}}(d_0)}{d_{Ls}-d_0} & , A_{ed} > 0 \\ \frac{A_{ed}+m_d d_{Ls}-A_{\text{los}}(d_1)}{d_{Ls}-d_1} & , A_{ed} < 0 \end{cases} \tag{3.26}$$

where

$$d_0 = \min(\frac{d_L}{2}, 1.908 k h_{g,RX} h_{g,TX})$$
$$d_1 = \max(A_{ed}/m_d, d_L/4)$$

A_{los} is also defined in [41] in terms of the 'extended diffraction attenuation', A_d and the 'two-ray attenuation', A_t:

$$A_{\text{los}} = (1-\omega)A_d + \omega A_t \tag{3.27}$$

Chapter 4

RESOURCE ALLOCATION TECHNIQUES FOR CELLULAR NETWORKS IN TV WHITE SPACE SPECTRUM

TV white space (TVWS) represents unused TV channels - resulting from the transition to digital over-the-air broadcasting - made available by FCC for unlicensed secondary users. This presents opportunities for new wireless networks and services, for example as a complement to licensed 4G cellular networks as a mechanism for data offloading, in analogy with the use of 802.11 WLAN hotspot networks for current 3G networks. However, certain design challenges must be addressed - TVWS spectrum is characterized by significant (spatial) variability in number and quality (measured by Signal to interference and noise ratio) of available channels. Therefore, channel allocation - that seeks to optimize some overall network performance metric - must be adapted to this variation while complying with FCC regulations. In this chapter, we explore the problem of resource allocation in TVWS spectrum by developing models for channel availability based on co-channel interferences among secondary users as well as primary-to-secondary interference. We define two formulations: a) based on maximizing number of allocated channels, and b) based on total network throughput. Techniques for solving these two formulations are explored and the results are compared through numerical evaluations.

4.1 Introduction

Cognitive radio (CR) systems allow dynamic access of secondary users (SU) to the licensed spectrum that is temporarily not used or underutilized by licensed (primary) users (PU). With the increasing usage of internet services by mobile users and the lack of sufficient spectrum, CR systems are becoming a popular solution for spectrum scarcity. For example the Federal Communication Commission (FCC) has opened unlicensed usage of TV band spectrum subject to specific regulations that prohibits harmful interference to TV broadcast services and other licensed users [18, 19, 22]. This possibility in TV band is mainly because

of the switch-over from analog to digital TV transmission that was obligated by FCC for full power TV broadcasters in the United States. These opportunities have pushed the wireless industry to standardize CR operation in IEEE 802.22 [51], 802.11af [52], etc. It is also expected that additional spectrum will be released for unlicensed use in the near future as result of the US National Broadband Plan [23].

A typical scenario for unlicensed operation requires SU to first detect the presence of unoccupied channels via spectrum sensing or by contacting a database administrator (DBA) to receive a list of available channels[1]. Every DBA models the protection region (or the so-called service contour) for each primary user based on FCC's protection rules and determines the list of available channels at each location/time. This framework for determining channel availability has two major effects. First, the computational burden of channel detection and incumbent protection is removed from secondary devices. Second, the DBA serves as an aggregation point for information about location and other technical specification of secondary devices, which can be utilized for possible centralized management solution (channel/power assignment) to secondary devices. This feature of TVWS networks (and possibly future WS spectrum) is unlike regular CR-based networks where devices are usually connected in adhoc mode without a centralized network controller/planner. This limitation eliminates the possibility of managing inter-network interferences that arise when independent networks utilize the shared spectrum, similar to the current situation of Wi-Fi networks that limits performance in dense urban areas [53]. Issues surrounding secondary network planning in TVWS is not well studied in the literature. Current FCC regulation for TVWS band are fully focused on protecting primary services [19] and does *not* consider interference management among TV based devices. This will eventually result in high interference floor for secondary devices and network throughput will degrade.

In this work, we focus on cellular secondary network design that operate on TVWS spectrum; however, the model and techniques apply to any WS scenario. Our model first and foremost accounts for FCC's protection contours of the primary sources. Second, the quality of each available WS channel is also location dependent, due to varying interference

[1]FCC has adopted a centralized approach to secondary TVWS use by authorizing a group of DBAs to provide spectrum availability information.

levels from primary transmitters. Third, transmit power allowed on secondary TV band devices is also location dependent because of FCC's adjacent channel rules. Therefore, traditional techniques for resource allocation in cellular networks cannot be utilized and new approaches are needed.

The rest of the chapter is organized as follows. Section 4.2 introduces secondary network architecture while coexisting with primary users. Section 4.3 reviews previous related work in this area. Channel allocation problem in secondary cellular networks is defined in section 4.4 and various solutions are discussed in section 4.5. Numerical results are provided in 4.6 and finally section 4.7 concludes the chapter.

4.2 Secondary Network Architecture

Cellular communication systems are based on the notion of frequency reuse which allows a channel to be spatially re-used by different users, as long as the co-channel interference is within acceptable bounds. However, for TVWS applications, the cellular layout of the secondary cells is further restricted by the primary protection regions, as shown in Fig. 4.1. This figure presents TV towers as an irregular primary network, where each primary cell corresponds to the coverage area (or service contour [19]) of the associated tower. r_i denotes the maximum distance at which the received TV signal is above the detection threshold and the channel is considered busy [18] with an additional distance for protecting primary receivers on the edge of the service contour. Therefore, primary cell sizes depend on transmitter power/height, receiver sensitivity, terrain height profile and other physical layer parameters (details of calculation of primary user's protection area for TVWS is provided in [54]). It is clearly highlighted in this figure that service contour for TV broadcasters is often irregular and $r_i(\theta)$ significantly depends on θ. The three protection regions in this example are obtained from [4]. This irregularity is mainly because of variations in terrain height along different directions (both average and variance) and the use of directional antenna by the transmitter.

Secondary networks can only be located outside of these protected contours subject to further FCC limitations imposed by need for protection of primary receivers. Secondary cells are usually much smaller in size compared to primary cells because of the lower trans-

mission power and antenna height, Fig.4.1. The location dependency of secondary cells can be observed in this figure. Suppose primary transmitters in different colors are utilizing different channels. The area outside *all* protection regions can access the same set of available channels. However, secondary cells inside primary's protection region (shown as dotted circles) are possible as long as channel separation and power limitation is met by the secondary user. Therefore, these cells will receive a reduced set of available channels and those cells that are inside the overlapping section of protected regions receive an even shorter list. In practice, the number of protected entities are so large and diverse that essentially no secondary cell is completely outside all protection regions and list of channels are highly varying. As a practical example, in a highly populated urban area such as downtown Los Angeles there are zero channels available while 40 miles away from down town 14 channels are available for secondary operation as shown in Fig. 4.2.

Furthermore, the quality of available channels changes from cell to cell. This is because primary transmitters are very high power[2] and although secondary cells are outside protection regions they are still prone to receiving high interference from primaries especially for cells that are close to service contours. In Fig.4.1, cell A and B have the same set of available channels but significantly stronger interference affects A compared to B.

4.3 Related Works

Traditional channel allocation techniques for cellular networks [55] seek to optimize channel reuse factor while maintaining signal-to-interference plus noise (SINR) constraints for any link, by designing appropriate dynamic channel assignment algorithms [56–58]. Such channel assignment algorithms are modeled as a graph color/multi-coloring problem in which each node (base station) is colored according to the number of requests (user calls) in the associated cell. To achieve this, each node is weighted by the number of calls in the cell that includes currently ongoing calls and new requests [56]. Therefore, the objective target is to achieve the point where all cell calls are responded (assuming it is feasible). The major question of interest in this case is whether the graph is color-able or not instead of

[2]For full power digital TV transmitters, the transmitted power can be as big as 1000 kWatt.

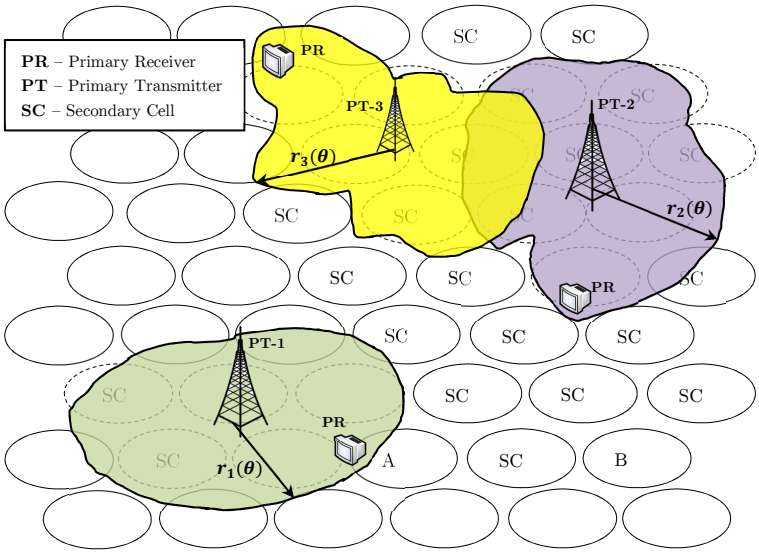

Figure 4.1: Coexistence between primary and secondary cells in cellular networks based on TV white space. Primary cells are protection contours for TV broadcasters, defined based on transmission power, receiver sensitivity and other link-budget parameters [4].

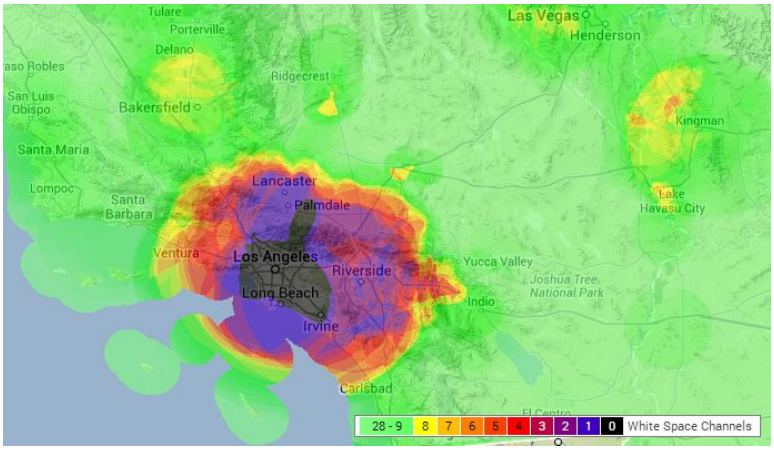

Figure 4.2: Variability of available channels in a highly populated area (Los Angeles). Color map data are obtained from [5].

optimizing the total network throughput [55, 58, 59]. Network planning in a data network is beyond just responding to current requests. It should improve quality of service to the end user by maximizing overall throughput. Therefore the objective function to be optimized

is network capacity (in its various forms and definitions) rather than the number of calls being covered.

What makes TVWS-based networks particularly interesting is the fact that the set of available channels changes from cell to cell and from device to device[3]. This is unlike regular cellular networks where there is no inherent differences among cells and potentially the same set of channels is available to every cell. In every primary-secondary paradigm, these variations in time/location/device-type complicate the channel assignment process and is not considered in the literature [59–66].

In [67], a distributed algorithm is considered for cognitive cellular networks using a game theory framework. However, major factors are overlooked in their problem formulations. Primary to secondary interference is not considered in calculating channel quality and the optimization metric is not the aggregate throughput. Only one channel is assigned to each AP which reduces the solution to a graph coloring instead of multi-coloring problem. Maximum power for each AP is decided solely based on primary limitations and not secondary-to-secondary interference and the method does not comply with FCC's vision of power selection [18,19]. The protection contour for each primary user is modeled as a single point in their LP formulation which is technically wrong because the whole area should be protected.

In [68–70] greedy and IP-based algorithms are considered for formulating spectrum allocation problem. However, the aforementioned constraints for TVWS paradigm are not considered and the objective function is limited to some utility functions (such as total revenue for spectrum broker) rather than overall network throughput.

Our contribution in this chapter is to formulate resource allocation problem in cellular networks from a data transfer perspective (rather than voice) and in a more generalized paradigm. We consider channel variation as well as different sources of interference (both secondary to secondary and primary to secondary) in the problem formulation in order to optimize overall network throughput.

---

[3]FCC defines different TVBD types (fixed versus portable) and regulations are different for each type. Hence, the set of available channels depends on the device type as well as other parameters.

4.4 Channel Allocation in Secondary Cellular Networks

An interesting question for a network planner in TV white space spectrum is *'how to assign available channels to different users?'* In regular cellular networks, repetitive patterns are used in which every channel is periodically (in space) assigned to nodes with specific distances. For example in a fully developed hexagonal structure, Fig. 4.3, channel assignment is defined by two shift parameters i, j. The resulting frequency reuse parameter $K = i^2 + ij + j^2$ determines the frequency-reuse rate of each channel across the network [46]. In contrast, the same method can be used in TVWS only for those channels that are available in every cell (which are very few). The availability of channels is significantly a function of location. Furthermore, channels are shared with primary users, here TV broadcasters, which is a different network with a variant requirement that makes network planning non-homogenous. The quality of each channel (in this context defined as *signal to noise and interference ratio*) depends on primary-to-secondary interference and is significantly channel and location dependent [54]. Therefore, any optimal channel allocation mechanism must consider these irregularities in the optimization process.

Let's define $\mathcal{C}$ as the set of all permissible white space channels [19]. Our focus is toward TV white space channels and therefore $\mathcal{C} = \{2, 3, ..., 36, 38, ..., 51\}$ with each channel representing 6 MHz bandwidth in V/UHF band (based on USA standard [45]). For every cell A_i, $\Upsilon(A_i) \subseteq \mathcal{C}$ is the set of all available channels that must be determined according to incumbents protections and FCC regulations. A minimum of one channel must be allocated to each cell (with the assumption that $\Upsilon(A_i) \neq \emptyset$, there is at least one available channel in that cell). For each available channel $c \in \Upsilon(A_i)$, we specify a quality factor $\gamma_{i,P}(c)$ as the level of interference from primary transmitter. This parameter includes co-channel and adjacent channel pollution from all licensed users in channel c.

Since more than one channel can be assigned to each cell, the overall network throughput depends on how many channels are utilized in each cell without severe mutual interference. Therefore an optimizing algorithm toward maximizing the network throughput (either average or worst-case user throughput) can be set differently according to the level of details involved. Here, we consider two problem formulations, one for maximizing the total num-

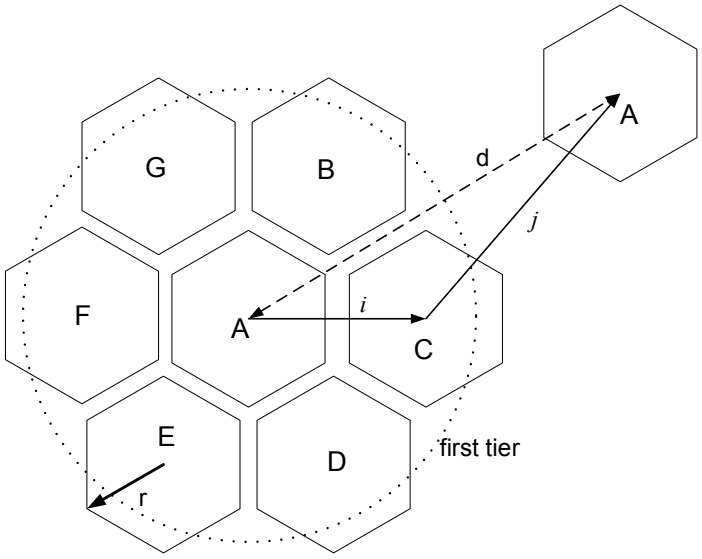

Figure 4.3: Spatial frequency reuse in a fully developed hexagonal cellular network. Cells with similar letter share the same channel. No channel sharing exists among the first tier neighbors. Shift parameters i, j defines how channel repeats in space.

ber of channels assigned to the entire network and another for maximizing total Shannon capacity of the network.

Problem definition 1: For a set of N cells $\{A_0, A_1, ..., A_{N-1}\}$, with channel set availability of $\{\Upsilon(A_0), ..., \Upsilon(A_{N-1})\}$, a channel selection function $f : \Upsilon(A_i) \rightarrow C_i \subset \Upsilon(A_i)$ is desired that assigns to each cell a subset of available channels $C_i \subset \Upsilon(A_i)$ so as to maximize f_{opt}:

$$f_{opt} = \arg\max_{f} \sum_{i=0}^{N-1} |C_i| \tag{4.1}$$

subject to:

$$\begin{aligned} & C_i \subset \Upsilon(A_i), \forall i \in [0, ..., N-1] \\ & C_i \neq \emptyset \\ & \sum_{j=0}^{N-1} \gamma_{i,j}(c) + \gamma_{i,P}(c) + \sigma_n^2 \leq \gamma_t, \forall c \in C_i \end{aligned} \tag{4.2}$$

where $\gamma_{i.j}(c)$ is the mutual interference between cell i and j on channel c, σ_n^2 is noise power and γ_t is the maximum acceptable noise and interference threshold (In terms of transmission power P and desired SNR, $\gamma_t = \frac{P}{SNR}$). The last inequality condition guarantees that channel noise floor is below a certain level and therefore an acceptable performance is achievable on the shared channels. If c_i is not shared by cell i and j then $\gamma_{i.j}(c_i) = 0$. This formulation maximizes the number of channels used by the cells but does not necessarily optimize throughput. This is because mutual interference is kept below a certain level rather than being optimized (minimized). The following more sophisticated formulation for this problem considers this issue.

Problem definition 2: For a set of N cells, $\{A_0, A_1, ..., A_{N-1}\}$, with channel set availability of $\{\Upsilon(A_0), ..., \Upsilon(A_{N-1})\}$, a channel selection function $f : \Upsilon(A_i) \rightarrow C_i \subset \Upsilon(A_i)$ is desired that assigns to each cell a subset of available channels $C_i \subset \Upsilon(A_i)$ as following:

$$f_{opt} = \arg\max_{f} \sum_{i=0}^{N-1} \sum_{c \in C_i} \log_2 (1 + SINR(c)) \tag{4.3}$$

$$SINR(c) = \frac{P}{\sum_{j=0}^{N-1} \gamma_{i,j}(c) + \gamma_{i,P}(c) + \sigma_n^2}$$

subject to:

$$C_i \subset \Upsilon(A_i), \forall i \in [0, ..., N-1]$$

$$C_i \neq \emptyset \tag{4.4}$$

Here, Shannon equation is used for the throughput of each channel utilized in each cell. Therefore, the answer to this optimization problem is optimal in the sense of overall secondary network's throughput.

4.5 Solutions to Channel Allocation Problem

Finding a solution to channel assignment is generally very challenging and it highly depends on the level of details involved. Here, problem definition 1 is focused toward maximizing the number of assigned channels that is a discrete function with continuous constraints. On

the other hand, problem definition 2 is optimizing a continuous function with continuous constraints. While both problems are discrete optimization, the latter is significantly more complicated that the former. In following sections, we explore possible solutions for both problems.

4.5.1 Suboptimal Greedy Solution for Problem 1

One sub-optimal solution for problem 1 is possible by considering this fact that in cellular systems, the strongest interferer is the first tier in a hexagonal structure as shown in Fig. 4.3. Because of this, any frequency reuse pattern avoids using the same channel in neighboring cells. Therefore, as a mechanism to ensure interference rejection, we force the solution to avoid reusing in neighboring cells (can be generalized to prevention against second and third tiers) while the total number of channels in all cells is maximized.

In order to generalize this idea for our problem, we modify the hard decision mechanism based on adjacency to a soft decision process that eliminates channels from neighbors based on comparing overall calculated interference with γ_t. Let's model the network as a graph $G = (V, E)$ where V, the set of vertices, represents the cell centers (base stations) and E, the set of edges, describes cell adjacency. Therefore, if $e = (v_1, v_2) \in E$ then v_1 and v_2 are two neighboring cells. This can be generalized to second/third-tier cells if cells are small and interference beyond the first neighbors are considerable. For every edge $v_i \in V$, the set of available channels is $\Upsilon(v_i) \subset \mathcal{C}$ as shown in Fig. 4.4. The set of assigned channels to each vertex v_i is $C(v_i)$.

Here we explore a greedy algorithm that seeks to assign non-shared channels first and then divide the remaining set of channels evenly between interfering cells. The algorithm, shown in Algorithm 1, starts with a vertex that has minimum number of assigned channels and minimum number of available channels. Every possible channel is explored on this node to find the one that results in minimum number of interfered nodes. A node v is considered interfered as the result of a channel assignment if one of the following happens:

- ◇ Total interference level in v crosses the threshold γ_t

- ◇ Assigning this channel to node v results in another currently assigned node to cross

Algorithm 1: Greedy algorithm for problem 1

Data: $G(V, E), \{\Upsilon(V)\}$ ▷ interference graph, channel availability vectors
Result: $\{C(v) : \forall v_i \in V\}$

Function `GreedyAssign()`
  while $\bigcup_{v_i \in V} \Upsilon(v_i) \neq \emptyset$ **do** ▷ some channels left unassigned
    $v_{cur} \leftarrow$ select $v \in V$ with min $|C(v)|$ and min $|\Upsilon(v)| \neq 0$ ▷ current cell
    $c_{\min} \leftarrow$ select $c \in \Upsilon(v_{cur})$ with min `InterferingNodes(`v_{cur}, c`)`
    $C(v_{cur}) \leftarrow C(v_{cur}) \cup c_{\min}$ ▷ assign selected channel to current cell
    $\Upsilon(v_{cur}) \leftarrow \Upsilon(v_{cur}) \backslash \{c_{\min}\}$ ▷ remove selected channel from set of available channels
    `UpdateChannels(`$c_{\min}, v_{cur}$`)`
  end while
  return
Function `InterferingNodes(`v_{cur}, c`)`
  $V_n \leftarrow$ set of neighbors of v_{cur}
  $V_{shrd}(c) \leftarrow \{v \in V_n : c \in \Upsilon(v)\}$
  $V_{own}(c) \leftarrow \{v \in V_n : c \in C(v)\} \cup \{v_{cur}\}$
  count $\leftarrow$ number of $v \in V_{shrd}(c)$ for which `TotalInterference(`c, v`)` $> \gamma_t$
  return count
Function `UpdateChannels(`c, v_{cur}`)`
  $V_n \leftarrow$ set of neighbors of v_{cur}; $V_{shrd}(c) \leftarrow \{v \in V_n : c \in \Upsilon(v)\}$; $V_{own}(c) \leftarrow \{v \in V_n : c \in C(v)\}$
  forall the $v \in V_{shrd}(c)$ **do** ▷ Check every nodes that has c available
    $V_{own}(c) \leftarrow V_{own}(c) \cup \{v\}$ ▷ Temporarily assign channel c to node v
    if `TotalInterference(`$c, V_{own}(c)$`)` $> \gamma_t$ **then** ▷ If any channel crosses threshold
      $\Upsilon(v) \leftarrow \Upsilon(v) \backslash \{c\}$
    end if
    $V_{own}(c) \leftarrow V_{own}(c) \backslash \{v\}$ ▷ Remove temporarily channel assignment
  end forall
  return

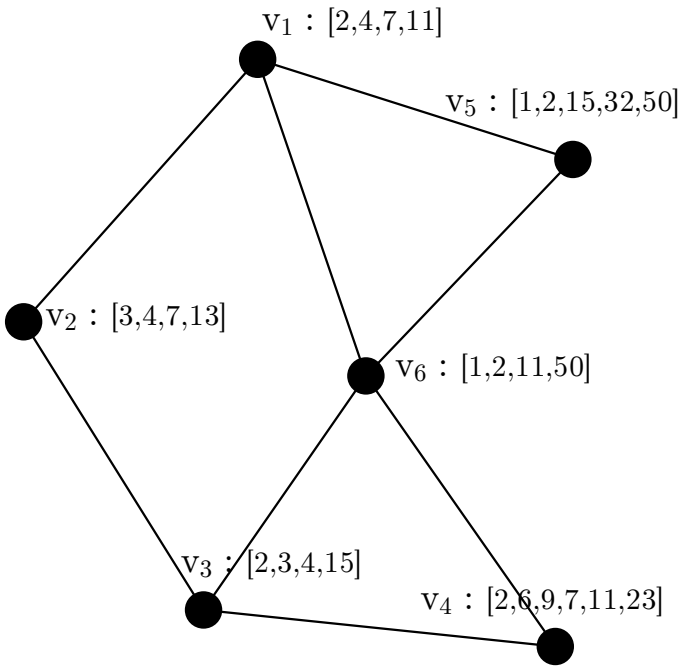

Figure 4.4: Graph based model for cellular networks in TVWS spectrum. Cells are represented by vertices, along with their corresponding set of channels and interfering cells are connected by edges.

the threshold

The channel $c_{\min}$ that causes minimum number of interfered nodes is assigned to current vertex and is removed from the set of available channels. The list of available channels for all neighboring nodes is updated after this assignment according to two condition above. This process is repeated until there is no available channel in all the vertices.

Greedy algorithm guarantees every assigned channel $c \in C_i$ has a total interference level less than threshold γ_t. However, it does not guarantee the condition of $C_i \neq \emptyset$ is met. The algorithm reaches most vulnerable nodes first to minimize the probability of having $C_i = \emptyset$ but the final results depend on the distribution of the available channels among nodes and the value of γ_t. There are very rare cases for large values of γ_t that there is a solution which meets the constraints but this algorithm barely misses that. However, all these cases are

for large and non-optimal values of γ_t as we will see in the numerical section results. For a wide range of γ_t that includes the optimal point, this algorithm also satisfies this criteria.

4.5.2 Integer Programming formulation for problem 1

In this section we formulate the channel assignment problem as an integer linear program (ILP). The reason for this translation is the availability of standard tools and libraries for solving ILP. Classic channel assignment problems are usually modeled as a graph multi-coloring (GMC) problem [71]. However, there are major differences between our resource allocation problem and GMC. In a typical GMC setup, the objective function is to minimize the number of required channels (colors) to cover a specific interference graph such that each node receives the minimum required channels. Therefore, there is a homogeneity in GMC that does not exist in our problem. Here, the set of channels that are available at each node is forced by the scenario and changes from node to node. There is a quality factor assigned to each channel that originates from primary to secondary interference and the objective function is to maximize the total number of assigned channels in the network.

For each node $v_i \in V$ $(i = 0, ..., N-1)$ let $\mathcal{A}_i^{|\mathcal{C}|\times 1}$ be a binary vector of length $|\mathcal{C}|$ (total number of channels) that defines availability/unavailability of each channel at node v_i. Also, let $\mathcal{L}_i^{|\mathcal{C}|\times 1}$ be the binary vector that shows what channels are currently assigned to node v_i. We define $\mathcal{A}$ and $\mathcal{L}$ as the concatenation of all $\mathcal{A}_i$ and $\mathcal{L}_i$ vectors, respectively:

$$\mathcal{A} = \begin{bmatrix} \mathcal{A}_0 \\ \mathcal{A}_1 \\ ... \\ \mathcal{A}_{N-1} \end{bmatrix}, \mathcal{L} = \begin{bmatrix} \mathcal{L}_0 \\ \mathcal{L}_1 \\ ... \\ \mathcal{L}_{N-1} \end{bmatrix} \tag{4.5}$$

The optimization problem is to find the optimum $\mathcal{L}$ that has maximum weight and yet satisfies the constraints. All the constraints in problem 1 are now defined in terms of $\mathcal{L}$ and $\mathcal{A}$. The availability constraint is specified as $\mathcal{L}^T.\mathcal{A}^c = 0$ where $(.)^T$ is matrix transpose operation and $\mathcal{A}^c$ is binary complement of $\mathcal{A}$. The minimum number of assigned channels

to each node (that must be non-zero $C_i \neq \emptyset$) is defined in terms of $\mathcal{L}$ as:

$$\sum_{j=0}^{|\mathcal{C}|-1} \mathcal{L}(|\mathcal{C}|i+j) > 0, \;\; i = 0, 1, ..., N-1 \tag{4.6}$$

In order to formulate mutual interference condition, let's translate the general from defined by (4.2) in our ILP problem. This constraint should be specified for every $v_i \in V$ and for every permissible channel $c_k \in \Upsilon(v_i)$. We assume the cross interference is known for every pair of (v_i, v_j) as $\gamma_{i,j}(c_k)$. For simplicity of notation, we assume $\gamma_{i,i}(c) = 0$. Thus, for every $v_i \in V$ and for every channel $c_k \in \Upsilon(v_i)$ we need an interference constraint as below:

$$\sum_{j\,=0}^{N-1} \mathcal{L}(j|\mathcal{C}|+k)\gamma_{i,j}(c_k) + \gamma_{i,P}(c_k) + \sigma_n^2 \leq [1 - \mathcal{L}(i|\mathcal{C}|+k)]\Lambda + \gamma_t \tag{4.7}$$

where $\Lambda \gg \gamma_t$ is a large constant number that is used here to make sure interference constraint is applied only when $\mathcal{L}(i|\mathcal{C}|+k) = 1$ (when channel c_k is actually assigned to v_i).

The ILP that finds the optimum solution to problem definition 1 is:

$$\max_{\mathcal{L}} \mathbf{1}^T.\mathcal{L} \tag{4.8}$$

Subject to:

$$\begin{aligned}
&\mathcal{L}^T.\mathcal{A}^c = 0 \\
&\sum_{j=0}^{|\mathcal{C}|-1} \mathcal{L}(|\mathcal{C}|i+j) > 0, \;\; i = 0, 1, ..., N-1 \\
&\sum_{j=0}^{N-1} \mathcal{L}(j|\mathcal{C}|+k)\gamma_{i,j}(c_k) + \gamma_{i,P}(c_k) + \sigma_n^2 \leq \\
&\qquad \gamma_t + [1 - \mathcal{L}(i|\mathcal{C}|+k)]\Lambda
\end{aligned} \tag{4.9}$$

The answer to this ILP, if exists, is the optimal solution for problem definition 1 in (4.2). Compared to greedy algorithm, this formulation finds the best answer that maximizes the desired metric (number of assigned channels) and satisfies all required constraints. Clearly, trade off here is significantly higher complexity than the greedy method. However, the set

of parameters here are sufficiently general that other restrictions can easily be applied to (4.9).

4.5.3 Suboptimal greedy solution for problem 2

A heuristic approach for finding a solution to problem 2 must consider maximizing the total throughput in (4.3) at every iteration. A greedy algorithm is shown in Algorithm 2. This procedure again starts with a node v that has minimum number of assigned channels $|C(v)|$ and minimum number of available channels $|\Upsilon(v)|$. This is essential for our fairness constraint of $C_i \neq \emptyset$.

The procedure for finding best available channel $c_{\max}$ for current node v is through estimating total achievable throughput (heuristically) for every available channel and choosing the one with maximum value. Estimation of total throughput is non-trivial. Our heuristic method (function BestChannel in Algorithm 2) starts by adding channel c_i (from set of available channels) to v and evaluate total throughput (considering mutual interferences). Afterwards, as long as the value of total throughput is increasing, it keeps assigning channel c_i to other nodes. This operation stops when total throughput is no longer increasing. This procedure is repeated for every channel and the maximum value of total throughput determines $c_{\max}$.

The neighbor removal process (function RemoveNeighbors in the Algorithm) is based on hypothetically assigning the channel to all eligible nodes and evaluating total throughput. If total throughput decreases as the result of such a channel assignment, the channel must be removed from set of available channels.

4.5.4 Nonlinear IP formulation for problem 2

Since the objective function in (4.3) is non-linear, regular integer programming formulation cannot be used here. Finding a solution to non-linear IP problems are generally NP-hard and therefore computationally they are not efficient. However, the result obtained from this formulation is optimal. This definition is mostly used as a benchmark against heuristic-based methods such as greedy algorithm in the previous section, to evaluate how close

those results are to the optimal answer. The non-linear IP in this case is defined as below:

$$\max_{\mathcal{L}} f_{obj}(\mathcal{L}) \tag{4.10}$$

Subject to:

$$\mathcal{L}^T.\mathcal{A}^c = 0$$
$$\sum_{j=0}^{|\mathcal{C}|-1} \mathcal{L}(|\mathcal{C}|i+j) > 0, \;\; i = 0, 1, ..., N-1$$

where the objective function $f_{obj}(\mathcal{L})$ is defined based on total throughput in (4.3). Therefore, in terms of channel assignment vector $\mathcal{L}$, it is defined as:

$$f_{obj}(\mathcal{L}) = B^{1\times N|\mathcal{C}|}.\mathcal{L}$$
$$B(i|\mathcal{C}|+k) = \log_2\left(\frac{P}{\sum_{j=0}^{N-1}\mathcal{L}(j|\mathcal{C}|+k)\gamma_{i,j}(c_k)+\gamma_{i,P}(c_k)+\sigma_n^2}+1\right)$$
$$i,k = 0, ..., N-1$$

4.6 Numerical Results

In this section, numerical results are provided for a typical network graph to compare introduced algorithms. Simulation parameters are provided in Table 4.1. There are 25 nodes in a grid topology, Fig. 4.5. All secondary users transmit with unit power. Mutual interference between nodes is determined in terms of cross distance and typical path-loss functions $\gamma_{i,j} \propto \frac{P}{d_{i,j}^2}$. There are a total of 10 available channels that are randomly available at each node (uniform distribution in range of 3 to 5 for each node). The quality of each channel, defined in terms of primary to secondary interference level is also randomized for each channel uniformly.

Each simulation scenario in the following two sections is repeated multiple times with different seeds for random generator and the results are averaged. The seed values however are fixed across different algorithm to provide a reasonable comparison. We keep a fixed seed for generating the number of available channels at each node but a variable seed is used for generating the actual channel numbers and channel quality factor. Therefore, the total

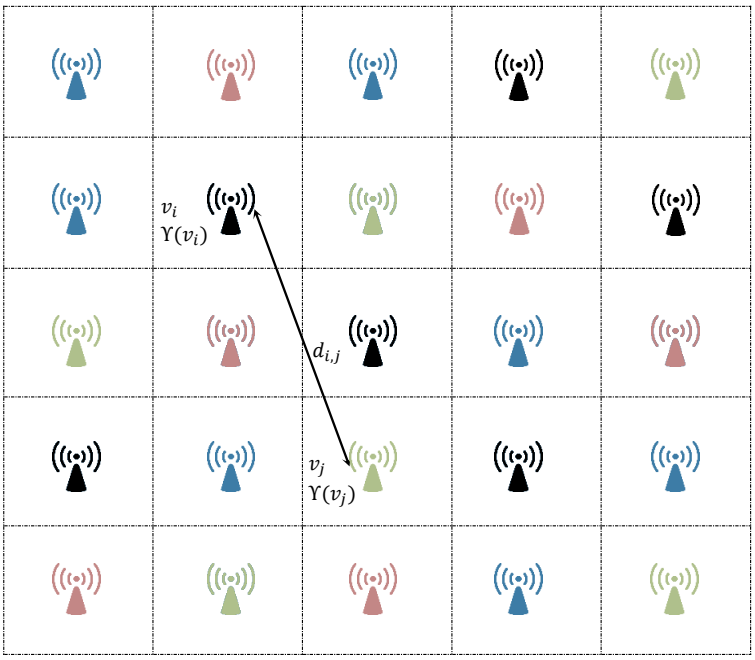

Figure 4.5: Network topology with multiple nodes in DSA scenario. Each node has a certain set of available channels $\Upsilon(v_i) \in \{1, 2, ..., 10\}$.

number of available channels are fixed in all cases but the interference pattern is different.

The two factors of interest are the total number of channels that are assigned to nodes and the total throughput of the network (bps/Hz). We normalize both metrics by the total number of available channels for easier comparison and to remove dependency of the results on this factor.

4.6.1 Comparing greedy algorithm with ILP in problem 1

An important factor in problem 1 is parameter γ_t. This defines how conservative the algorithm is in terms of accepting external interference in an assigned channel. Increasing γ_t will decrease the frequency reuse factor for the network and forces reused channels to be further away. Figure 4.6 shows the total number of assigned channels versus $SNR = \frac{P}{\gamma_t}$ for both greedy algorithm and ILP in problem 1. Decreasing SNR (increasing γ_t) will increase the total number of channels in both algorithms because higher level of interference is

accepted. The two algorithms present the same behavior and their performance is relatively close.

Figure 4.7 shows the normalized total throughput of the network in terms of bps / Hz / (Available Channel) for both methods. The total throughput is calculated by considering total interference at each node as sum of mutual interference, primary to secondary interference and noise power for every assigned channel and utilizing Shannon capacity equation. The trade-off between throughput and γ_t can be seen in this figure. For smaller values of γ_t, throughput decreases because the fewer number of channels becomes dominant. For larger values of γ_t it also decreases because excessive interference becomes dominant. While both methods present a similar behavior overall, the trade-off is more visible in ILP. This is because in ILP problem, the algorithm forces one channel per node and the target function is to maximize the total channels. This can result in multiple channels at one node while another node has only one channels assigned. On the other hand, greedy algorithm provides a more homogenous distribution of channels among nodes because always the node with minimum $|C(v)|$ is selected. Therefore, this algorithm shows less sensitivity to threshold value.

4.6.2 Comparing problem 2 with problem 1

With the lack of standard tools for solving nonlinear IP problems, our work in providing the most optimal answer through second problem definition is an ongoing effort for future works. However, in this section we can compare the results of greedy algorithm for problem 2 versus one. Problem definition 2 is based on maximizing total throughput without utilizing hard decision threshold for channel assignment. Therefore, the choice of γ_t does not affect the result. Hence, we compare this result with best results obtained from problem 1 through a search in γ_t. Table 4.2 compares the results for both definitions. In addition to greedy method in Algorithm 2 , we simulated a different greedy method that runs an integer quadratic programming (IQP) for minimizing total interference in every iteration inside method BestChannels. The results show slightly better performance than the previous heuristic based method. By comparing the results in this table, it is inferred that ILP

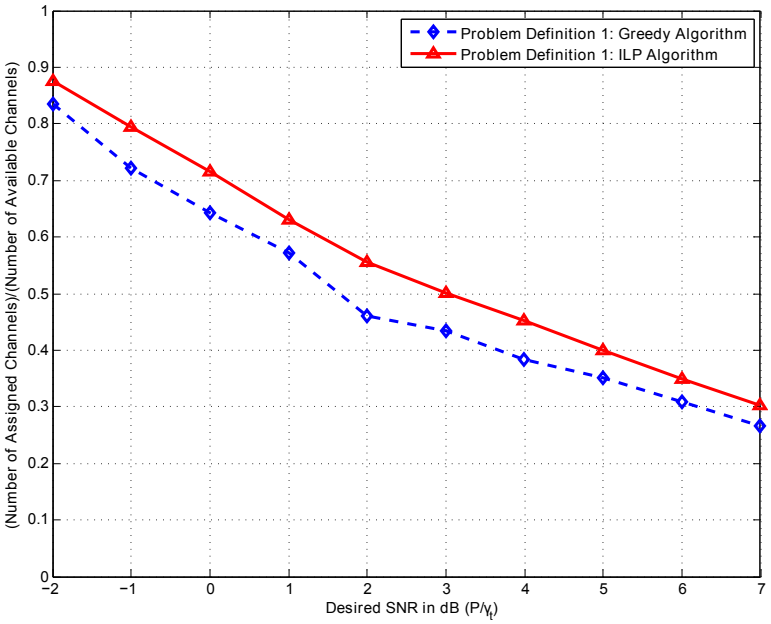

Figure 4.6: Number of assigned channels normalized to total number of available channels versus SNR $= \frac{P}{\gamma_t}$ in (4.2) for first problem formulation.

presents the best results and Greedy for problem 1 which has the worst performance is only 12% below ILP. Greedy for problem 2 is very close to ILP, only 2.8% below.

Considering both performance and computational requirements, greedy algorithm for problem 2 has the best performance. This is because of multiple reasons. First, problem formulation 2 does not depend on threshold and automatically finds the optimal point. Thus, no exhaustive search is needed. Second, greedy algorithm is significantly faster in every iteration. Third, the complexity of greedy algorithm is polynomial in number of nodes while ILP is exponential. Therefore, greedy method is better scalable. Finally, the overall result of greedy is sufficiently close to ILP.

4.7 Conclusion

In this chapter, we explored the problem of resource allocation in TVWS based networks with a focus on cellular networks. Major issues in TVWS were addressed including variability of available channels w.r.t. location as well as quality of each channel. Two problem

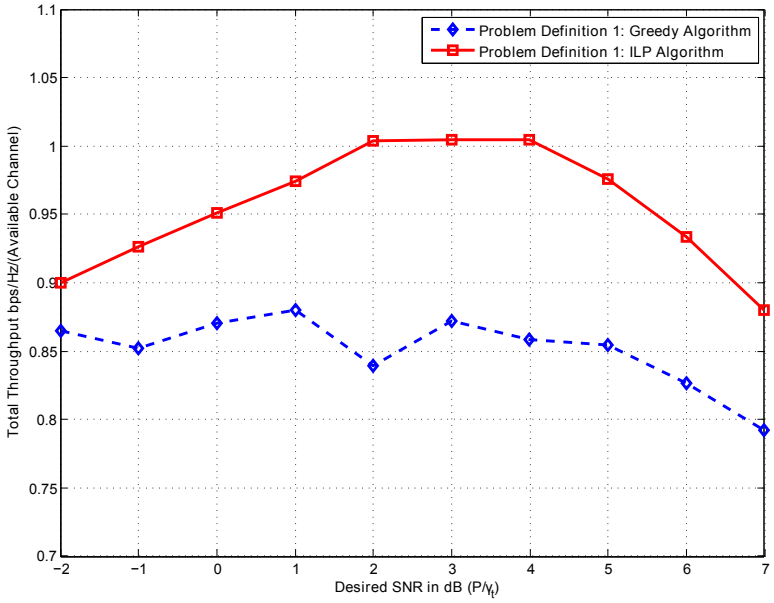

Figure 4.7: Total throughput across the network normalized by total number of available channel versus SNR $= \frac{P}{\gamma_t}$ in (4.2) for first problem formulation. Mutual interference between nodes, primary to secondary interference and noise variance is considered in calculation of throughput.

definitions were presented for allocating channels to cells with different objective functions and constraints. First problem formulation, based on maximization of total number of channels, proved to be an integer linear programming problem for which standard tools are available. Second problem formulation was based on maximization of total Shannon throughput explicitly which resulted in a non-linear IP problem. Greedy algorithms were provided for both definitions.

Numerical results showed a trade off between total throughput and γ_t for problem 1 and that careful choice of γ_t is needed to obtain optimum results. In practice, exhaustive/binary search techniques are required to find optimum γ_t. By choosing the best value of γ_t, ILP showed the best results which was slightly better than greedy solution for problem 2 with the cost of enormously higher computation.

Algorithm 2: Greedy algorithm for problem 2

Data: $G(V,E), \{\Upsilon(V)\}$ ▷ interference graph, channel availability vectors
Result: $\{C(v) : \forall v_i \in V\}$
Function `GreedyAssign()`
  while $\bigcup_{v_i \in V} \Upsilon(v_i) \neq \emptyset$ **do** ▷ some channels left unassigned
    $v_{cur} \leftarrow$ select $v \in V$ with min $|C(v)|$ and min $|\Upsilon(v)| \neq 0$ ▷ current cell
    $c_{\max} \leftarrow$ `BestChannel(`v_{cur}`)` ▷ find best channel for current cell
    $C(v_{cur}) \leftarrow C(v_{cur}) \cup c_{\max}$ ▷ assign best channel to current cell
    $\Upsilon(v_{cur}) \leftarrow \Upsilon(v_{cur}) \backslash \{c_{\max}\}$ ▷ remove selected channel from set of available channels
    `RemoveNeighbors(`$c_{\max}$`)`
  end while
Function `BestChannel(`v`)`
  Input: v: Node $v \in V$
  Output: $c_{\max}$: Best channel $c \in \Upsilon(v)$ with maximum total throughput
  $f_{\max} \leftarrow -\infty$
  forall the $c_i \in \Upsilon(v)$ **do** ▷ Test every available channel
    $D_1 \leftarrow \{v | c_i \in C(v)\} \cup \{v\}$ ▷ All channel that currently use c_i
    $D_2 \leftarrow \{v | c_i \in \Upsilon(v)\}$ ▷ All channel that can potentially use c_i
    forall the $v_j \in D_2$ **do**
      if `TotalThroughput(`c_i, $D_1 \cup v_j$`)` $>$ `TotalThroughput(`c_i, D_1`)` **then**
        $D_1 \leftarrow D_1 \cup v_j$
      end if
    end forall
    if `TotalThroughput(`c_i, D_1`)` $> f_{\max}$ **then**
      $f_{\max} \leftarrow$ `TotalThroughput(`c_i, D_1`)`; $c_{\max} \leftarrow c_i$
    end if
  end forall
  return $c_{\max}$
Function `TotalThroughput(`c, V`)`
  Input: V: Set of nodes, c: specific channel
  $f \leftarrow 0$
  forall the $v_i \in V$ **do** ▷ Assume c is assigned to all nodes in V
    $I \leftarrow \gamma_{i,P}(c) + \sum_{v_j \in V \backslash \{v_i\}} \gamma_{i,j}(c)$
    $f \leftarrow f + \log_2\left(1 + \frac{P}{I+\sigma_n^2}\right)$
  end forall
  return f
Function `RemoveNeighbors(`c`)`
  $D_1 \leftarrow \{v | c_i \in C(v)\}$; $D_2 \leftarrow \{v | c_i \in \Upsilon(v)\}$
  forall the $v_j \in D_2$ **do**
    if `TotalThroughput(`c, $D_1 \cup v_j$`)` $<$ `TotalThroughput(`c, D_1`)` **then**
      $\Upsilon(v_j) \leftarrow \Upsilon(v_j) \backslash \{c\}$
    end if
  end forall

Table 4.1: Simulation Parameters

Parameter	Value
Number of nodes $\|V\|$	25
Number of channels $\|\mathcal{C}\|$	10
Available channels $\Upsilon(v)$	$\sim U[3,5]$
Primary Interference $\gamma_{i,P}(.)$	$\sim U[0.0,0.1]$
Secondary User's Power	1.0
Mutual Interference $\gamma_{i,j}$	$\propto \frac{P}{d_{i,j}^2}$
Noise Power σ_n^2	0.01

Table 4.2: Comparing simulation results for problem 2 versus problem 1

Method	Norm. No. Assigned Channels	Norm. Throughput
Greedy Prob. 2 with IQP	0.534	0.976
Greedy Prob. 2 with Heuristic	0.546	0.973
ILP Prob. 1	0.5	1.005
Greedy Prob. 1	0.57	0.88

Chapter 5

SPECTRUM SHARING BETWEEN ROTATING RADAR AND SECONDARY WI-FI NETWORKS

Recently, the feasibility of white space based unlicensed device operation has been explored for the 3 GHz band where spectrum sharing is to be achieved with terrestrial (e.g. Air Traffic Control) and shipborne radars[1]*. Similar to every primary-secondary coexistence scenario, interference from unlicensed devices must be within acceptable bounds to avoid degradation of primary user's performance. In this chapter, we formulate the spectrum sharing problem between a pulsed, search radar (primary) and 802.11 WLAN as the secondary. We compute the protection region for a rotating terrestrial search radar for both a single secondary user (initially) as well as random spatial distribution of multiple secondary users. Furthermore, we also analyze the interference* to *the WiFi devices from the radar's transmissions to estimate the impact on achievable WLAN throughput as a function of distance to the primary.*

5.1 Introduction

The scarcity of available RF spectrum and technological limitations for usage of higher frequency bands (above 60 GHz) obligates more efficient allocation of spectrum. This has motivated spectrum regulatory bodies such as FCC (US) and Ofcom (UK) to allow use of unused 'spatio-temporal' access opportunities by unlicensed users, subject to cognitive rules of usage [19,54]. In this chapter, we focus on spectrum sharing between primary radar systems and secondary 802.11 WLAN networks - a topic on which little work exists beyond the studies in [72–81]. The re-emergence of interest in this topic is based in part on large amount of licensed spectrum allocated to radar operations - over 1700 MHz in 225 MHz to 3.7 GHz band, are set aside for radar and radio-navigation [82] in the US. Given that

[1] In the US, airport radars are allocated 2700-2900 MHz, and 3100-3650 MHz for military radar operations for national defense.

terrestrial radar locations are fixed and have predictable operational patterns, it is possible to model their behavior and utilize it for a database-driven coexistence solution, akin to the architecture espoused by the FCC for TV white spaces [83].

Database-driven spectrum sharing uses a geo-location database that determines available spectrum for a secondary user (SU) requesting access based on their location. This coexistence mechanism is currently mandated by the FCC for operation in TV band; its main impact was to remove the burden of spectrum sensing from secondary devices thereby simplifying receiver design for clients (by obviating the need for a highly sensitive design) and also avoids the challenges in distributed spectrum sensing such as the well-known hidden terminal problem, that is aggravated by channel conditions such as fading. By rules of cognitive access, overlay secondary users are prohibited from re-using a primary operating channel within an area defined as the *protection region*. The geo-location database has access to relevant information of primary users such as location, transmit power, interference tolerance, etc. that it utilizes to estimate this protection region to enable any secondary transmitter to meet the interference protection conditions.

The actual implementation of any incumbent protection rule depends strongly on the usage scenario, i.e., features of the primary and secondary systems and the consequent coexistence requirements. In this chapter, we consider a *rotating search radar* as the licensed transmitter and WiFi networks as unlicensed devices. First, we review the known design equations that represent performance characteristics of a typical search radar for the purely noise limited case in terms of the desired probability of detection P_D and false alarm P_{FA}. This determines the minimum SNR requirements at the boundary of the radar operating range and sets the baseline for comparison with any spectrum sharing regime.

In order to permit overlay transmission by secondaries, we need to define the rules for co-existence. A recent DARPA program suggests drop of 5% in P_D for fixed P_{FA} [73] at the edge of radar operating range; this defines the protection regime for the primary receiver (from secondary interference). However, the fundamental objective of any WS type spectrum sharing scenario is to *promote* secondary usage subject to the primary protection constraints; we thus analyze the effect of (high power) radar pulse sequences transmitted by rotating radar on the throughput of WiFi network. Any successful spectrum sharing

system must balance the rights of the incumbent (primary protection) with encouraging new services, and we hope that our work fundamentally highlights the inherent trade-offs in this design space.

5.1.1 Related Works

There is growing interest in radar spectrum sharing from both regulators and researchers [72–81, 84–89]. SSPARC program from DARPA [73] is a good example that seeks to support two types of sharing: a) Military/military sharing between military radars and military communication systems to increase capabilities of both and b) Military/commercial sharing between military radars and commercial communication systems to preserve radar capabilities while meeting the need for increase commercial spectrum.

In [74–76], the author studies coexistence between radar and a cellular base station. The focus of this work is to present available white/gray spectrum for secondaries as a result of radar rotation by considering variable transmission power level for secondary users and assuming a pre-known maximum tolerable interference by radar. Therefore, no discussion is made on calculation of this maximum interference level, its dependency on main radar parameters and how it can affect achievable SU throughput. The authors consider only one sharing scenario in which SU is perfectly synchronized with radar rotations which is not practical. Different secondary traffic types such as VoIP, file download and video-on-demand are inspected and the result of radar interference on each case is studied. Similarly in [72], temporal variations of radar antenna's main lobe is exploited to support more white space users when their location is not within the main lobe. In [77], spectrum sensing is combined with database approach to create a hybrid spectrum sharing technique. The authors in [80] study the potential for secondary LTE usage in 2.7-2.9 GHz radar bands for different scenarios such as home eNodeB at street levels (HeNb), HeNb at high-rise buildings, macro LTE transmitters and so on. They use a fixed INR of -10 dB for sharing without any discussion on radar performance and how it relates to this threshold. Their analysis does not consider radar rotation and mostly focused on single-user sharing with radar. In case of multiple SU, no spatial distribution is considered and a simplifying assumption is made

for all users to be in the same distance from radar.

Signal processing aspects of spectrum sharing between a MIMO radar and a wireless communication system is analyzed in [81]. Their interference mitigation approach is shown to eliminate wireless interferences from main/side lobe while maintaining target detection performance.

Technical characteristics for various types of radars that are operating in the 2700-2900 MHz as well as 5250-5850 MHz bands are introduced in [86, 87]. Protection criteria against external interference is determined through experimental measurements by injecting three types of unwanted emissions, continuous wave, CDMA-QPSK, and TDMA-QPSK. Depending on interference type, maximum tolerable interference is measured in each case. In [88], the authors evaluate interference from broadband communication transmitters such as WiMax to radars in the 2700-2900 MHz band. They use WSR-88D next-generation weather radar in their investigations and their analysis is based on field measurements. A computation model for calculating aggregate interference from radio local area networks to 5-GHz radar systems is provided in [89]. Their analysis methodology is based on using point to point path loss models between radio networks and radar as well as other link-budget parameters such as antenna gains and frequency-dependent rejection. The aggregate interference is simply calculated from summation over a set of N known transmitters. Similar studies are performed in [84] and [85].

Our novel contribution in this work is a complete characterization of Radar - WiFi coexistence as a function of all the relevant system parameters and design constraints/objectives. First, the maximum tolerable interference *from* WiFi networks *to* radar is estimated for both a a) single WiFi network and b) a (random) spatial distribution of multiple WiFi networks. Depending on how much information about radar is available to secondary (WiFi) networks, various sharing scenarios are considered, resulting in different protection distances. Second,the (time-varying) interference *from* radar *to* WiFi networks is modeled and achievable secondary throughput is estimated.

The rest of this chapter is organized as follows. In section 5.2, baseline performance for a noise limited radar is formulated. Section 5.3 considers coexistence between radar and a single SU. Multiple SU with spatial distribution is discussed in 5.4. In section 5.5,

interference from radar to SU is studied as a limiting factor to available white space capacity. Numerical results are provided in 5.6 and finally 5.7 concludes the chapter.

5.2 Search Radar: Noise Limited Operation [1]

In this section, we review operational characteristics of a typical search radar in the noise limited regime with no external source of interference. For a radar transmitting a pulse train $x(t) = \sum_n \sqrt{P_T} s(t - \frac{n}{f_R})$ with instantaneous power P_T and pulse repetition frequency of f_R, the power of reflected signal from the target at the radar receiver, assuming free space propagation is given by the well-know *Radar Equation*, i.e.,

$$P_R = \frac{P_T G^2 \lambda^2}{(4\pi)^3 d^4} \sigma \tag{5.1}$$

where G is the radar's antenna gain (relative to isotropic antenna) on both transmit and receive, λ is the wavelength and d the distance from source to the target of interest, and σ represents the target's *radar cross section*.

For a single received pulse, the signal-to-noise ratio (SNR) at the receiver input is calculated as

$$\text{SNR}_p = \frac{P_T G^2 \lambda^2}{(4\pi)^3 d^4 N_0 f_{BW}} \sigma \tag{5.2}$$

with f_{BW} representing the pulse bandwidth and N_0 being the one-sided noise spectral density.

$$N_0 = FKT_E \tag{5.3}$$

where F is the receiver noise figure and T_E is the ambient temperature. Radar detection typically operates based on processing of multiple pulses received from the target. For a *coherent* radar receiver that uses M pulses, the energy of the pulses are integrated such that the resulting SNR at the detector input is increased by a factor of M, i.e.,

$$\text{SNR}_{\text{eff}} = M \frac{P_T G^2 \lambda^2}{(4\pi)^3 d^4 N_0 f_{BW}} \sigma \tag{5.4}$$

where $M = T_I \ f_R$, product of illumination time T_I and pulse repetition frequency f_R. The

target illumination time T_I depends on radar scan rate as well as antenna pattern. Let θ_V and θ_H (in radian) denote the vertical and horizontal antenna beam width, respectively, then the antenna gain can be approximated as

$$G \approx \frac{4\pi}{\theta_H \theta_V} \rho_A \tag{5.5}$$

where ρ_A is the antenna efficiency, i.e., the radar antenna is concentrating an otherwise uniformly distributed power into an area of $\theta_V \theta_H$ with efficiency of ρ_A where the latter is typically around 0.5. If radar is scanning over an area of Ω (steradians), within a scan time of T_S, then illumination time is determined as:

$$T_I \approx T_S \frac{\theta_H \theta_V}{\Omega} \approx T_S \frac{4\pi \rho_A}{\Omega G} \tag{5.6}$$

For a radar that searches the entire azimuth/elevation plane, $\Omega = 4\pi$.

Using (5.4)-(5.6) yields

$$\text{SNR}_{\text{eff}} = \frac{T_S}{\Omega} \frac{P_T G \lambda^2 f_R}{(4\pi)^2 d^4 N_0 f_{BW} L} \sigma \tag{5.7}$$

Here, antenna efficiency ρ_A is replaced by L that represents total losses in the system, including antenna efficiency, transmission lines mismatch, perfect coherence in pulse detector, etc.

5.2.1 Minimum Required SNR

Radar detection performance is defined in terms of two probabilities, detection P_D and false alarm P_{FA}, which in turn depend on SNR at the detector input. The latter is determined by the pulse integration method that is utilized by the receiver, namely *coherent* versus *non-coherent*.

a) Single pulse, hard detection: If the received signal at the detector input is

$$e_0(t) = r(t) \cos\left(\omega_c t + \phi(t)\right) \tag{5.8}$$

then the PDF of the detected envelope for a single pulse is *Rician*, i.e.,

$$p(r) = \frac{r}{\beta^2} e^{\frac{-(r^2+A^2)}{2\beta^2}} I_0\left(\frac{rA}{\beta^2}\right) \tag{5.9}$$

where A is the amplitude of the base band pulse and $\beta = \sqrt{N_0 f_{BW}}$. Therefore, P_{FA} is determined by setting $A = 0$ and integrating over 0 to detection threshold V_T as:

$$P_{FA} = e^{\frac{-V_T^2}{2\beta^2}} \tag{5.10}$$

A similar general closed-form equation for P_D does not exist in general. However, for *high-SNR* cases, $p(r)$ is well approximated as Gaussian, for which case P_D is given by [1]

$$P_D = \frac{1}{2}\left[1 - erf\left(\frac{V_T}{\beta\sqrt{2}} - \sqrt{\text{SNR}_p}\right)\right] \tag{5.11}$$

The relationship between P_D, P_{FA} and SNR is fairly accurately expressed via the following empirical equation [1]:

$$\text{SNR}_p = \ln\left(\frac{0.62}{P_{FA}}\right) + 0.12\ln\left(\frac{0.62}{P_{FA}}\right)\ln\left(\frac{P_D}{1-P_D}\right) + 1.7\ln\left(\frac{P_D}{1-P_D}\right) \tag{5.12}$$

b) Coherent Integrator: For a coherent receiver integrating M pulses, the SNR-performance relationship is described in (5.12) in which SNR_p should be replaced with the effective SNR at the detector input (SNR_{eff}), determined by (5.7).

c) Noncoherent Integrator: If radar utilizes a linear (rather than square-law) detector for single pulse and then combines M pulses non-coherently, the required SNR per pulse for desired P_D, P_{FA} is [90]:

$$\begin{aligned} \text{SNR}_{p,dB} &= -5\log_{10}(M) + \left[6.2 + \frac{4.54}{\sqrt{M+0.44}}\right]\log_{10}(A + 0.12AB + 1.7B) \\ A &= \ln\frac{0.62}{P_{FA}}, B = \ln\frac{P_D}{1-P_D} \end{aligned} \tag{5.13}$$

Overall, the baseline performance of a noise-limited radar can be evaluated in two ways:

- ◇ Assuming that maximum operational range of the radar is known, calculate SNR from (5.2) or (5.7) for the maximum distance d. Then, using either (5.12) or (5.13), we can trade-off between P_D and P_{FA}.

- ◇ Assuming that target P_D and P_{FA} is specified, estimate required SNR from (5.12) or (5.13) and then determine maximum range from (5.2) or (5.7).

For our calculations in the following sections, we consider a detector with coherent integration, using effective SNR in (5.7) with (5.12).

5.3 Interference Limited Radar - Single Secondary

In this section, we consider spectrum sharing with a single Wi-Fi user as the secondary device by treating secondary signals as an external interference to radar receiver. Wi-Fi transmissions use OFDM signals, whereby each OFDM symbol is a linear combination of many randomly modulated sub-carriers. Hence, using central limit theorem, it is a reasonable assumption to consider the resulting waveform as a Gaussian random process that is independent of the (thermal) noise at the radar receiver [91]. Therefore, the power of interference can be directly added to AWGN noise, effectively raising noise floor, in calculation of Signal-to-Interference plus Noise ratio (SINR) at radar receiver input. Thus using (5.7), the total SINR at the receiver input is

$$\text{SINR} = \frac{T_S}{\Omega} \frac{P_T G \lambda^2 f_R}{(4\pi)^2 d^4 L \left(N_0 f_{BW} + I\right)} \sigma \tag{5.14}$$

where I represents total interference power received from secondary user. The latter depends on various factors: the distance and frequency dependent path loss between secondary source and radar receiver, the azimuth between SU direction and radar's main antenna beam, etc. as below:

$$I_{SU \rightarrow Radar} = \frac{P_{SU} G(\alpha_H, \alpha_V)}{L_1(d_{Rd-SU}) \text{FDR}(\Delta f)} \tag{5.15}$$

where $G(\alpha_H, \alpha_V)$ defines radar's antenna gain in the direction of SU (considering azimuth and elevation), FDR(Δf) is *frequency dependent rejection* factor that depends on spectral shape of transmitted signal $P(f)$ and receiver receive input filter $H(f)$, i.e.

$$\text{FDR}(\Delta f) = \frac{\int_0^\infty P(f)df}{\int_0^\infty P(f)H(f+\Delta f)df} \tag{5.16}$$

represents the out-of-band emission from the WiFi source into the radar RF receiver front-end as a function of $\Delta f = f_t - f_r$, the difference between interferer and receiver tuned center frequency. For a special case of exact co-channel operation $\Delta f = 0$; for a perfectly flat filter response $H(f) = 1$, FDR simplifies as the ratio of WiFi to radar bandwidth:

$$\text{FDR} = \max\left(\frac{\text{WiFi BW}}{f_{BW}}, 1\right) \tag{5.17}$$

The minimum required SINR for normal operation of the radar was defined in previous section. Therefore maximum additional interference level I that can be tolerated is determined as:

$$\begin{aligned} \text{SINR}_0 &\leq \frac{T_S}{\Omega}\frac{P_T G\lambda^2 f_R \sigma}{(4\pi)^2 d^4 L\,(N_0 f_{BW} + I)} \\ I &\leq \frac{T_S}{\Omega}\frac{P_T G\lambda^2 f_R \sigma}{(4\pi)^2 d^4 L\,\text{SINR}_0} - N_0 f_{BW} = I_{\max} \end{aligned} \tag{5.18}$$

Using (5.15) and (5.18), we can calculate the minimum separation distance between radar and SU[2] as:

$$d_{Rd-SU} \geq L_{Rd-SU}^{-1}\left(\frac{P_{SU}G(\alpha_H, \alpha_V)}{\text{FDR}(\Delta f) I_{\max}}\right) \tag{5.19}$$

Where $L_{Rd-SU}(.)$ is the path-loss between radar and SU as a function distance. As this equation suggests, the minimum separation distance depends on the instantaneous antenna gain, $G(\alpha_H, \alpha_V)$.

[2]Or equivalently maximum transmission power for a known distance

5.3.1 Numerical Results

For the computations in this section, we use radar parameters from ITU document, Rec. ITU-R M.1464-1, for a typical aeronautical radio-navigation radar in 2.8 GHz band. Table 5.6 in Appendix provides parameters for the so-called type-B radar in [86]. We choose performance points (of ROC) shown in Table 5.1 for the radar in noise and interference limited cases. As suggested by SSPARC, a drop of 5% in performance is permitted to

Table 5.1: Target ROC for Noise/Interference Limited Performance

Mode	P_D	P_{FA}	SNR/SINR (dB)
Noise Limited	0.90	10^{-6}	13.14
Interference Limited	0.85	10^{-6}	12.80

provide an interference margin for the secondary user, which is equivalent to an SNR loss of 0.34 dB.

To calculate max allowable interference level, $I_{\max}$ in (5.18), maximum operational range d and minimum target's radar cross section σ are required which is not provided by Table 5.6. Any variation in values of these two parameters can significantly affect resulting $I_{\max}$. For example, if the SNR of the noise-limited regime in (5.7) is 16.14 dB (3-dB above the required SNR in table 5.1) then $I_{\max}$ can be about as high as noise level $N_0 f_{BW}$ (INR of 0 dB), which brings SINR down to 13.14 dB. However, if we assume that SNR is already at the minimum level, then we only have 0.34 dB room for the interference which reduces the maximum INR down to -11 dB.

The type-B radar, as outlined in [86], employs high and low-beam horns in the antenna feed array. The high-beam horn receives returns from high-altitude targets close to the antenna, while the low-beam horn receives returns from low-altitude targets at greater distances. Overall, it is designed for monitoring air traffic in and around airports within a range of 60 Nm (approximately 111 km). A coverage pattern is also provided for a target with 1 m^2 radar cross section. Therefore, using $d = 111$ km and $\sigma = 1$, the resulting SNR (5.7) will be 30.6 dB that is significantly bigger than required SNR of 13.14 dB. This is unrealistic and does not represent radar's borderline operation. Therefore, in order to

remove the effect of d and σ in our calculation, we normalize them such that SNR in (5.7) matches with required SNR in (5.12)[3]. Based on these normalized parameter values, Table 5.2 shows the maximum permitted interference level and resulting INR. For noise limited case, no external interference is allowed because the radar's performance is already at the edge.

The results of two administrative tests, performed in [86] by injecting three types of interfering signals (Continuous Wave, CDMA-QPSK, TDMA-QPSK) to radar's receiver input, have also concluded that and an INR of -10 dB can fully protect radar type B and other aeronautical radionavigation radars operating in the 2700-2900 MHz.

Table 5.2: Maximum Permitted Interference Level

Mode	$I_{\max}$ (dBm)	INR (dB)
Noise Limited	$-\infty$	$-\infty$
Interference Limited	-122.64	-10.96

5.3.2 Protection Distance

The maximum interference level that was calculated in previous section can be used in (5.19) to define minimum separation between SU and radar receiver. SU is assumed to be a Wi-Fi AP with following parameters:

Table 5.3: Secondary User Specification

Parameter	**Value**
Emission Power (EIRP) P_{SU}	1 Watt
Bandwidth (MHz)	20.0
Antenna Height (m)	3.0
Interference Type	Co-channel, $\Delta f = 0$
Antenna Gain (Dipole)	2.15 dBi
Noise Figure (dB)	8.0

[3]By increasing the value of d or decreasing σ, effective SNR is reduced to match with (5.12)

Since SU and Radar are assumed to be co-channel, the FDR is calculated as the ratio of corresponding bandwidths FDR $= \frac{20MHz}{653KHz} = 30.6$. Note that we have used IF 3-dB bandwidth for radar's receiver which is significantly smaller than RF 3-dB bandwidth of 10 MHz, since radar signal detection happens at IF.

A statistical antenna gain model is introduced in [89] to determine the radar antenna gain in the azimuth and elevation orientations. For high gain values of $22 < G_{\max} = 33.5 < 48$ dBi, following piece-wise function is suggested:

$$G(\theta) = \begin{cases} G_{\max} - 0.0004 * 10^{G_{\max}/10}\theta^2 & \theta \in [0, \theta_M] \\ 0.75G_{\max} - 7 & \theta \in [\theta_M, \theta_R] \\ 53 - G_{\max}/2 - 25\log(\theta) & \theta \in [\theta_R, \theta_B] \\ 11 - G_{\max}/2 & \theta \in [\theta_B, 180] \end{cases} \tag{5.20}$$

where $\theta_M = 50\sqrt{0.25G_{\max} + 7}/10^{G_{\max}/20}$, $\theta_R = 250/10^{G_{\max}/20}$ and $\theta_B = 48$. Figure 5.1 shows antenna gain versus azimuth with a main lob of 33.5 dBi. The 3-dB beam width in this pattern is 3.7 degree. Using this antenna pattern and Longley-Rice path loss model [42] between secondary user and radar's receiver, Figure 5.1 also shows protection region as a function of relative azimuth between SU and radar's antenna main beam. *It is clear that protection region follows the same pattern as radar's antenna pattern as suggested by (5.19).*

5.4 Interference Limited Radar - Multiple Secondary Networks

Equation (5.18) defines a maximum interference level that a radar can tolerate while its performance is in the acceptable range. From radar's point, if multiple secondary users coexist with the radar simultaneously, the accumulated signal power at radar's location must also be bounded by (5.18). In practice, this is the more common scenario due the proliferation of WiFi networks.

The characterization of the aggregate interference from multiple WiFi APs as seen by a radar receiver, is fundamentally determined by the multiple access protocol employed by WiFi nodes. Users within a single WiFi network *time-share* the common channel based on

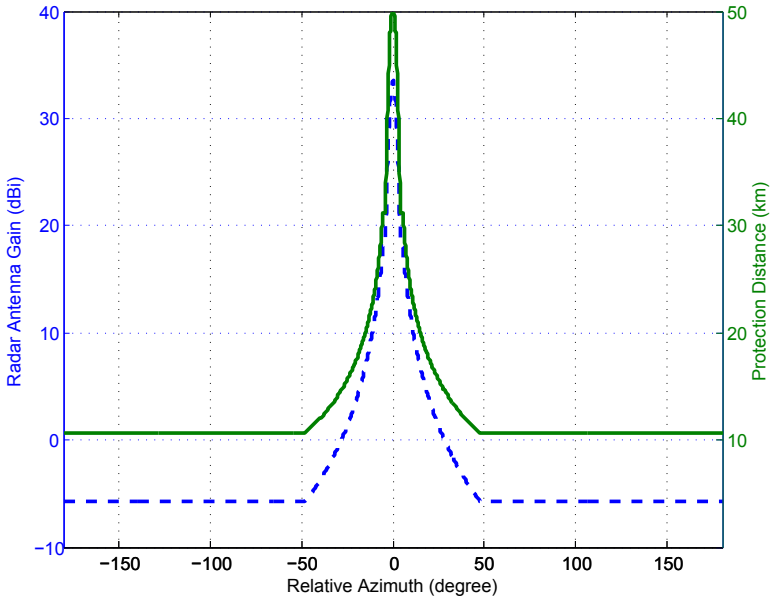

Figure 5.1: Radar antenna gain as well as Protection distance between SU and Radar v.s. azimuth.

CSMA-CA, i.e., the WiFi DCF protocol prohibits simultaneous multiple user transmissions. However, *different* WiFi networks can simultaneously operate in the vicinity of a radar and the aggregate interference across different networks needs to be accounted for, as shown in the scenario in Figure 5.2.

Wi-Fi APs and their associated users are randomly distributed in space which is suitably modeled as a Poisson Point Process (PPP). For a radar located at point $y \in R^d$ and randomly distributed access points at $x \in R^d$, the aggregate interference from secondary users to radar is described as a generalized shot noise process in space [92]:

$$I_{aggr}(y) = \sum_{x \in \Phi} \frac{P_x G(\theta_x)}{\mathrm{FDR}(\Delta f)} l(||y - x||) \tag{5.21}$$

where P_x is the SU transmit power at location x (an i.i.d random variable) and $||y - x||$ describes the distance between radar and secondary access point. $l(.)$ is the impulse response function that models signal attenuation (inverse of path loss) and $G(.)$ is radar's antenna gain in the direction of interferer, θ_x. Stochastic distribution of I_{aggr}, plays an important

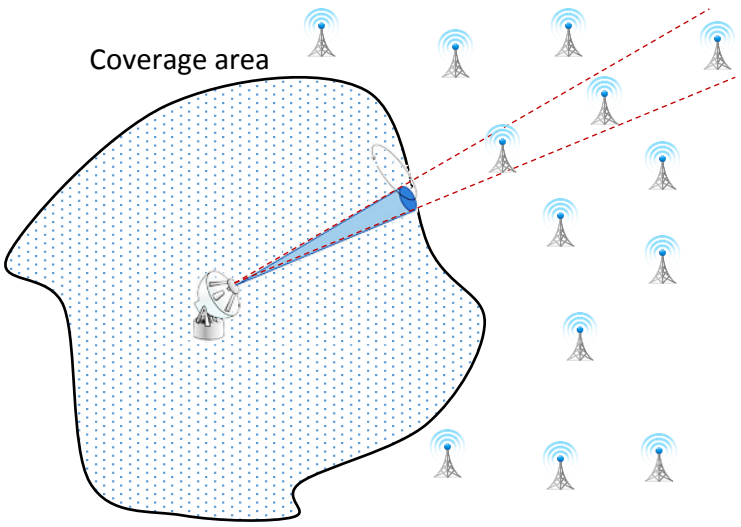

Figure 5.2: Aggregate interference from multiple WiFi access points to radar receiver.

role in performance analysis for radar. We assume all WiFi networks form a PPP of intensity λ and each network is independently active with probability p. Hence, it is effectively a PPP of intensity $p\lambda$ with all nodes being active simultaneously. Furthermore, we consider a fixed transmit power for all WiFi networks (which is common in practice) of $P_x = P_{SU}$.

The aggregate interference I_{aggr} in (5.21) is a weighted sum of received power from many independent APs that are distributed over a large area. Hence, it is reasonable to assume that I_{aggr} has a Gaussian distribution with mean and variance of μ_I and σ_I^2, respectively [93]. For a PPP of density λ, the mean and variance of the sum $\sum_{x\in\Phi} f(x)$ is calculated from Campbell's theorem [92] as

$$E\left[\sum_{x\in\Phi} f(x)\right] = \lambda \int_{\mathcal{R}^d} f(x)dx \tag{5.22}$$

$$var\left[\sum_{x\in\Phi} f(x)\right] = \lambda \int_{\mathcal{R}^d} f^2(x)dx \tag{5.23}$$

5.4.1 Average and Variance of Interference (μ_I, σ_I^2)

The average interference that is received at radar receiver is calculated from (5.22) by integrating over the $\mathcal{R}^2$ plane. Assuming that radar receiver is at the origin ($y = 0$):

$$\mu_I = E[I_{aggr}] = \frac{p\lambda P_{SU}}{\mathrm{FDR}(\Delta f)} \int_{\mathcal{R}^2} G(\theta_x) l(||x||) dx \tag{5.24}$$

Here we assume there is a minimum separation distance between radar and SU which could potentially be a function of θ, $d(\theta)$. Using polar coordinates for the integral and considering $l(r) = K_0 r^{-\alpha}$ we obtain:

$$\begin{aligned} \mu_I &= \frac{p\lambda P_{SU} K_0}{\mathrm{FDR}(\Delta f)} \int_\theta \int_{d(\theta)}^{\infty} G(\theta) r^{1-\alpha} dr d\theta \\ &= C_{\mu_I} \int_\theta G(\theta) d^{2-\alpha}(\theta) d\theta \\ C_{\mu_I} &= \frac{p\lambda P_{SU} K_0}{\mathrm{FDR}(\Delta f)(\alpha - 2)} \end{aligned} \tag{5.25}$$

with an important assumption of $\alpha > 2$ to guarantee convergence of inner integral. This assumption is valid in practical cases because except for the free space path loss, where $\alpha = 2$, in all practical cases $\alpha > 2$.

This equation allows variation in protection distance according to current direction of the radar's main antenna beam. The total interference highly depends on the choice of function $d(\theta)$ as a systematic parameter that trade-offs protection distances between main beam interferer versus side lobe ones. This is clearly chosen based on $G(\theta)$ and optimized subject to some constraints, as shown in the following sections.

The variance of aggregated interference is calculated from (5.23). Similar to the approach taken for μ_I, the variance σ_I^2 is calculated by the following double integral over r and θ:

$$\begin{aligned} \sigma_I^2 &= \frac{p\lambda P_{SU}^2 K_0^2}{\mathrm{FDR}^2(\Delta f)} \int_\theta \int_{d(\theta)}^{\infty} G^2(\theta) r^{-\alpha} r dr d\theta \\ &= C_{\sigma_I^2} \int_\theta G^2(\theta) d^{2-2\alpha}(\theta) d\theta \\ C_{\sigma_I^2} &= \frac{p\lambda P_{SU}^2 K_0^2}{\mathrm{FDR}^2(\Delta f)(2\alpha - 2)} \end{aligned} \tag{5.26}$$

with the assumption that $\alpha > 1$ to ensure convergence of the integration over r.

5.4.2 Protection Region

With multiple secondary users being active simultaneously, protection region for radar can be defined in terms of *probability of outage*, i.e. probability of effective radar SINR dropping below the minimum threshold. This is also equivalent to limiting aggregate interference $I_{aggr} < I_{\max}$. Since I_{aggr} has a normal distribution $N(\mu_I, \sigma_I^2)$, the outage probability can be determined as following:

$$\begin{aligned} P_{outage} &= \Pr\{I_{aggr} > I_{\max}\} \\ &= Q\left(\frac{I_{\max} - \mu_I}{\sigma_I}\right) \end{aligned} \tag{5.27}$$

where $Q(.)$ function is the tail probability of the standard normal distribution. It is desired to set an upper bound for probability of outage, $P_{out,\max}$:

$$\begin{aligned} &P_{outage} \leq P_{out,\max} \rightarrow Q\left(\frac{I_{\max} - \mu_I}{\sigma_I}\right) \leq P_{out,\max} \\ &I_{\max} \geq \mu_I + \sigma_I Q^{-1}\left(P_{out,\max}\right) \end{aligned} \tag{5.28}$$

This equation defines the relationship between maximum tolerable interference by the radar receiver and average/variance of aggregate interference from secondary WiFi networks. Depending on how much information about radar rotation is available at the SU, different scenarios are plausible for determining protection distance $d(\theta)$. Here we consider three special cases. *First*, optimal protection distance is defined and calculated for a secondary network that has full knowledge about current radar antenna beam with respect to its location. *Second*, an SU that has no knowledge about radar rotation pattern and therefore is not capable of synchronizing its transmission instances with it. This results in a constant $d(\theta) = d_{\min}$ and a circular protection region. *Third*, a secondary user that is partially aware of radar's rotation schedule and is capable of identifying radar's main lobe from side lobe is evaluated as a pragmatic sub-optimal solution.

In order to better estimate protection distance, we need a more accurate path loss model

than free space model. We use the well-known Longley-Rice (LR) model that is based on field measurements and is relatively more accurate. However, previous analysis needs a closed form attenuation function of the form $l(r) = K_0 r^{-\alpha}$. Accordingly, we performed exponential curve fitting on LR with parameters in tables 5.3 and 5.6 to estimate α and K_0. LR defines three propagation regions, namely *line of sight*, *diffraction* and *scattering*. By using line-of-sight region for curve fitting, $l(r) = 259\, r^{-3.97}$ is obtained.

Optimal Distance

Using (5.28), the coexistence criteria is defined by limiting average and variance of aggregate interference $\mu_I + \sigma_I Q^{-1}\left(P_{out,\max}\right) \leq I_{\max}$. This inequality has a trivial answer that is achieved by letting $d(\theta) \to \infty$ (apparent from (5.25) for example). In order to avoid this, one must minimize the total protection area subject to total interference limit as formulated in following optimization problem:

$$d_{opt} = \arg\min_{d(\theta)} \int_0^{2\pi} \frac{d^2(\theta)}{2} d\theta \tag{5.29}$$

subject to:

$$\mu_I + \sigma_I Q^{-1}\left(P_{out,\max}\right) \leq I_{\max} \tag{5.30}$$

For the most general antenna pattern model of $G(\theta)$, it is proven in the appendix that optimum protection distance $d_{opt}(\theta)$ is proportional to $G^{1/\alpha}(\theta)$ with an eqality constant that is determined by numerically solving following equation:

$$\begin{aligned} & d_{opt}(\theta) = \gamma G^{\frac{1}{\alpha}}(\theta) \\ & \mathcal{A}\gamma^{2-\alpha} + \mathcal{B}\gamma^{1-\alpha} - I_{\max} = 0 \end{aligned} \tag{5.31}$$

in which $\mathcal{A}$ and $\mathcal{B}$ are constant determined by:

$$\begin{aligned} \mathcal{A} &= C_{\mu_I} \int_0^{2\pi} G^{\frac{2}{\alpha}}(\theta) d\theta \\ \mathcal{B} &= Q^{-1}\left(P_{out,\max}\right) \sqrt{C_{\sigma_I^2} \int_0^{2\pi} G^{\frac{2}{\alpha}}(\theta) d\theta} \end{aligned} \tag{5.32}$$

Radar-Blind SU

For this type of SU, protection distance $d(\theta) = d_{\min}$ is constant and it simplifies equations (5.25) and (5.26). By using simplified mean and variance in (5.30), $d_{\min}$ is found as the solution of following equation:

$$d_{\min}^{2-\alpha}\left[C_{\mu_I}\int G(\theta)d\theta\right] + d_{\min}^{1-\alpha}\left[Q^{-1}(P_{out,\max})\sqrt{C_{\sigma_I^2}\int G^2(\theta)d\theta}\right] = I_{\max} \tag{5.33}$$

Main/Side Lobe Interferer

While equation (5.31) determines best protection distance in its general form, SUs have limited resolution in synchronizing with radar rotation in any practical scenario. A more pragmatic assumption is that secondaries can estimate when radar's main antenna beam is directed toward their location and stop their transmission accordingly. Here, radar antenna pattern is split into two regions of *main lobe* with a width of θ_H and *side lobe* that is $2\pi - \theta_H$ wide. Protection distance is similarly divided to two distances of $d_{\max}$ and $d_{\min}$ for the main lobe and side lobe, respectively. One of these two distances should be specified intentionally and the other distance is calculated from total interference constraint. This degree of freedom allows us to optimize (minimize) total protection distance.

Let $\beta = \frac{d_{\max}}{d_{\min}}$ be the radio of main beam protection distance to side beam. For any choice of β, protection distances $d_{\min}$ and $d_{\max}$ can be determined from the constraint in (5.30), which results in following:

$$\begin{aligned}
&d_{\min}^{2-\alpha}C_{\mu_I}\xi_1 + d_{\min}^{1-\alpha}Q^{-1}(P_{out,\max})\sqrt{C_{\sigma_I^2}\xi_2} = I_{\max}\\
&\xi_1 = \int_{\frac{\theta_H}{2}}^{2\pi-\frac{\theta_H}{2}} G(\theta)d\theta + \beta^{2-\alpha}\int_{\frac{-\theta_H}{2}}^{\frac{\theta_H}{2}} G(\theta)d\theta\\
&\xi_2 = \int_{\frac{\theta_H}{2}}^{2\pi-\frac{\theta_H}{2}} G^2(\theta)d\theta + \beta^{2-2\alpha}\int_{\frac{-\theta_H}{2}}^{\frac{\theta_H}{2}} G^2(\theta)d\theta\\
&d_{\max} = \beta d_{\min}
\end{aligned} \tag{5.34}$$

The best ratio β is selected to minimize total protection area of $Area = [\beta^2\theta_H/2 + \pi - \theta_H/2]d_{\min}^2$. For $p\lambda = 10^{-6}$ (time-space density product), figure 5.3 shows total protection

area as a function of β for various values of $\frac{G_{\max}}{G_{\min}}$ (radio of maximum to minimum radar antenna gain).

Figure 5.4 shows protection distance as a function of relative azimuth with radar's main beam for three cases of *Radar-Blind SU*, *Optimal Distance* and *Main/Side lobe interferer*. It is evident from this figure that a radar-blind SU will lose a significant portion of available white space spectrum as protection distance is significantly larger than other two cases. Main/Side interferer is plotted for the optimum choice of β. It provides a much closer distance to optimal results. A comparison between optimal distances here and that of single user in figure 5.1 reveals that distances are significantly increased (10-km for side lobes is expanded to 239-km) because of accumulated interference from spatial distribution of users. Table 5.4 compares total protection area for the three cases above. While total area occupied by *main/side lobe interferer* is about twice as optimal area, the required area for radar-blind user is 11.5 times larger than optimal which again highlights inefficiency of this method.

Table 5.4: Protection Area Comparison

	Optimal	**Main/Side Lobe**	**Radar Blind**
Total Area (1000,000 km^2)	0.54	0.98	6.2
Min. Distance (km)	239	437	1403
Max. Distance (km)	2331	2140	1403

5.5 Interference to WiFi devices

The main goal of spectrum sharing is to create new secondary networks, while providing protection to the incumbents (primary). Therefore, it is essential to study *primary to secondary* interference. In most sharing scenarios, secondary transmitters use a significantly lower power profile compared to the primary[4], rendering them very sensitive to interference from the primary.

[4]For example, in TV white spaces, TV station may output upto 1000 KW as against portable secondary devices transmitting at 100 mW.

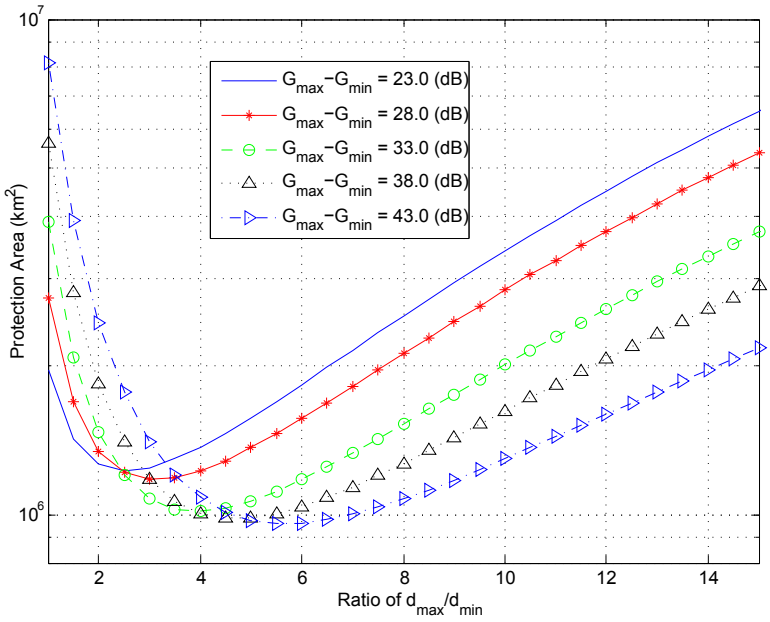

Figure 5.3: Total protection area v.s. $\frac{d_{\max}}{d_{\min}}$ ratio for various values of $\frac{G_{\max}}{G_{\min}}$; $p\lambda = 10^{-6}$.

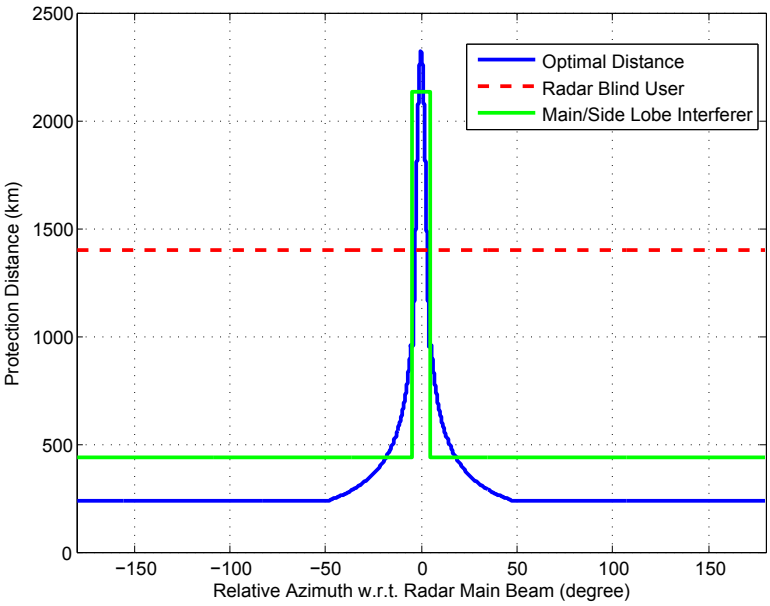

Figure 5.4: Protection region v.s. relative azimuth between SU and radar's main antenna beam for following cases: Radar-Blind SU, Optimal Protection Distance and Main/Side lobe interferer; $p\lambda = 10^{-6}$, $P_{out,\max} = 0.1$

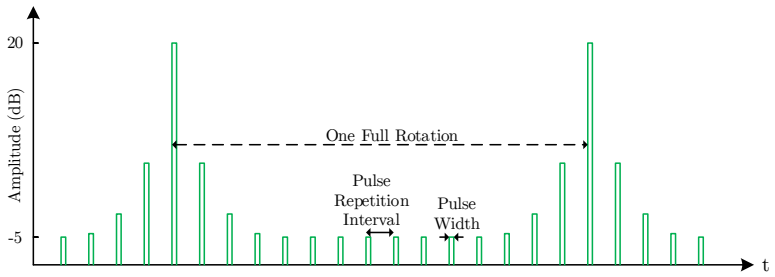

Figure 5.5: Radar signals received at WiFi receiver behave as a non-stationary source of interference.

The radar signal received at a WiFi receiver is given by

$$y(t) = \sum_n \sqrt{\frac{G_{SU} G(\theta(t)) P_T}{L_{Radar \to SU}}} s(t - \frac{n}{f_R})$$

where $G(\theta(t))$ is the time-varying, radar antenna gain and $L_{Radar \to SU}$ is the path loss from radar to SU. By reciprocity, the path loss from SU to radar is thus $L_{Radar \to SU} = \frac{1}{K_0 r^{-\alpha}}$. The instantaneous interference power from the radar and resulting SINR at the input to the WiFi receiver can be written as

$$\begin{aligned} P_R(t) &= P_T G_{SU} G(\theta(t)) K_0 d_{Radar-SU}^{-\alpha} \sum_n \Pi(\frac{t}{PW} - \frac{n}{f_R}) \\ \text{SINR}_{SU}(t) &= \frac{P_{SU} G_{SU}}{L_{SU-SU}(N_0 BW + P_R(t))} \end{aligned} \tag{5.35}$$

The radar interference to WiFi receivers is *non-stationary* for two reasons. *First*, due to radar rotation, the interference power varies periodically as a characteristic for search radars. Depending on rotation speed, this period is typically of the order of seconds. *Second*, the transmitted signals by radar $s(t - n/f_R)$ consists of short pulses as shown in Figure 5.5. For our typical aeronautical radar, the pulse width is $1\mu s$ and pulse repetition internal is about $1ms$. Therefore, even when the radar main beam is directly aligned with WiFi receiver ($G(\theta(t))$ is maximum), there are inter-pulse durations with zero interference.

Analytical evaluation of WiFi performance against a non-stationary interferer such as a pulsed radar is substantially more complicated than stationary ones for several reasons.

First, depending on WiFi packet size and radar pulse repetition interval, the impact of radar signal on WiFi packet reception can vary greatly. For example, packet lengths in 802.11n can be vary from few hundreds of microseconds to several tens of milliseconds. Therefore, for pulse repetition interval of $1ms$, short packets can fall in between inter-pulse intervals with significant probability, while longer packets almost surely overlap with radar pulses. *Second*, WiFi packets are composed of multiple OFDM symbols each of duration $4\mu s$ (for 802.11n in a 20-MHz channel) [94]. A radar pulse of 1-μs width will collide with one symbol (or few symbols when packet is very long) out of many in the packet. Depending on the channel code (convolutional or LDPC) and selected MCS as well as the SNR of the interference-free channel, packet might still be decodeable. In addition, certain OFDM symbols are more crucial than the others. A collision between PLCP header and radar pulses will leave the entire packet undecodeable while impacted data symbols may be recovered by interleaving and channel coding. *Third*, all practical implementations of WiFi MAC/PHY layers include rate adaptation mechanisms to choose the best MCS based on channel condition. These algorithms are typically designed to converge to a steady state response in presence of *stationary* noise and interference. A non-stationary interferer can degrade the performance drastically unless smarter adaptation methods are designed which are aware of coexistence scenario.

A comprehensive WiFi performance study that considers all the aforementioned concerns is beyond the scope of this work. Here, our focus is the achievable throughput in WiFi given the sharing scenario. Therefore, we assume that best MCS selection in WiFi is made for the current SINR. We consider a pair of 802.11n-based SUs in a 20-MHz channel with one spatial stream (1x1 SISO). The standard modulation and coding schemes in 802.11n as well as achievable rates are shown in Table 5.5. The minimum required SNR for each MCS, corresponding to a 10% packet loss, is also provided. The SNR values are obtained from [95] which are based on experimental measurements on an Intel Wireless Wi-Fi Link 5300 a/g/n.

The achievable throughput $R_{SU}(t)$ is a function of two factors; the instant SINR as in (5.35) that determines date rate through table 5.5 and the fraction of time SU is allowed to transmit, $\rho(d)$. From previous analysis for a single user or multiple users, there is a minimum separate distance $d(\theta(t))$ that depends on the direction of radar's main beam.

Table 5.5: Standard modulation and coding schemes and achievable data rates for 802.11n specifications. Minimum required SNR for each MCS, corresponding to 10% packet loss, is also provided.

MCS	**Modulation**	**Coding Rate**	**Data Rate(Mbps)**	**SNR**
0	BPSK	1/2	6.5	4.5
1	QPSK	1/2	13.0	6.5
2	QPSK	3/4	19.5	8.0
3	16-QAM	1/2	26.0	10.5
4	16-QAM	3/4	39.0	13.5
5	64-QAM	2/3	52.0	17.5
6	64-QAM	3/4	58.5	19.5
7	64-QAM	5/6	65.0	21.5

$\rho(d)$ defines the fraction of time when $d_{Radar-SU} \geq d(\theta(t))$. Therefore, SU throughput is:

$$R_{SU}(t) = \begin{cases} f(\text{SINR}(t)) & d_{Radar-SU} \geq d(\theta(t)) \\ 0 & d_{Radar-SU} < d(\theta(t)) \end{cases} \tag{5.36}$$

Therefore, a closer SU to radar has a lower throughput not only due to reduced SINR but also diminished transmission opportunity. The $\rho(d)$ factor also depends on our sharing policy. For example, for a *Radar-Blind* SU, $\rho(d)$ is a binary function while for *Main/Side lobe interferer*, it is constant as long as $d < d_{\max}$.

Figure 5.6 shows achievable throughput by SU for a single user sharing scenario with radar. Three different users are considered at different distances from the radar and throughput variation is depicted with respect to radar rotation. The path loss between WiFi AP and station is set to 80 dB, corresponding to free space loss for a 100-meter link at 2.7GHz. As a first order approximation, SINR is set to instantaneous SINR as defined by (5.35), treating radar pulses as a continuous waveform (CW) interfering with WiFi OFDM symbols.

In order to differentiate radar pulses from a CW signal, we need to estimate effective SINR from (5.35). Since WiFi data are interleaved in time, an OFDM symbol (4-μs long) that falls within a radar pulse is later extended to (after de-interleaving) a significantly larger time interval. This is equivalent to extending radar pulse width while reducing its power level. Therefore, if we assume that WiFi interleaver is sufficiently long, effective

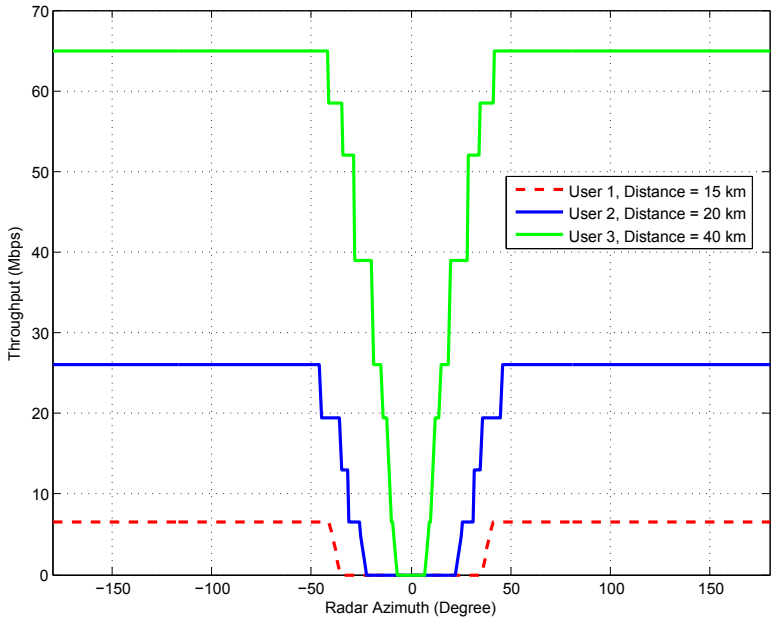

Figure 5.6: Secondary user throughput for single-SU sharing with radar.

radar interference is $\overline{P_R(t)} = \mathrm{PW} f_R P_T G_{SU} G(\theta(t)) K_0 d_{Radar-SU}^{-\alpha}$, which is averaged over pulse repetition interval. Here, radar interference to WiFi receiver is scaled by a factor of pulse width/pulse repetition interval. The average SINR and throughput experienced by the SU is:

$$\overline{\mathrm{SINR}(t)} = \frac{P_{SU} G_{SU}}{L_{SU-SU}(N_0 BW + \overline{P_R(t)})}$$
$$\overline{R_{SU}} = \int_{<T_S>} \overline{R_{SU}(t)} dt \tag{5.37}$$

where integration is over the scan time of radar, T_S. Figure 5.7 shows average SU throughput based on (5.37) for single and multiple SU sharing.

5.6 Numerical Results

In this section, protection distance and SU throughput is evaluated against various systematic parameters. In previous sections, we made a conservative assumption that the SNR of radar pulses reflected from a target at the edge of radar's coverage area are already at

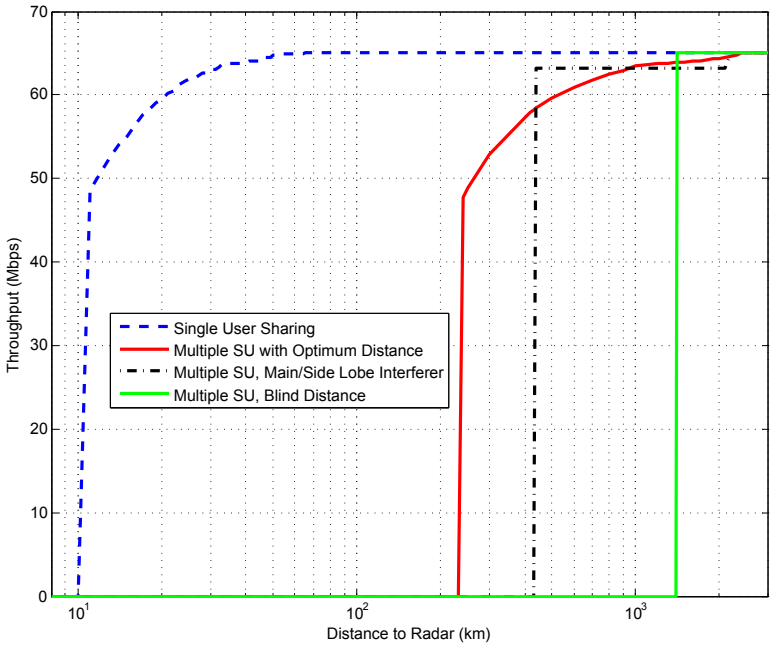

Figure 5.7: Average secondary user throughput for single/multiple SU sharing with radar.

the minimum required level specified by (5.12). This condition will leave a small room for additional interference from secondaries and therefore results in a larger protection distance. Here, we relax this condition by estimating SNR from (5.7) and estimating permitted interference from SU.

Figure 5.8 shows maximum permitted INR caused by SU as a function of radar performance drop (reduction in P_d). Original P_d is set to 0.9 and reduction of down to 0.7 is evaluated in this figure. Different curves in the figure correspond to various initial SNR (without SU interference) at the radar. Bigger initial SNRs open more room for external interference and result in larger INRs, as can be seen in this chart. For example at initial SNR of 16.14 and with 0% performance drop, INR can be as large as 0 dB. This is because initial SNR is 3 dB above minimum required SNR of 13.14 dB, therefore a 3 dB drop is allowed.

Using radar parameters in table 5.6, radar initial SNR is estimated to be 30.57 dB which allows maximum INR of +17.69 dB for 5% drop in P_d. We use this INR in the following to determine a less conservative protection distance then previous sections as well as achievable

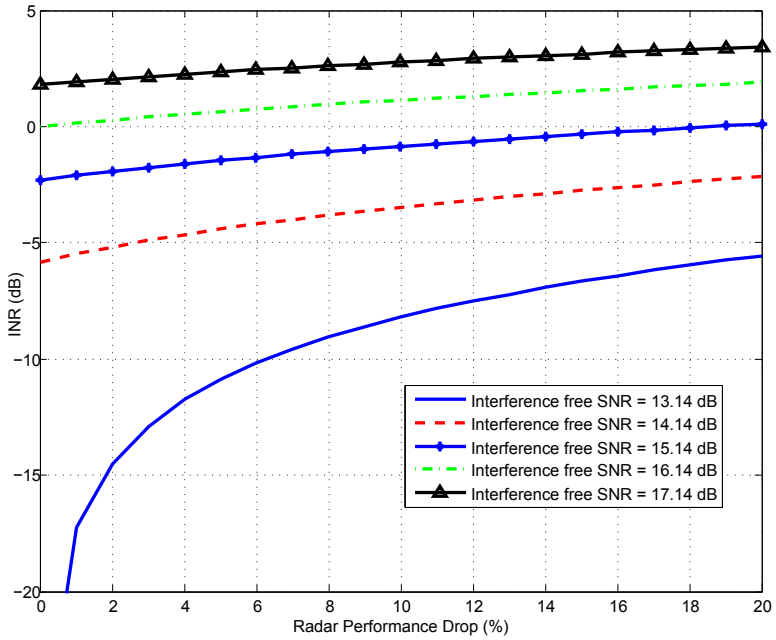

Figure 5.8: Maximum permitted INR versus radar performance drop for various values of original SNR (interference-free SNR)

SU throughput.

5.6.1 Protection Distance

Figure 5.9 shows protection distances for single and multiple SU sharing. Comparing this with figures 5.1 and 5.4 reveals that protection distances are immensely reduced because INR is increased from -10.96 dB to +17.69 dB. To better investigate the effect of initial radar SNR on required protection distances, figure 5.10 shows protection distance for single/multiple radar-blind secondary users with different initial radar SNR. The minimum required SNR for target ROC point of P_d=0.90 and $P_{fa} = 10^{-6}$ is 13.4 dB. Therefore, for the initial SNR of 13.14 dB, allowing radar performance to drop because of additional interference is very critical and reducing this drop can increase the distance to a large extent. However, if initial SNR is above this limit by only a few dB, the dependency of protection distance on radar performance drop is significantly reduced. For example at SNR of 17.14 dB, increasing radar P_d drop from 90% to 70% will reduce the distance from 315 km to 260 km (multiple

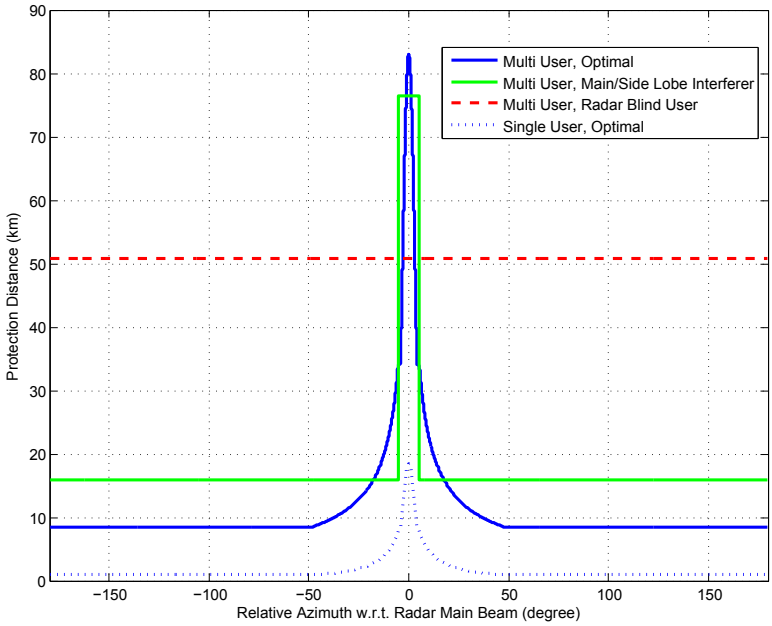

Figure 5.9: Protection distance versus azimuth for single and multi-user sharing

SU, radar-blind).

In sharing radar spectrum with distributed SUs, average interference is also highly affected by population density and probability of WiFi network's activity. Figure 5.11 shows this dependency by evaluating protection distance for radar-blind users versus the product of $p\lambda$ and for different initial radar SNR. A constant performance drop of 5% is utilized for radar. It is clear from this figure that in the logarithmic scale, protection distance is a linear function of $p\lambda$.

5.6.2 SU Throughput

By increasing initial radar SNR or allowing further drop in its performance, we observed significant reductions in protection distances as it was shown in previous results. Reduced distances provide additional white space opportunities for WiFi devices in spatial domain. On the other hand, closer distances to radar means additional interference from transmitted pulses.

The average interference from radar to WiFi receiver was calculated in (5.37) by scaling

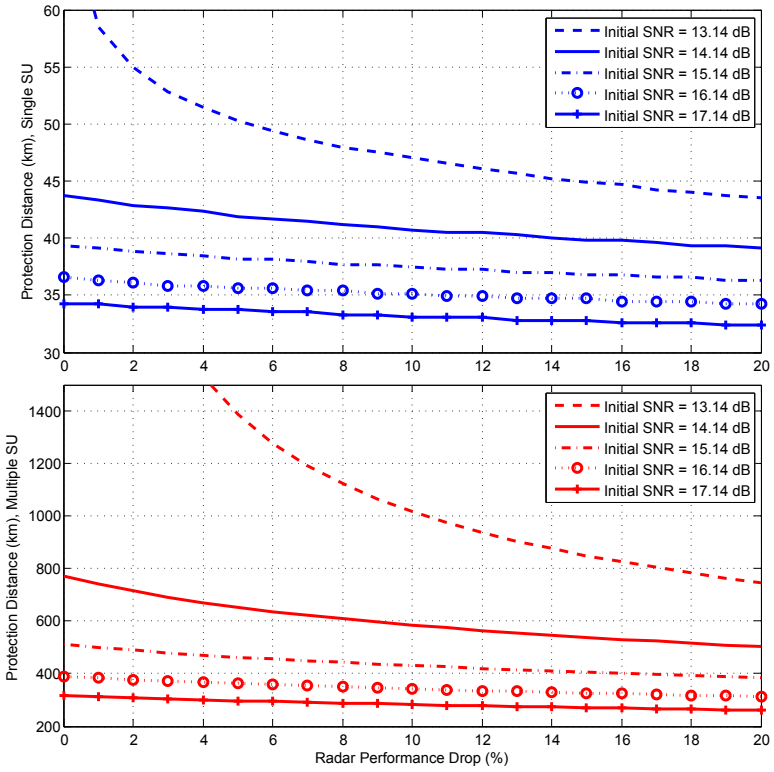

Figure 5.10: Protection distance versus radar performance drop for single/multiple radar-blind secondary users. Initial SNR corresponds to noise-limited SNR at radar receiver.

peak power with the ratio of pulse width to pulse repetition interval. For our radar parameters, this translates to $\frac{1\mu s}{896\mu s} \approx 29.5$ dB reduction in effective radar interference level which significantly improves WiFi SINR at close distances to radar. Figure 5.12 shows achievable SU throughput for both cases of using peak radar interference (a) and average/effective radar interference (b) to WiFi receivers (29.5 dB reduction w.r.t. peak). Initial radar SNR is set to 23.14-dB which is 10-dB above minimum required level and radar performance drop is set to 5%. For a radar-blind SU that can only coexist with radar at large distances of >120 km, throughput is the same in both cases because radar interference is negligible. However, at close distances of single-user sharing and multi-user with optimal distance, throughput drop due to radar interference is very clear in (a). Particularly for the case of single-user sharing, protection distance is reduced to about 2-km, but practical throughput is still zero up to 12 km from radar.

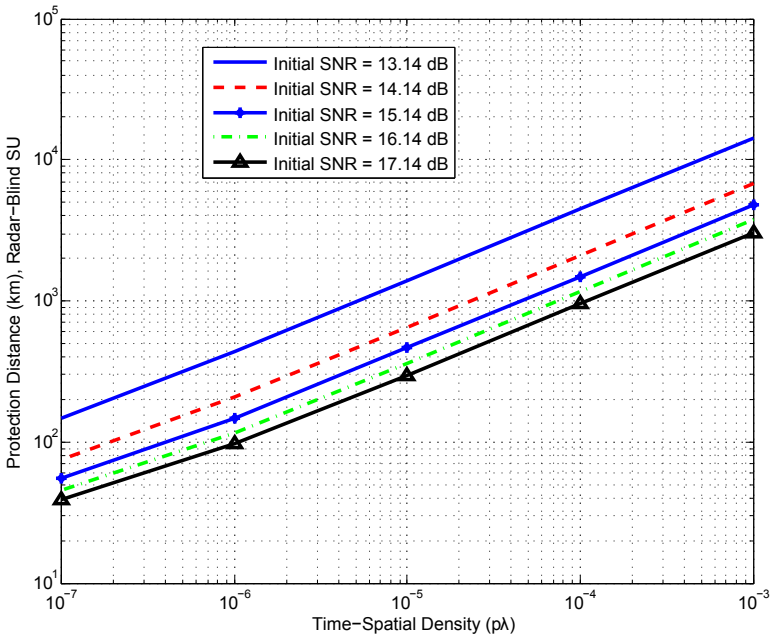

Figure 5.11: Protection distance versus time-spatial density of WiFi networks, $p\lambda$

5.7 Conclusion

In this chapter, we considered the problem of spectrum sharing between a rotating radar and WiFi networks. Minimum required SNR for noise-limited operation of the radar was defined as a function of basic radar parameters, including probability of *detection*. Coexistence with WiFi users was made possible by permitting a certain drop in radar's detection performance. We showed that this performance drop is very essential when radar SNR (without interference from WiFi users) is very close to the minimum required SNR. This determined maximum tolerable interference by the radar from WiFi devices (INR). Evaluating INR for various values of radar detection drops revealed that INR falls abruptly at small performance detection drops, when radar SNR is already at its minimum; otherwise INR changes are slow.

Protection distance - the minimum required distance between SU and radar receiver - was calculated for both single-SU case as well as multiple spatially distributed SUs. The latter formed a Poisson point process in space and an aggregate interference to radar that

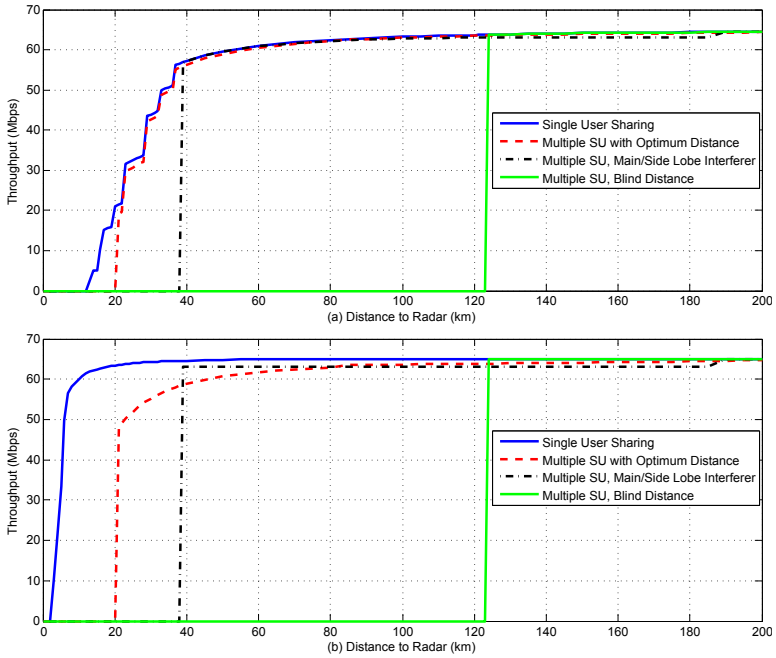

Figure 5.12: Achievable SU throughput versus distance for various sharing policies. (a) is based on peak radar interference to WiFi receiver and (b) is based on average radar interference.

was approximated as Gaussian. Outage probability was utilized as the defining metric for protection distance calculation and different sharing scenarios was introduced based on how much radar-related data is available to the SU.

The optimal protection distance was defined in terms of minimizing total protected area. It was shown to be proportional to $G^{\frac{1}{\alpha}}(\theta)$. For a radar-blind SU, a constant protection distance was defined which was significantly larger than optimal distance. Comparing total protected area for these two showed that radar-blind area is about 12 times (for our settings) larger than optimal area. A more pragmatic solution is an SU with sufficient side information about radar to distinguish main lobe from side lobe. Protection distance for this type of SU was calculated and shown to be very close to optimal distance.

The effect of interference caused by radar pulses on performance of WiFi networks was modeled and achievable throughput (as a function of radar rotation as well as average) was estimated. For close distances to radar, throughput was shown to be very low even though

SU is allowed to transmit. Since radar interference is non-stationary, two cases were considered as the upper and lower bounds of effective radar interference. First, instantaneous interference from radar pulses was utilized for calculating effective SINR. Second, the power of radar pulses was normalized by the ratio of pulse-width/pulse-repetition-interval. The former showed significant throughput reduction at close distance (single SU and optimal multiple SU).

APPENDIX

5..1 Radar Parameters

Radar parameters used for simulation purposes in this chapter are presented in table 5.6.

5..2 Optimum Protection Distance

Based on equations (5.29) and (5.30), optimal protection distance by limiting maximum outage probability is obtained as:

$$d_{opt} = \arg\min_{d(\theta)} \int_0^{2\pi} \frac{d^2(\theta)}{2} d\theta$$
$$\mu_I + \sigma_I Q^{-1}\left(P_{out,\max}\right) \leq I_{\max}$$

where μ_I and σ_I are calculated in (5.25) and (5.26):

$$\mu_I = C_{\mu_I} \int_\theta G(\theta) d^{2-\alpha}(\theta) d\theta$$
$$\sigma_I = \sqrt{C_{\sigma_I^2} \int_\theta G^2(\theta) d^{2-2\alpha}(\theta) d\theta}$$

Optimal $d(\theta)$ is attained by reducing inequality constraint to equality. This is simply because for any $d(\theta)$ that the strict inequality constraint holds (strict $<$), we can scale down $d(\theta)$ accordingly to increase μ_I, σ_I and achieve equality constraint (note that $2-\alpha < 0$ and $2-2\alpha < 0$). This will clearly result in a smaller objective function.

Having equality constraint, we use Lagrange multiplier method with a dummy variable

---

[2]P0N: No modulating signal and no information transmitted [96]

[3]Options are: continuous, random, 360 deg, sector, etc.

Table 5.6: Technical Parameter for Type B Aeronautical Radar

Characteristics	**Radar B**
Platform Type	Ground, ATC
Tuning Range (MHz)	2700 - 2900
Modulation	P0N[5]
Tx power into antenna	1.32 MW
Pulse Width (μs)	1.03
Pulse rise/fall time (μs)	–
Pulse repetition rate (pps)	1059 - 1172
Duty Cycle	0.14 maximum
Chirp BW	NA
Compression Ratio	NA
RF emission BW (-20 dB)	5 MHz
RF emission BW (3 dB)	600 kHz
Antenna Parameters	
Type	Parabolic reflector
Pattern type (degrees)	Cosecant-squared +30
Polarization	Vertical or right hand circular
Main beam gain (dBi)	33.5
Elevation beamwidth (degree)	4.8
Azimuthal beamwidth (degree)	1.3
Horizontal scan rate (degree/s)	75
Horizontal scan type[6](degrees)	360
Vertical scan rate (degree/s)	N/A
Vertical scan type (degree)	N/A
Side-lobe levels (1st and remote)	7.3dBi
Height (m)	8.0
Receiver Parameters	
IF 3 dB bandwidth	653 kHz
Noise figure (dB)	4.0 maximum
Minimum discernible signal (dBm)	-108
Receiver RF 3 dB bandwidth (MHz)	10

ϵ to redefine objective function as

$$d_{opt} = \arg\min_{d(\theta)} \int_0^{2\pi} \frac{d^2(\theta)}{2} d\theta + \epsilon \left(\mu_I + \sigma_I Q^{-1} \left(P_{out,\max} \right) - I_{\max} \right)$$

Taking partial derivatives of the new objective function with respect to $d(\theta)$ results in:

$$\frac{\partial f}{\partial d(\theta)} = 0$$
$$d(\theta) + \epsilon \left[\frac{\partial \mu_I}{\partial d(\theta)} + Q^{-1}(P_{out,\max}) \frac{\partial \sigma_I}{\partial d(\theta)} \right] = 0$$

Replacing μ_I and σ_I:

$$d(\theta) + \epsilon \left[(2-\alpha) C_{\mu_I} G(\theta) d^{1-\alpha}(\theta) + \frac{Q^{-1}(P_{out,\max}) C_{\sigma_I^2} (2-2\alpha) G^2(\theta) d^{1-2\alpha}(\theta)}{2\sqrt{C_{\sigma_I^2} \int_\theta G^2(\theta) d^{2-2\alpha}(\theta) d\theta}} \right] = 0$$

Let $X = G(\theta) d^{-\alpha}(\theta)$, the above equation can be written as $1 + \epsilon \left[\Gamma X + \Lambda X^2 \right] = 0$, where Λ and Γ are constant. Solving for X results in $G(\theta) d^{-\alpha}(\theta) = \frac{-\epsilon\Gamma \pm \sqrt{\epsilon^2\Gamma^2 - 4\epsilon\Lambda}}{2\epsilon\Lambda}$. Therefore, $d(\theta)$ is proportional to $G^{\frac{1}{\alpha}}(\theta)$. The proportionality constant is found from the constraint equation:

$$d(\theta) = \gamma G(\theta)^{\frac{1}{\alpha}}$$
$$C_{\mu_I} \int_\theta G(\theta) \gamma^{2-\alpha} G^{\frac{2-\alpha}{\alpha}}(\theta) d\theta + Q^{-1}\left(P_{out,\max}\right) \sqrt{C_{\sigma_I^2} \int_\theta G^2(\theta) \gamma^{2-2\alpha} G^{\frac{2-2\alpha}{\alpha}}(\theta) d\theta} = I_{\max}$$

which is simplified to:

$$\gamma^{2-\alpha} C_{\mu_I} \int_\theta G^{\frac{2}{\alpha}}(\theta) d\theta + \gamma^{1-\alpha} Q^{-1}\left(P_{out,\max}\right) \sqrt{C_{\sigma_I^2} \int_\theta G^{\frac{2}{\alpha}}(\theta) d\theta} = I_{\max}$$

Chapter 6

SDR PLATFORM FOR WIRELESS OPERATION IN WHITE SPACE SPECTRUM

6.1 Introduction

In previous chapters, we studied various problems in the context of spectrum sharing or coexistence between an unlicensed secondary user and a licensed primary owner. The fundamental purpose behind all these coexistence analysis is to enable end users to build and operate wireless networks in the shared RF spectrum without interfering with licensed users. Also in academic world, developing new ideas for interference management and coexistence necessitates open source test wireless networks. Building a practical network which operates in these newly available bands can be very challenging due to multiple reasons:

- ◇ Commercial products such as WiFi cards and access points are not readily available for these bands. Typically, large manufacturers of these commercial devices need a certain demand to consider a new frequency band in their product line. Clearly, this means the lengthy standardization process must be finalized before any supporting hardware appears in the market.

- ◇ Even with the existence of access points for setting up WiFi networks in the emerging bands, current user devices (laptops, tablets, cellphones, etc.) cannot exploit any of these networks due to their hardware incompatibility. Hence, practical performance evaluation requires developing hardware prototypes.

- ◇ All commercial devices are designed for and implemented on ASIC[1]. This leaves minimum configurability, particularly for lower layers of the network stack (PHY/MAC) and RF front-end. Therefore, each new device is still limited to one or few bands

[1]Application Specific Integrated Circuit

without possibility of changing bandwidth, power, aggregating multiple discontinuous bands, etc.

There are very important features that are essential in any potential wireless test-bed. *High configurability* is the key enabler for researchers which allows them to change basic settings on the processing chain of transmitter and receiver in order to mimic any desired scenario. This capability is more difficult at the lower layers of PHY and MAC, where most of the real-time processing happens. *Portability* of nodes is a fundamental characteristic in wireless networks. It is often necessary to evaluate overall user throughput or other performance metrics in a dynamic environment with users roaming around. Especially, for cognitive radio experiments based on spectrum sensing or DBA, spatial variation of available spectrum and its quality (as discussed in chapter 3) is a key feature and a portable wireless platform is essential. The achievable user throughput in a high-rate network such as WiFi is highly affected by processing delays in the physical and lower MAC layer[2]. *Real-time processing* at these layers is crucial to achieve rates that are comparable with the standard. This feature is often traded-off by high configurability. For example, a fully-software implementation of network stack provides highest configurability while severely affecting real-time capability of the lower layers.

The focus of this chapter is around design and implementation of an open-source hardware platform as a wireless test-bed which provides the required features discussed above. The outcome of this chapter is utilized in a longer-term project, called *CampusLink*, with the purpose of providing wireless connectivity through shared spectrum access in the University of Washington campuses. Further details are provided in the next sections. The rest of this chapter is organized as follows. Section 6.2 provides background and related works in this area. Selected SDR for our implementations is presented with details in section 6.3. Implementation details of physical layer is presented in section 6.4 and MAC layer is discussed in section 6.5. Integration of different layers in the hardware is discussed in section 6.6.

---

[2]Lower MAC layer is responsible for time-critical tasks such as sending ACK after receiving a successful packet or running CSMA-CA state machine.

6.2 Background and Related Works

A Software Defined Radio (SDR), also known as software based radio or just software radio, is a radio in which the properties of carrier frequency, signal bandwidth, modulation, and network access are defined by software. Modern SDR also implements any necessary cryptography, forward error correction coding, and source coding of voice, video, or data in software as well [6]. The multidimensional aspects of SDR spans from radio implementation to user application level. At radio level, SDR is viewed as an efficient technique for construction of wireless devices, offering a wide range of advantages including adaptability, reconfigurability and multifunctionality [97,98]. Depending on usage, an SDR can have one or some of following features [99]:

- ◇ *multi-band*: which is supporting more than one frequency band in a wireless standard, such as LTE-700, LTE-1700 and LTE-1900.

- ◇ *multi-standard*: that is supporting more than one wireless standard, such as LTE-TDD, LTE-FDD, GSM and WLAN.

- ◇ *multi-service*: which provides different wireless services to user, such as telephony, data and video streaming.

- ◇ *multi-channel*: that supports multiple transmission and reception channels independently and simultaneously.

Here, our focus is on multi-band and multi-standard features which contributes to its reconfigurability. The adaptability of SDR platforms is well-aligned with cognitive radio systems requirements to the extent that CR is sometimes defined as an SDR with additional sensing capability [99]. Therefore, this is an excellent target for our wireless test-bed complying with the required features.

The basic hardware architecture for a modern SDR is shown in figure 6.1. The RF front-end is designed to support a large frequency range using tunable filters, mixers and local oscillators. The digital back end is the highly configurable processing chain which

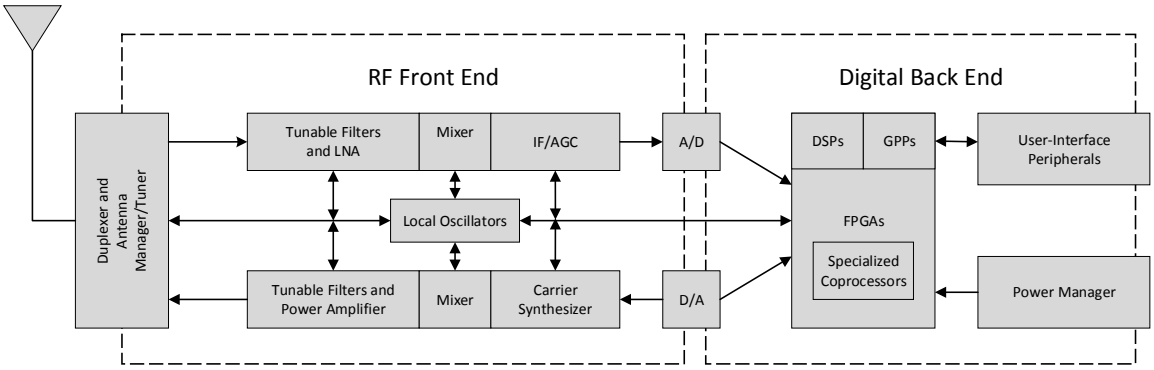

Figure 6.1: Basic hardware architecture of an SDR modem. It provides resources to define carrier frequency, bandwidth, modulation and source coding. The hardware resources may include mixtures of GPP, DSP, FPGA and other specialized processors [6].

comprises DSPs, general purpose processors and FPGAs. The software architecture in the digital back-end is created based on application programming interfaces (APIs) for the major components to ensure portability across different hardware implementations.

The flexibility offered by SDRs has motivated researchers to design and build various SDR boards with different capabilities [100–103]. Major differences between these SDRs are in the supported RF frequency span, instantaneous baseband bandwidth, full/half duplex capabilities, and available on-board processing units. Most of these platforms are designed for down-conversion of RF signal to base-band (zero IF), sampling and sending raw I/Q data to a host PC for processing. Therefore, user applications are entirely implemented in the host PC while on-board processors are handling I/Q transfer between A/D (D/A) and host, mainly through USB[3] port. While this framework is useful for certain applications in which SDR acts in only-RX mode (sniffer) or only-TX mode, it is severely limiting for wireless network operation due to following:

- ◇ There are large latencies in data transmission through most common ports such as USB[4]. However, in an interactive wireless protocol such as WLAN, AP and station

[3]Universal Serial Bus

[4]Currently, the minimum possible latency for for USB-3.0 is $128\mu s$ and on average it is in the order of few milliseconds.

are sending requests/acknowledgments back and forth with very short inter-spacing durations (few μs). Therefore, port latencies are added to each transmission time slot which increases inter-spacing from few micro-seconds to milliseconds. This not only affects the overall throughput severely but also breaks distributed real-time algorithms such as CSMA-CA that manages cross interference between users.

- ◇ I/Q signals are sampled at a very high rate. For a 20-MHz WiFi channel, this can be as high 80 MS/s and with 12-bits precision it results in $\sim$ 2-Gbps data transfer rate between SDR and host PC. This is a very high data transfer rate, even for state of the art USB ports. At this rate, port latencies can vary significantly, further breaking real-time processing operations.

Our wireless test-bed needs to perform I/Q level processing on the board (using configurable FPGA or DSP) so that conversion between raw information bits and actual TX/RX waveforms is carried out locally. Therefore, data transfer between SDR and host is limited to information bits which are smaller in size than I/Q samples by multiple orders of magnitude. This design choice together with other criteria such as platform dimensions and portability restricts us in our SDR selection. In the next section, we discuss our selected SDR platform in details.

There are some prior works in the area of TVWS focused on building hardware prototypes for experimental evaluation of available spectrum. KNOWS platform that is utilized for some TVWS measurements in [104–106] is designed from a commodity 2.4-GHz WiFi card by converting original 22-MHz bandwidth to 6-MHz. A UHF translator is used for re-tuning waveforms from 2.4 GHz to UHF TV bands. Spectrum sensing is implemented in a separate USRP unit. The overall design is suitable for some limited WS measurements in UHF however it is very large and it lacks configurability and portability. Testing in [107] is based on a WiMax IEEE 802.16d chipset that is capable of operating below 1 GHz. Carrier frequencies are modified through a policy file to match with TV band and the data traffic are eventually routed to a WiFi network through a host PC.

A CR system based on IEEE 802.11a is discussed in [108] for UHF TVWS. This prototype includes two carrier boards each consists of three processors and two Mezzanine

card slots for XMC-3321 (Dual Transceiver XMC Module). The overall design is a rack-mounted system with the same limitation mentioned before. WARP platform in [109] is a programmable wireless platform that implements PHY and MAC layers on an FPGA-based hardware. Other than previous limitations, the radio interface is only limited to 2.4 and 5.0 GHz bands.

There are very few commercial products, such as ACRS developed by Adaptrum [110], which are designed for point-to-point links. The main use cases are for back-haul connections or to provide internet in rural areas, in which case the receiving client is bridged back to a WLAN network for end users.

6.3 CampusLink: A WS-based Campus Network

CampusLink project is defined for development of a WS-based wireless network at University of Washington campuses. According to our discussion in chapter 2, current FCC suggestion for WS-based network architecture is based on using a central DBA that determines available spectrum based on location of requesting user, primary users' data and local FCC regulation. Therefore, each AP in CampusLink network initializes its local WLAN setup by first contacting DBA and registering for an available channel. Figure 6.2 shows the overall network architecture with multiple APs for larger coverage. Through an IP connection, each AP is connected to DBA for receiving channel information such as available spectrum, corresponding quality and maximum permitted power. Intelligent spectrum allocation is performed for registered users by running channel allocation algorithms on the server which minimizes cross interference between APs. Each AP also acts as a spectrum sensor node by providing spectrum utilization data to DBA. These additional data which are gathered from various locations are extremely useful in evaluation of current FCC rules for defining coexistence opportunities in TV band (and others in the future).

The main goals that are pursued in CampusLink project can be summarized as following:

1. Building a fully-functional wireless network that is entirely based on white space spectrum (TVWS as well as future WS opportunities). This network is designed similar to current WiFi networks. However, it extends WLAN capability by:

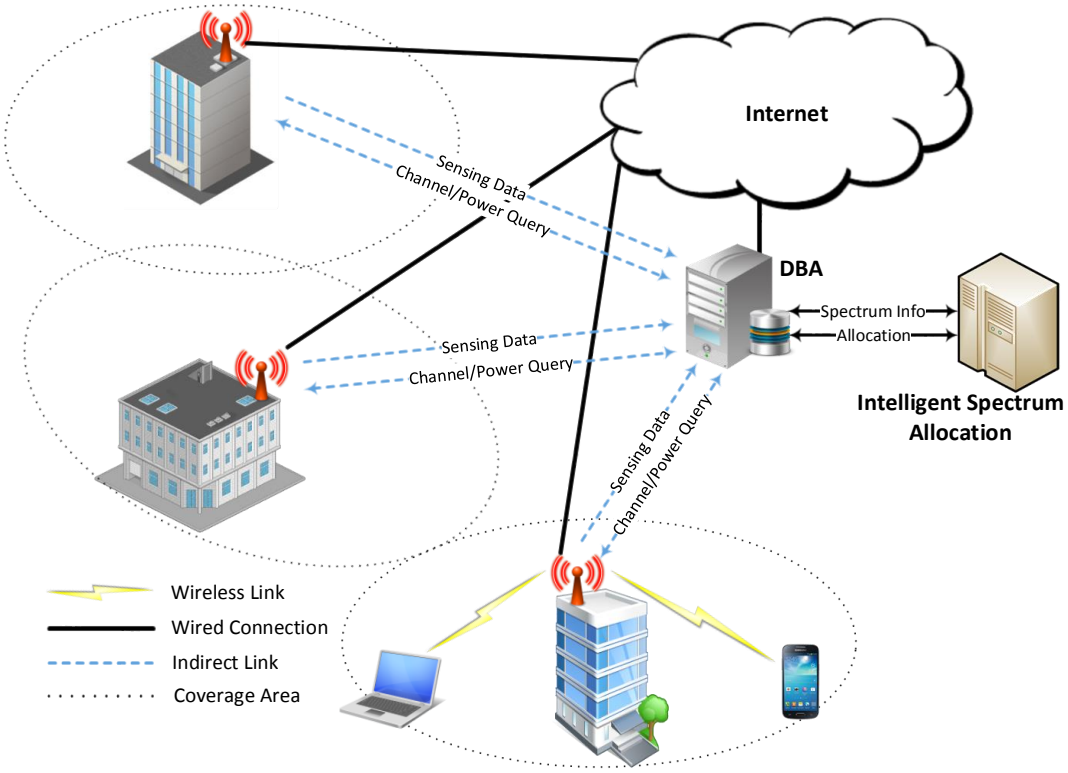

Figure 6.2: Wireless network architecture in *CampusLink* project

- ◇ Available spectrum is significantly increased.
- ◇ Best channel selection is automatically performed by AP for optimal cross-network performance, using an intelligent central spectrum allocator.
- ◇ Network coverage is significantly improved because TVWS spectrum (<700 MHz) is well below standard WiFi band (ISM 2.4GHz and 5.0 GHz). This improves signal quality at receivers as well as providing outdoor WLAN coverage.

2. Providing portable devices for end-users which enables wireless connectivity in a very wide-band spectrum (entire UHF band and beyond).

3. Using sensing data in the DBA, indoor/outdoor primary to secondary interference level is measured which is critical for optimal channel allocation. In addition, sensing

data are utilized for creating radio environment maps which are based on distributed measurement of radio spectrum activity and performing spatial interpolation techniques such as Kriging [111].

4. Functioning as a practical network with dynamic end-users, it is a comprehensive test-bench for following evaluations:

   ◇ Interference management and channel allocation algorithms

   ◇ Achievable throughput per available channels using IEEE 802.11 standard

   ◇ TV band channel characteristics such as delay/power profiles, fading, etc.

The first step in CampusLink project is implementation of an SDR-based wireless platform with required portability and configurability that was discussed before. The rest of this chapter presents implementation details of this platform.

6.3.1 BladeRF SDR

BladeRF is a an open-source SDR board that is designed and implemented by Nuand [102]. It is fully powered by USB-bus (no external power source needed) and is manufactured in a portable and handheld form factor (5.0x3.5 $inch^2$); hence very suitable for a portable wireless test platform. The basic block diagram for BladeRF hardware is shown in figure 6.3. The three major components are:

◇ *Field Programmable RF*: Designed by Lime-Microsystems [112], this is a fully programmable RF transceiver IC that directly converts digital baseband I/Q samples to analog RF waveforms and vice versa. Without the need for external oscillator (only clock signals), this chip combines following common modules in a wireless transceiver to a single IC: LNA, Amplifiers, Mixer, ADC, DAC. It covers a frequency range of 300 MHz to 3.8 GHz, capable of achieving full-duplex 28 MHz channels. Independent RX/TX 12-bit quadrature sampling provides up to 40 MS/s.

◇ *USB Controller*: This is a USB-3.0 controller providing Super Speed data transfer between SDR and host PC of up to 400 MB/s (3.2 Gbps). It is equipped with a

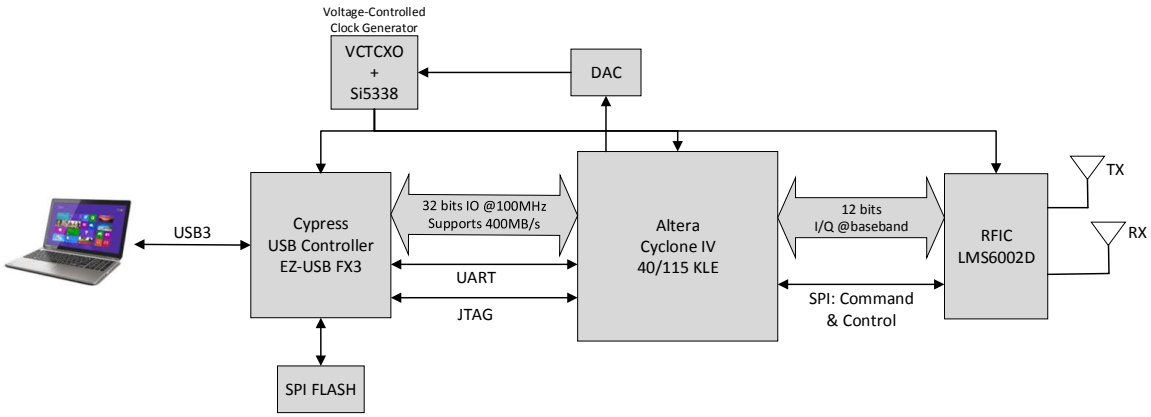

Figure 6.3: Block diagram of BladeRF hardware architecture.

200MHz ARM-9 processor that runs our firmware and it can also be used for signal processing on the board.

◇ *Altera FPGA*: In the heart of the board is an Altera FPGA that has access to all the components on the SDR board. It sends/receives I/Q samples to/from RF chip and transfer data to host computer through USB controller. This large FPGA has sufficient resources (40 or 115 KLE[5]) for real-time implementation of IEEE 802.11 PHY and MAC layers as well as spectrum sensing algorithms for cognitive radio purposes.

Table 6.1 summarizes technical specification for BladeRF SDR platform.

6.3.2 Overall SDR Architecture

The OSI reference model defines seven layers for network stack from Physical layer (lowest) to Application layer (highest) [113]. Internet protocol stack is based on five layers out of seven OSI layers, shown in table 6.2. Lower layers (physical and part of link layer) are delay-sensitive and they require real-time processing. Therefore, in most commercial WiFi cards, PHY and Link layers are implemented on-board. Upper layers are less time-critical and typically they are implemented in the host operating system. Our target platform

[5]Kilo Logic Element

Table 6.1: Specification of BladeRF SDR

Fully bus-powered USB 3.0 Super Speed SDR
Portable, handheld form factor: 5” by 3.5”
Extensible gold plated RF SMA connectors
300MHz - 3.8GHz RF frequency range
Independent RX/TX 12-bit 40MSPS quadrature sampling
Capable of achieving full-duplex 28MHz channels
16-bit DAC factory calibrated 38.4MHz +/-1ppm VCTCXO
On-board 200MHz ARM9 with 512KB embedded SRAM
On-board 40KLE or 115KLE Altera Cyclone 4 FPGA
2x2 MIMO configurable with SMB cable, expandable up to 4x4
Modular expansion board design for adding GPIO, Ethernet, and 1PPS sync signal and expanding frequency range, and power limits
DC power jack for running headless
Highly efficient, low noise power architecture
Stable Linux, Windows, Mac and GNURadio software support
Hardware capable of operating as a spectrum analyzer, vector signal analyzer, and vector signal generator

is designed to operate with Microsoft Windows and Linux environments. Both operating systems handle network stack from Network layer. Therefore, our implementation is focused on Link and Physical layers, based on IEEE 802.11 standard [9].

Table 6.2: 5-layer Internet protocol stack and 7-layer OSI reference model

Application
Transport
Network
Link
Physical

Application
Presentation
Session
Transport
Network
Link
Physical

IEEE 802 family is a series of specification for local area network (LAN) technologies. These specifications are focused on the two lowest OSI layers as all 802 networks have both MAC (sublayer of Link) and PHY components [9, 114]. Figure 6.4 shows the relationship

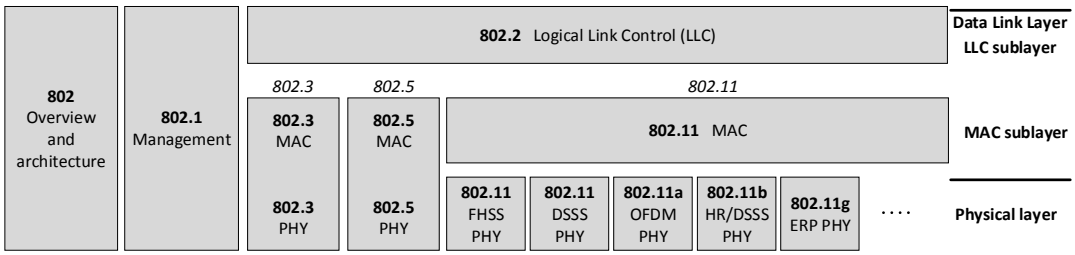

Figure 6.4: The IEEE 802 family and its relation to the OSI model

between components of the 802 family and OSI model. 802.2 defines a common link layer, the logical link control (LLC), which can be used by any lower-layer LAN technology.

The IEEE 802.11 [7] is one link layer that uses 802.2/LLC encapsulation. It specifies a common MAC sublayer and various PHY revision, some of which are shown in figure 6.4 (802.11a, 802.11g). Newer 802.11 specifications such as 802.11n and 802.11ac also modify MAC sublayer to achieve higher efficiencies. Our SDR implementation covers the 802.11 component for the MAC and PHY layers as well as parts of the LLC sublayer. The details for each layer implementation as well as their mapping to SDR hardware resources are discussed in the next sections.

Figure 6.5 shows the overall architecture of hardware/software design for SDR platform. The processing is divided between following resources: *FPGA Core* handles real-time components by assigning dedicated logic elements; *NIOS-II* processor is an embedded processor inside FPGA core that is capable of running custom software codes. Since it is implemented as part of FPGA design, along with other low level elements, it has direct access to all the modules and is capable of time-sensitive operations [115]. NIOS is clocked at 200 MHz; *Host PC* handles non-critical aspects of link layer such as conversion between Ethernet and WiFi frames or rate adaptation algorithms. Processing responsibility of each of these blocks is discussed below:

- PHY RX/TX: These dedicated FPGA blocks implement OFDM transceiver for 802.11 physical layer, responsible for time/frequency synchronization, FFT, channel equal-

ization, modulation/demodulation, interleaving, coding and scrambling. The input to TX sub-block is a stream of information bits that are divided to a number of OFDM symbols (after scrambling, encoding and interleaving) and converted to I/Q samples. RX sub-block performs the reverse chain.

◇ Lower MAC: Distributed Coordination Function (DCF), which manages channel access between multiple users connected to a single AP, is based on CSMA/CA with binary exponential back-off algorithm. It requires sensing channel before transmission with precise timers for running DCF state machine. These features are implemented by the lower MAC block as part of FPGA core. It also schedules TX PHY and monitors incoming RX frames from physical layer.

◇ Upper MAC: Certain aspects of DCF are implemented as part of the software running in NIOS II processor. This includes handling of received frames by sending acknowledgments, segmentation of large WiFi frames to multiple smaller sub-frames, and responding to various pre-defined control or management frames. These are time-sensitive tasks that cannot be handed over to host PC, yet they are sufficiently slow to avoid using customized FPGA blocks.

◇ LLC: IEEE 802.2 specifies LLC which constitutes the top sublayer of data link layer and is common to different MAC methods [116]. This is implemented in the host PC in our SDR design and performs as an interface between MAC sublayer and network layer. LLC is primarily responsible for (in general) node-to-node flow and error control as well as multiplexing different protocols that are transmitting over the MAC layer. In wireless LAN communication, however, error management is handled by the MAC. Hence, LLC is mostly focused on multiplexing (between WiFi and Ethernet frames) and flow control through rate adaptation algorithms (MCS[6] selection).

---

[6]Modulation and Coding Scheme

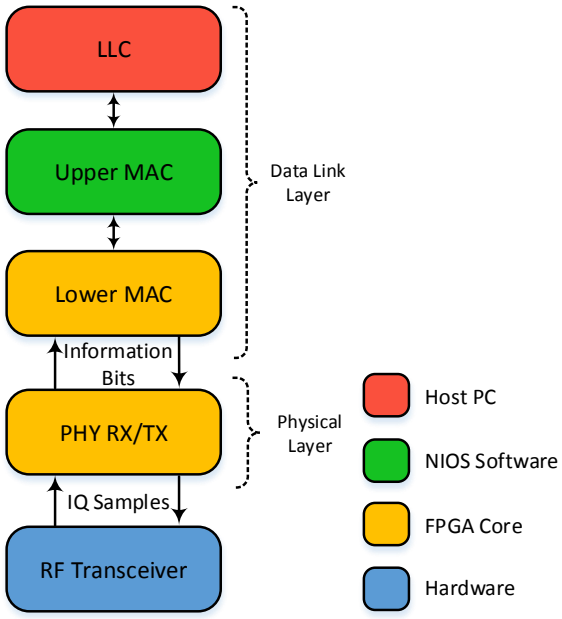

Figure 6.5: The overall architecture of SDR design

6.4 Physical Layer

The PHY layer defined under IEEE 802.11 for WLAN services can consist of two protocol functions as below [7]:

1. A PMD[7] system whose function defines the characteristics of, and method of transmitting and receiving data through a wireless medium between multiple stations.

2. A PHY convergence function that adapts the capabilities of PMD to the PHY service. This function is supported by the PLCP[8] sublayer as shown in figure 6.6. It defines mapping from MPDU[9] to a suitable framing format for sending and receiving data between multiple stations, using the associated PMD.

---

[7]Physical Medium Dependent

[8]Physical Layer Convergence Procedure

[9]MAC Protocol Data Unit

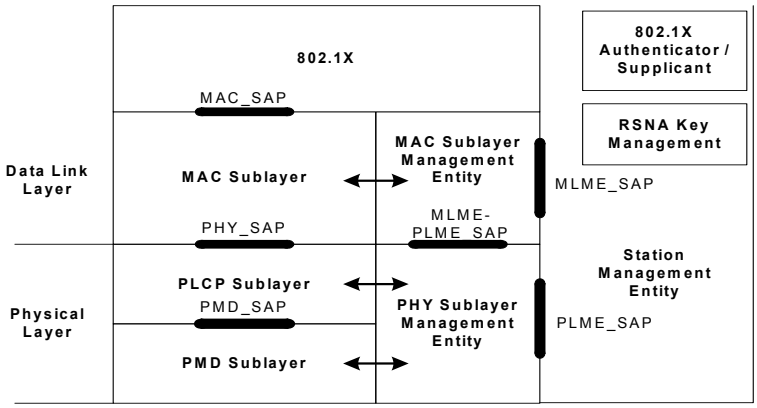

Figure 6.6: Reference model for PHY and MAC layers and corresponding management entities [7].

An additional function entity, PLME (Physical Layer Management Entity), can also exist which performs management of the local PHY functions in conjunction with MLME (MAC Layer Management Entity).

6.4.1 PLCP Sublayer

The format of protocol data unit generated by PLCP is shown in figure 6.7. It includes preamble, PLCP header, PSDU, tail bits and pad bits. The PLCP header contains following information: *Length*, *Rate* and *Service*. Rate and length are encoded with the most robust MCS (BPSK, r=1/2) to ensure decodability in worst scenarios. The *Rate* field determines the utilized MCS for OFDM symbols in the DATA field. This is necessary for the receiver to demodulate and decode the received data. Table 6.3 shows the standard modulation and coding schemes defined in 802.11 specification.

The *length* parameter in PLCP header indicates the number of octets in the PSDU that is requested by the MAC layer. PSDU is the frame payload which is essentially the same as MPDU. Permitted values for length is 1 to 4095. The six tail bits following PSDU are set to '0', which are utilized to return the convolutional encoder to zero state. The number of bits in the DATA field should be a multiple of N_{CBPS}, as shown in table 6.3. This is achieved by using pad bits to extend total coded bits, accordingly. Depending on length

Table 6.3: Modulation Dependent Parameters in IEEE 802.11 [7]

Modulation	Coding rate	Coded bits per subcarrier	Coded bits per OFDM symbol (N_{CBPS})	Data bits per OFDM symbols (N_{DBPS})	Data rate for 20-MHz channel(Mbps)
BPSK	1/2	1	48	24	6
BPSK	3/4	1	48	36	9
QPSK	1/2	2	96	48	12
QPSK	3/4	2	96	72	18
16-QAM	1/2	4	192	96	24
16-QAM	3/4	4	192	144	36
64-QAM	2/3	6	288	192	48
64-QAM	3/4	6	288	216	54

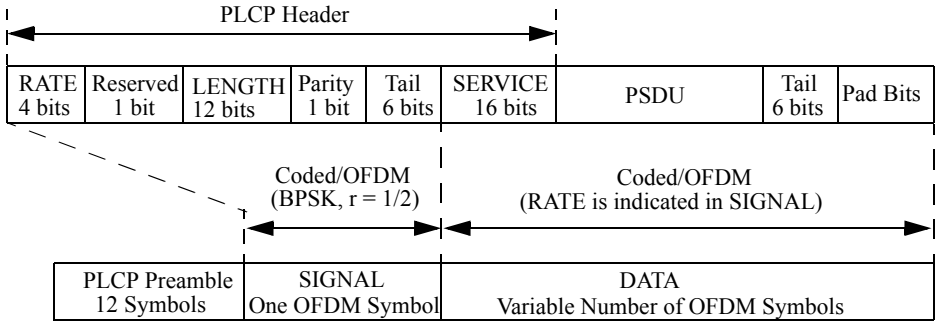

Figure 6.7: PPDU frame format [7].

and rate fields, *Data* field is split to multiple OFDM symbols, N_{SYM}:

$$N_{SYM} = \left\lceil \frac{16 + 8 * \text{LENGTH} + 6}{N_{DBPS}} \right\rceil \tag{6.1}$$

For 20-MHz bandwidth, each OFDM symbol is $3.2\mu s$ long with a $0.8\mu s$ guard interval (Cyclic Prefix extension). PLCP preamble includes two training sequences (known as short and long sequences), each of $8.0\mu s$ duration which are used for signal detection, AGC, diversity selection, frequency and time synchronization. The total duration of transmitted

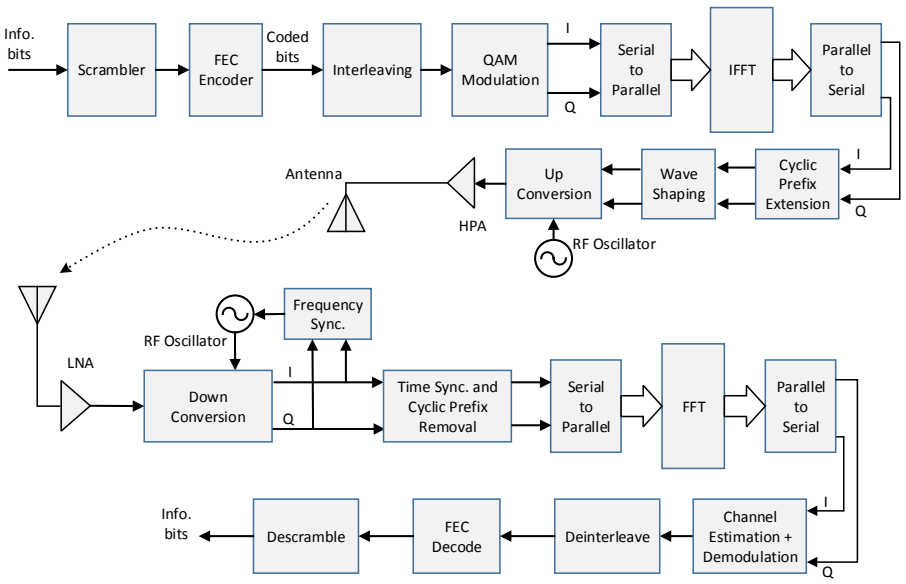

Figure 6.8: Block diagram of an OFDM-based transceiver in PMD sublayer

PPDU frame in time-domain is:

$$T_{PPDU} = (20 + N_{SYM} * 4.0)\frac{20}{\text{BW(MHz)}} \quad (\mu s) \tag{6.2}$$

where BW(MHz) is the utilized bandwidth for OFDM symbols in MHz, assuming that bandwidth variation is achieved by down/up-clocking the entire frame. Bandwidth variation is required to match signal bandwidth with available white space channel, such as 6-MHz TV channels in TVWS.

6.4.2 PMD Sublayer

The actual transmission and reception of OFDM-based PPDU through wireless medium is performed by PMD sublayer. Figure 6.8 shows transmitter and receiver chain for OFDM PHY. The FFT/IFFT block is 64-point long out of which 52 subcarriers are utilized. 11 subcarriers on the edge are not used, hence effective bandwidth is $\frac{53}{64}$ of nominal bandwidth (16.6 MHz effective bandwidth in case of 20 MHz).

FEC encoder in figure 6.8 is a convolutional code of rate 1/2, 2/3 or 3/4. Higher rates

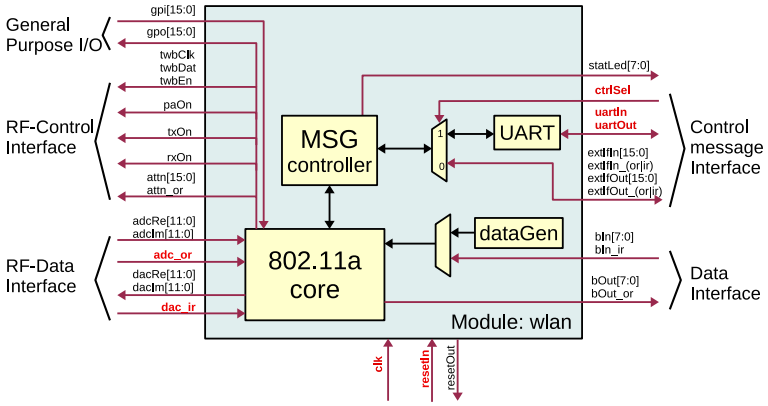

Figure 6.9: 802.11a FPGA core overview [8]

are possible by employing puncturing methods. A block interleaver is applied to all coded bits corresponding to each OFDM symbol. Therefore, interleaver block size is the number of coded bits per symbol, N_{CBPS}. It is defined by a two-step permutation. The first permutation maps adjacent coded bits to nonadjacent subcarriers. The second permutation maps adjacent coded bits to less and more significant bits of the constellation alternately. This avoids long runs of low reliability bits (LSB).

6.4.3 Hardware Implementation

Physical layer is entirely implemented in the Altera FPGA core that is available on BladeRF SDR. We use 802.11a physical layer IP core that is available in [8]. Figure 6.9 shows an overview of the IP core, highlighting various interfaces for control and data. The data interface is for providing PSDU bytes to WLAN core while in TX operation as well as receiving decoded bytes from any incoming RX frame.

Control message interface consists of fast parallel input/output lines for command and control as well as slow UART lines. This is used for sending various requests to the core and receiving related confirmations. Detection of any incoming frame is also indicated by the core through this interface. The RF data interface provides 12-bits input/output lines for complex I/Q samples at IF or base-band (zero-IF).

The core is clocked at 80-MHz for 20-MHz WiFi bandwidth (4 times over-sample).

However, by changing the clock frequency through SDR software, any desired bandwidth can be obtained for the application. Currently, we use 24-MHz to generate 6-MHz WiFi frames for operation in TVWS spectrum. In summary, the main features of the core are listed in table 6.4.

Table 6.4: 802.11a FPGA core specifications

Full IEEE 802.11a compliant, 802.11p is possible using half the clock frequency
Support for all data rates 6-54 Mbit/s
80-MHz target frequency
Generic message interface for configuration, operation, and debugging
Separate interfaces for control messages and data input/output
RF control signals included (PA/TX/RX on/off, 16 parallel AGC lines)
Digital up/down conversion for zero IF or 20 MHz low IF mode

6.5 MAC Layer

Considering MAC as a data service, it provides LLC entities the ability of exchanging MSDUs. Each local MAC utilizes PHY-level services to transfer MSDU to the other MAC entity and eventually delivering to LLC. MSDU transport is asynchronous and on a connectionless basis [7]. In a wireless media (unlike wired connection), this task is faced with multiple challenges as follows, which are to be resolved by the MAC [9]:

- ◇ RF Link Quality: Data transmission through radio links is prone to failure due to noise, interference and radio channel conditions such as multipath fading. Physical layer does not provide an error-free channel between peers. Hence positive acknowledgment is used in 802.11 protocol to recover from packet drop.

- ◇ Hidden Node Problem: Unlike wired connection (such as Ethernet) in which every node is able to detect transmission from all other nodes, wireless networks have fuzzy boundaries. Transmission from one node is strong enough for the AP but not necessarily for all the stations. This is solved in MAC through RTS-CTS mechanism in

which AP (that is visible to all nodes) issues transmission grant for the requesting user.

6.5.1 DCF/PCF/HCF

With multiple users requesting transmission in the shared wireless media, a distributed coordination function (DCF) is required to manage cross-interference and avoid collision. The standard DCF in 802.11 is based on CSMA/CA with binary exponential backoff algorithm. Every node senses the channel before transmission. Once clear, every waiting node generates a random slot number and starts decrementing. The first node that reaches zero wins the channel.

DCF is the base service that is defined by the MAC and other services are defined on top of it. Point coordination function (PCF) is a contention-free service that is implemented above DCF. PCF is implemented by APs and it makes sure that medium is provided without contention. Hybrid coordination function (HCF) allows the stations to have multiple service queues for different service qualities. Therefore, access to the wireless medium by various applications is balanced according to their quality of service.

6.5.2 Physical and Virtual Carrier Sensing

Carrier sensing determines channel status in DCF. There are two ways to accomplish this: physical carrier sensing and virtual carrier sensing. If any of these methods declares a busy channel, DCF avoids transmission.

Physical sensing is performed by the PHY on the received I/Q samples, through energy detection, signal correlation or other known sensing techniques. With the hidden node problem, physical sensing cannot provide all the required information to avoid collision. Virtual carrier sensing in 802.11 is performed through a mechanism known as Network Allocation Vector (NAV). The MAC frame header contains a duration field that specifies transmission time required for the frame. The NAV is a timer that indicates the amount of time the media is reserved, in microseconds. By setting the NAV timer to the expected duration of channel usage and counting from NAV to 0 by the other stations, it can be used

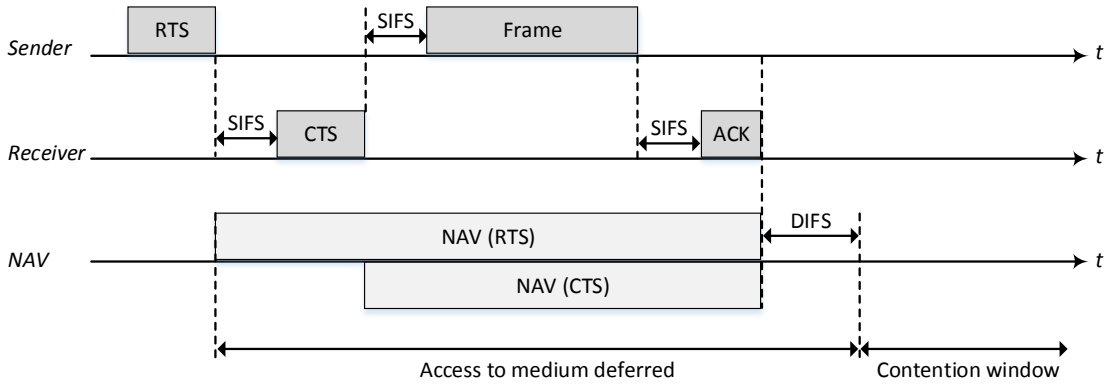

Figure 6.10: Virtual carrier sensing through NAV [9]

to indicate channel status. Media is considered busy as long as the NAV is non-zero [9].

Figure 6.10 shows the virtual sensing process that is initiated by reading the duration field from RTS packet (if station receives it) or from CTS (that is sent by the AP and has a smaller NAV). All the stations defers their access to the medium until NAV timer reaches zero with an additional delay of DIFS.

6.5.3 Interframe Spacing

There are four different types of interframe spacings between MAC frames. Three of them are used for medium access with different length for various priorities, as shown in figure 6.11. Different interframe delays are used as part of the MAC protocol to differentiate high priority traffic from low priority ones. The higher priority traffic uses the shorter delays (SIFS $<$ PIFS $<$ DIFS) so that it can grab the channel before lower traffic. The interframe spaces are fixed regardless of transmission speed to help with compatibility of different protocol speeds.

SIFS is the shortest interframe spacing for highest priority traffic such as RTS/CTS and ACK. The contention-free service that is offered by the PCF is using PIFS for operation. Stations are allowed to transmit data after PIFS period and before contention window starts. DIFS is used by the contention-based services (normal DCF behavior) such that they are allowed access to the medium after it is idle for DIFS. EIFS, which is not a fixed interval,

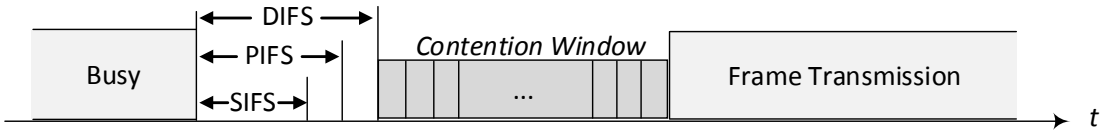

Figure 6.11: Various interframe spacings in 802.11 [9]

is used when error happens during frame transmission.

6.5.4 Channel Access Rules

In 802.11 DCF, sending node is responsible for making sure that transmitted frame is successfully received at the destination. The basic rules for getting access to channel are as follows:

1. If medium has been idle for longer than DIFS, data frame transmission can start immediately.

2. If medium is currently busy, sending is delayed until the end of current transmission (NAV) with an additional DIFS interval. A random slot number is chosen between 0 and CW-1 and following is performed:

   - ◇ The slot number is decreased in slot-time interval, as long as channel is idle
   - ◇ If transmission is detected on channel, wait until channel is idle again (NAV) with an additional DIFS period
   - ◇ When slot counter reaches zero, transmission can start

3. If length of data frame is less than RTS level, it is transmitted without RTS. Otherwise, an RTS is sent by the station, waiting for a valid CTS. If CTS is received correctly, data frame transmission can follow.

4. If ACK is required (normal 802.11 frames), transmitting node expects an ACK within SIFS interval from transmission. If received correctly, frame transmission and ACK

reception is repeated for the number of data fragments, after which process returns to idle state.

5. If CTS is not received after sending RTS, retry counter (SRC) is incremented. Similarly, if ACK is not received after sending data frame, SRC or LRC (depending on data frame size) is incremented. In both cases, the retry counter is compared with maximum threshold values and if maximum retry limit is reached then current frame is skipped and process goes back to idle. Otherwise, CW is doubled in size and exponential backoff algorithm is repeated.

Figure 6.12 shows the flowchart for DCF operations including channel acquisition process as well as data transmission.

6.5.5 Frames

There are different frame formats defined in WiFi that follow a similar structure to Ethernet frames. The most notable difference between Ethernet and WiFi frames is that 802.11 MAC frames do not include type/length and preamble fields. Preamble is part of the physical layer and type and length are present in the header on the data carried in the 802.11 frame The MAC also adopts several unique features to meet the challenges posed by the wireless data link, such as the use of four addresses [9].

Figure 6.13 shows different frame types that are commonly used in WiFi. Every frame starts with a two-byte Frame Control field that contains following main components. *Protocol version* indicates what version of the 802.11 MAC is utilized in this frame. *Type and sub-type* field identifies the type of current frame such as management, control or data frames. *More fragments bit* is set when original higher layer packet is fragmented into multiple frames and current frame is not the last frame. *Retry bit* is used with the ARQ mechanism to indicate re-transmission of lost frames and to avoid duplicates at the destination. *fromDS* and *toDS* bits indicate whether or not a frame is destined for the distribution system. In infrastructure mode, the frame is either sent to AP or transmitted by the AP; hence one of the bits is always set. For wireless bridge operations, both bits are set and for Adhoc mode both are cleared.

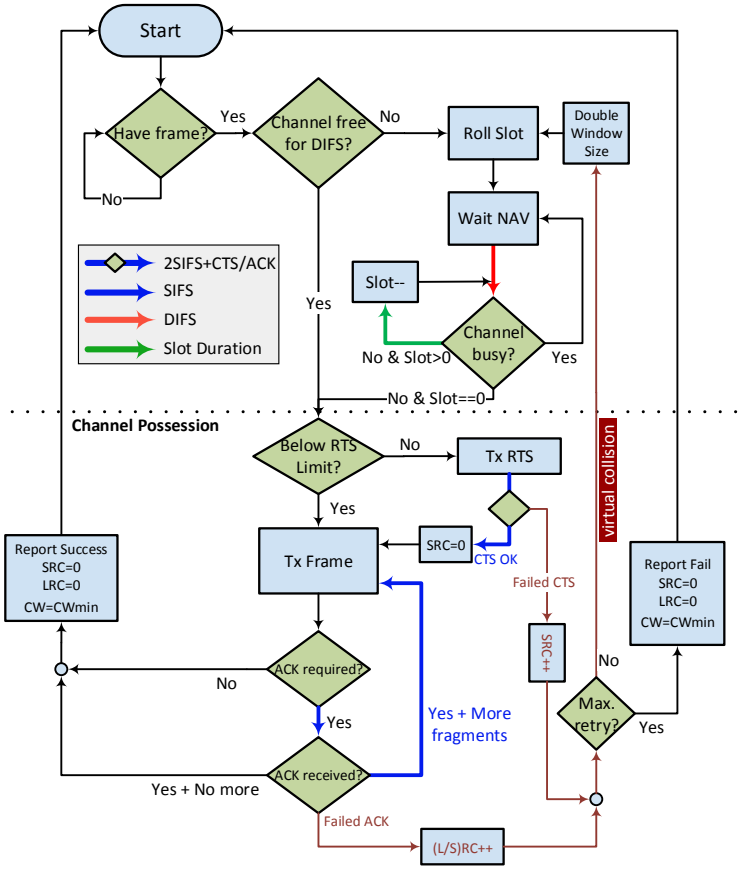

Figure 6.12: DCF Flowchart

Duration ID is a two-byte sequence that follows the frame control field. The main usage of duration ID is for NAV purposes in DCF as discussed previously. The value of this field represents the number of microseconds that the medium is expected to remain busy for current active transmission.

Addresses: Common WiFi frames consist of three different addresses, however, it can include up to four addresses while acting as a wireless bridge. Precise definition of each address field depends on frame type. The general rule of thumb is that address-1 is used for the receiver, address-2 for the transmitter and address-3 is for filtering by the receiver. *Destination address* corresponds to final recipient that will send the frame to higher network layers for processing. *Source address* identifies the source of the transmission which is only

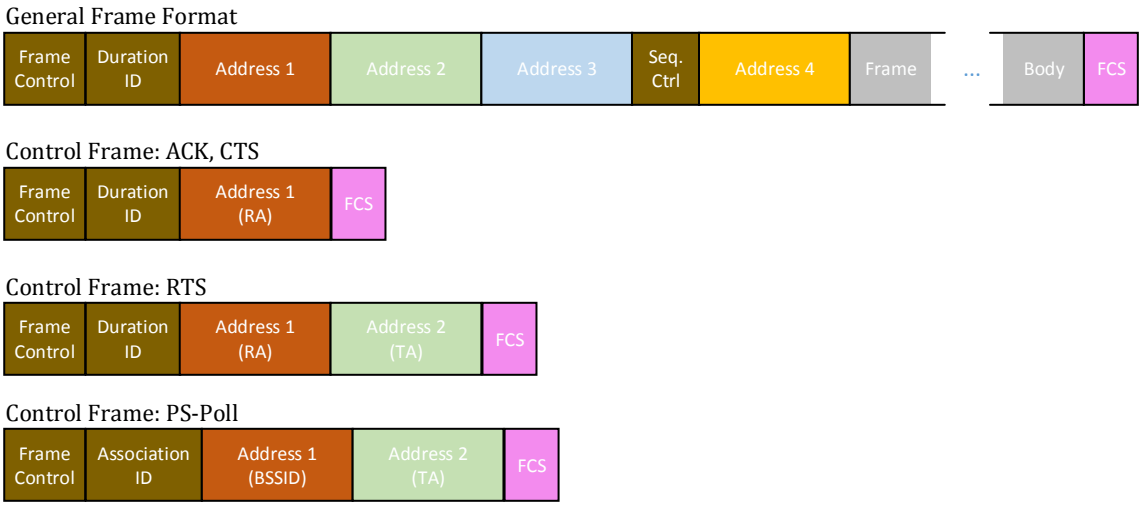

Figure 6.13: Different Frame Types in IEEE 802.11

a single station. *Receiver address* determines which station should process the frame. If it is the final recipient, this address will be the same as destination address. Otherwise, this can be BSSID when packet is routed through AP. *Transmitter address* that is used in wireless bridging identifies the wireless interface that transmitted the frame to the wireless medium [9].

Sequence Control Field is a two-byte sequence that is used for numbering frames when fragmentation is applied. This is also used by the receiver to discard duplicate receipt of the same frame. It is composed of a 4-bit fragment number and a 12-bit sequence number. The sequence number for each frame is assigned by the higher layer and it is constant among fragmented frames.

Frame Body has a variable size and it contains the higher layer data to be transmitted from one station to another.

Frame Check Sequence (FCS) is a 4-byte sequence that is used for error detection and added to the end of the frame. FCS is calculated using cyclic redundancy check (CRC-32) over the entire frame and transmitted with the rest of the frame. The receiving station will recalculate the FCS from the received frame and compares it with the transmitted FCS for error detection.

6.6 Hardware Integration

Figure 6.14 presents integration of different layers in the SDR platform. FX3 is the USB controller that provides super-fast USB-3.0 connection between the host software and FPGA core. It is equipped with an ARM-9 processor that handles USB requests as well as additional processing through its customizable firmware. USB end-points are connected to FPGA ports using DMA[10] channels. The benefits of DMA is that FX3 processor does not handle USB transactions and therefore packets are routed with minimal latencies. Different USB end-points are defined for various purposes. Command and control are send through UART-terminated end-point and data buffers are send by GPIF[11].

GPIF data are stored on FIFO's in the FPGA core. These FIFOs interact directly with PHY layer core and they transfer uncoded bytes (MAC frames). NIOS-II is a general purpose processor that is programmable through its firmware. It sends command and control messages to PHY core through its parallel lines and it also receives any message that is sent by PHY core. This core is directly reachable from the host PC through USB endpoints. Hence, all the requests from host software are processed by NIOS. Standard output messages (StdOut) are also available from its UART output port.

Lower MAC layer that is time-sensitive (interframe spacings, random backoff, etc.) requires precise timing calculations. Hence, MAC timers are implemented as a separate module on FPGA to generate very accurate timings for MAC state machine. The timers are used to interrupt the NIOS to continue its processing. Energy detection (as part of CSMA/CA sensing mechanism) is implemented as a separate module that calculates average energy of incoming IQ samples.

Setting various LMS parameters such as RF frequency, sampling time, bandwidth, internal gain values, etc. is through SPI connection (serial port). Since PHY core also needs to change RF gains for its internal AGC[12] operation, the SPI lines for LMS chip is multiplexed between NIOS and PHY core. The baseband IQ samples that are generated by the

---

[10] Direct Memory Access

[11] General Programmable Interface

[12] Automatic Gain Control

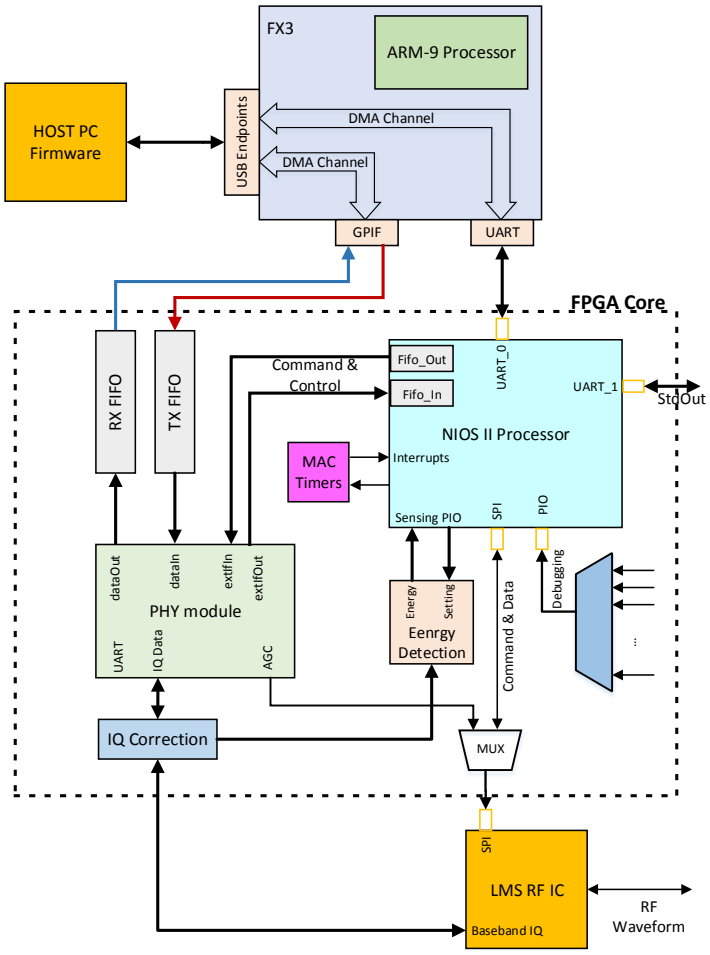

Figure 6.14: Hardware/Firmware Integration

PHY core or received from LMS must pass through IQ-correction module. This block is responsible for removing DC offset as well as correcting for any IQ imbalance that might exist.

For debugging purposes, various signal in the FPGA core are accessible through NIOS parallel IO (PIO) ports and can be accessed from the host software.

Chapter 7

FUTURE WORKS

In this work, we studied spectrum sharing in white spaces from different perspectives such as "how much TV white space capacity is available in the United States" or "how to coexist with a dynamic primary user as radar". We identify further works to be performed in each direction, some of which are presented below.

7.1 White Space Detection

Current FCC regulation for determining availability of a TV channel for unlicensed operation is mainly based on modeling of TV broadcasters. This solution is promising in terms of removing the burden of sensing from client devices and reducing device complexity. However, path-loss models are only accurate on an average basis and no model works for all terrains. Therefore, the actual white space availability can be significantly different from what model predicts.

7.1.1 Sensing as a Complement

The result of current DBA approach can be combined with optional localized sensing data from active users to improve accuracy of white space detection at the DBA. Due to centralized architecture of DBA-based spectrum sharing, DBA can perform as an aggregation point by collecting local sensing data from participating users and improving efficiency of its white space detection model.

FCC regulation should consider cooperative spectrum sensing from active users at different location as an amendment to DBA-based method. Since sensing data is being utilized cooperatively, highly sensitive receivers are not required to be used at the client side. A less-sensitive receiver, combined with collaboration will improve detectability of white space channels. It will be interesting to study the extent of variation in available TV white spaces

by incorporating sensing with PU modeling.

7.1.2 Indoor Users

All path loss models used by FCC are designed for outdoor areas. Coverage area of a broadcaster as well as cross-interference between a secondary user and primary receivers are all based on outdoor propagation. On the other hand, on common use-case for white space spectrum is WiFi devices that are located inside the buildings. Considering penetration loss of buildings in link budget calculation could significantly affect white space opportunities. A study can define sharing paradigms in case of indoor users and calculate the difference (in terms of available channels) with the outdoor case.

7.2 Coexistence with Radar

Primary users such as radars transmit high power and narrow pulses. Transmission power is a function of radar antenna direction that is time varying. Therefore, it performs as a non-stationary source of interference for secondary devices, such as WLAN networks. The effect of narrow interference (in time domain) on WiFi protocol (or in general OFDM modulation) is not well understood. A comprehensive study can analyze WiFi packet drop as a function of total SINR for various values of radar pulse widths, WiFi MCS and packet length.

Following to this analysis, Physical and MAC layer design in WiFi can be improved for further resistance against narrow and burst interference. Example improvements are in the interleaver that is currently applied on each OFDM symbol separately. Therefore, a burst error is not propagated over the entire packet for stronger robustness.

7.3 CampusLink Network

7.3.1 Network Setup

In chapter 6, we developed a fully functional SDR-based platform for WiFi operation in any band from 300MHz to 3.8GHz. This platform implements MAC and PHY layers based on IEEE 802.11 standard. The next step is to setup WiFi networks over the campus and to connect each bladeRF board to our central database (SpecObs server). The server is

responsible for assigning channels to each device and then each bladeRF board will set up its local WiFi network in the white space spectrum.

7.3.2 Fully Portable Devices

A fully portable device for white space operation should be in the form of a USB dongle. Our current SDR platform is suitable for access point as well as prototype stations. Final stations (client devices) will be in USB dongle form factor that is easily utilized by the end users.

7.3.3 Radio Environment Map

Spectrum sensing was discussed previously as a complement to white space detection mechanism. *CampusLink* project provides a suitable infrastructure for distributed sensing, performed by access points. The sensing results are sent to DBA where it can be used for various purposes. Two main use cases are:

1) Performing channel assignment based on real sensing data and the algorithms provided in chapter four.

2) Redefining coverage boundaries for TV broadcasters based on actual measurements.

For both purposes, it is often required to estimate signal power at locations where no measurement is performed; simply because the number of measurements are limited and they are scattered in a wide area. Here, interpolation techniques such as Kriging is used to approximate unknown signal power from limited set of measurements. The result is a radio environment map that can be used for the two purposes above.

BIBLIOGRAPHY

[1] Nadav Levanon, *Radar Principles*, 1st ed. United States of America: John Wiley and Sons, 1988.

[2] (2013, May) Cisco Visual Networking Index: Forecast and Methodology, 2012 - 2017.

[3] *Draft Recommended Practice for Measurement of 8-VSB Digital Television Mask Transmission Compliance for the USA* , IEEE Std. P1631/D3, Feb. 2008.

[4] F. Hessar and S. Roy. Cloud Based Simulation Engine for TVWS. [Online]. Available: http://specobs.ee.washington.edu/

[5] Google Spectrum Database. [Online]. Available: https://www.google.com/get/spectrumdatabase/

[6] Bruce Alan Fette, *Cognitive radio technology*, 2nd ed. Burlington, USA: Academic Press, 2009.

[7] *IEEE Standard for Information technology - Telecommunications and information exchange between systems - Local and metropolitan area networks - Specific requirements - Part 11: Wireless LAN Medium Access Control (MAC) and Physical Layer (PHY) Specifications*, IEEE Computer Society Std. 802.11-2012, March 2012.

[8] D. Sommer, "802.11a Physical Layer IP," Ingenieurbro BAY9, Dresden, Germany, Tech. Rep., 2014. [Online]. Available: http://www.bay9.de

[9] Matthew S. Gast, *802.11 Wireless Networks: The Definitive Guide*, 2nd ed. O'Reilly Media, 2005.

[10] Leslie M. Marx. (2012, June) The Spectrum Crisis. [Online]. Available: http://sites.duke.edu/marx/2012/06/

[11] (2013, November) Telebriefing: Ericsson Mobility Report. [Online]. Available: http://www.ericsson.com/res/investors/docs/2013/131111-ericsson-mobility-report-telebriefing.pdf

[12] D. Tse and P. Viswanath, *Fundamentals of Wireless Communication.* New York, NY, USA: Cambridge University Press, 2005.

[13] M. Dohler, R. Heath, A. Lozano, C. Papadias, and R. Valenzuela, "Is the phy layer dead?" *Communications Magazine, IEEE*, vol. 49, no. 4, pp. 159–165, 2011.

[14] P. Xia, "Interference Management in Heterogeneous Cellular Networks," Ph.D. dissertation, University Of Texas At Austin, December 2012.

[15] R. Chiang, G. Rowe, and K. Sowerby, "A quantitative analysis of spectral occupancy measurements for cognitive radio," in *Vehicular Technology Conference, 2007. VTC2007-Spring. IEEE 65th*, 2007, pp. 3016–3020.

[16] M. Wellens, J. Riihijarvi, M. Gordziel, and P. Mahonen, "Spatial statistics of spectrum usage: From measurements to spectrum models," in *Communications, 2009. ICC '09. IEEE International Conference on*, 2009, pp. 1–6.

[17] J. M. Peha, "Spectrum Sharing in the Gray Space," *Telecommunications Policy*, vol. 37, no. 2-3, pp. 167 – 177, 2013, cognitive Radio Dynamic Spectrum Assignment.

[18] *In the Matter of Unlicensed Operation in the TV Broadcast Bands: Second Memorandum Opinion And Order*, FCC Std. 10-174, September 2010.

[19] *In the Matter of Unlicensed Operation in the TV Broadcast Bands: Third Memorandum Opinion And Order*, FCC Std. 12-36, April 2012.

[20] White Space Database Administrator Group, "Channel Calculations For White Spaces Guidelines," Federal Communications Commission, Tech. Rep. Revision 1.29, March 2013, http://apps.fcc.gov/ecfs/document/view?id=7022134609.

[21] M. Hata, "Empirical Formulas for Propagation Loss in Land Mobile Radio Services," *IEEE Trans. Veh. Technol.*, vol. VT-29, no. 3, pp. 317–325, Aug. 1980.

[22] *In the Matter of Unlicensed Operation in the TV Broadcast Bands: Second Report and Order and Memorandum Opinion and Order*, FCC Std. 08-260, November 2008.

[23] FCC, "The National Broadband Plan: Connecting America," Federal Communications Commission, Tech. Rep., March 2010, http://www.broadband.gov/plan/.

[24] Global mobile data traffic forecast update, 2011-2016. From Cisco visual networking index. [Online]. Available: http://www.cisco.com/en/US/solutions/collateral/ns341/ns525/ns537/ns705/ns827/white_paper_c11520862.html

[25] President's Council of Advisors on Science and Technology, "Realizing the full potential of government-held spectrum to spur economic growth," Executive Office of the President, PCAST Report, July 2012.

[26] NTIA, "An assessment of the near-term viability of accommodating wireless broadband systems in the 1675-1710 MHz, 1755-1780 MHz, 3500-3650 MHz, and 4200-4220 MHz, 4380-4400 MHz bands," National Telecommunication and Information Administration, (Presidents spectrum plan report)–NTIA Report, November 2010. [Online]. Available: http://www.ntia.doc.gov/report/2010/assessment-near-term-viability-accommodating-wireless-broadband-systems-1675-1710-mhz-17

[27] ——, "An assessment of the viability of accommodating advanced mobile wireless (3G) systems in the 1710-1770 MHz and 2110-2170 MHz bands," National Telecommunication and Information Administration, NTIA Report, 2002. [Online]. Available: http://www.ntia.doc.gov/report/2002/assessment-viability-accommodating-advanced-mobile-wireless-3g-systems-1710-1770-mhz-and

[28] ——, "Background study on efficient use of the 2700-2900 MHz band," National Telecommunication and Information Administration, NTIA Report TR-83-117, April 1983. [Online]. Available: http://www.ntia.doc.gov/reports-publications/1983/background-study-efficient-use-2700-2900-mhz-band

[29] TRID, "Potential for accommodating third generation mobile systems in the 1710-1850 MHz band: Federal operations, relocation costs, and operational impacts," Transport Research International Documentation, TRID Report NTIA-SP-01-46, March 2001. [Online]. Available: http://144.171.11.39/view.aspx?id=863347

[30] C. Ghosh, S. Roy, and M. Rao, "Modeling and validation of channel idleness and spectrum availability for cognitive networks," *Selected Areas in Communications, IEEE Journal on*, vol. 30, no. 10, pp. 2029–2039, November 2012.

[31] D. Makris, G. Gardikis, and A. Kourtis, "Quantifying TV White Space Capacity: A Geolocation-Based Approach," *Communications Magazine, IEEE*, vol. 50, no. 9, pp. 145–152, September 2012.

[32] K. Harrison, S. M. Mishra, and A. Sahai, "How much white-space capacity is there?" in *Proc. IEEE Symposium on New Frontiers in Dynamic Spectrum DYSPAN'10*, 2010, pp. 1–10.

[33] M. Nekovee, "Quantifying the Availability of TV White Spaces for Cognitive Radio Operation in the UK," in *Communications Workshops, 2009. ICC Workshops 2009. IEEE International Conference on*, 2009, pp. 1–5.

[34] J. van de Beek, J. Riihijarvi, A. Achtzehn, and P. Mahonen, "UHF white space in Europe - A quantitative study into the potential of the 470-790 MHz band," in *New Frontiers in Dynamic Spectrum Access Networks (DySPAN), 2011 IEEE Symposium on*, 2011, pp. 1–9.

[35] R. Murty, R. Chandra, T. Moscibroda, and P. Bahl, "Senseless: A database-driven white spaces network," *Mobile Computing, IEEE Transactions on*, vol. 11, no. 2, pp. 189–203, Feb 2012.

[36] FCC, "Longeley-Rice Methodology for Evaluating TV Coverage and Interference," Federal Communication Commission, Washington DC, Tech. Rep. OET BULLETIN No. 69, February 2004.

[37] ITU, "Method for point-to-area predictions for terrestrial services in the frequency range 30 MHz to 3000 MHz," International Telecommunications Commission (ITU), RECOMMENDATION ITU-R P.1546-3, November 2007.

[38] FCC, "List of All Class A, LPTV, TV Translator, PLMRS and CMRS Stations," Federal Communication Commission, Tech. Rep., 2008. [Online]. Available: http://www.dtv.gov/MasterLowPowerList.xls

[39] NTIA, "Digital mobile radio towards future generation systems, final report," National Telecommunication and Information Administration, Tech. Rep. European Communities, EUR 18957, 1999, COST Action 231.

[40] P. L. Rice, A. G. Longley, K. A. Norton, and A. P. Barsis, "Transmission loss predictions for tropospheric communication circuit," U.S. Department of Commerce, Tech. Rep. Technical Note 101, Volumes I and II, 1967, available from NTIS, Access. No.AD-687-820.

[41] G. A. Hufford, "The its irregular terrain model, version 1.2.2, the algorithm," NTIA - ITS, 325 Broadway Boulder, CO 80303-3328, U.S.A., Tech. Rep. August, 2002, available on http://flattop.its.bldrdoc.gov/itm.html.

[42] ——, "The ITS Irregular Terrain Model," Institute for Telecommunication Services, Tech. Rep., September 1984, version 1.2.2, The Algorithm Available on ITS website.

[43] A. G. Longley and P. L. Rice, "Prediction of tropospheric radio transmission loss over irregular terrain - a computer method," EESA, Tech. Rep. ERL65-ITS67, 1968, available from NTIS, Access. No. AD-678-874.

[44] G. A. Hufford, A. G. Longley, and W. A. Kissick, "A guide to the use of the ITS Irregular Terrain Model in the area prediction mode," NTIA, Tech. Rep. NTIA Report 82-100, 1968, available from NTIS, Access. No. PB82-217977.

[45] *IEEE P1631/D3 Draft Recommended Practice for Measurement of 8-VSB Digital Television Mask Transmission Compliance for the USA*, IEEE Broadcast Technology Society Std. P1631/D3, February 2008.

[46] W. C. Y. Lee, *Wireless and Cellular Telecommunication*, 3rd ed. McGraw-Hill, 2005.

[47] SRTM3 - Shuttle Radar Topography Mission. [Online]. Available: http://www.webgis.com/srtm3.html

[48] National Geophysical Data Center. [Online]. Available: http://www.ngdc.noaa.gov/mgg/topo/gltiles.html

[49] TVStudy Software - OET Bulletin No. 69. [Online]. Available: http://data.fcc.gov/download/incentive-auctions/OET-69/

[50] "Implementation Guideline for White Space Operations: Geographic Contour Calculation Guidelines," Key Bridge Global LLC, 1600 Tysons Blvd., Suite 1100, McLean, VA 22102, Tech. Rep. KB-CCG-01r9, October 2011.

[51] "IEEE Recommended Practice for Information Technology - Telecommunications and information exchange between systems Wireless Regional Area Networks (WRAN) - Specific requirements - Part 22.2: Installation and Deployment of IEEE 802.22 Systems," *IEEE Std 802.22.2-2012*, pp. 1–44, Sept 2012.

[52] *Part 11: Wireless LAN Medium Access Control (MAC) and Physical Layer (PHY) specifications Amendment 5: TV White Spaces Operation*, 802.11 Working Group of the 802 Committee Std. P802.11af/D5.0, June 2013.

[53] M. A. Ergin, K. Ramachandran, and M. Gruteser, "Understanding the effect of access point density on wireless lan performance," in *Proceedings of the 13th annual ACM international conference on Mobile computing and networking*, ser. MobiCom '07. ACM, 2007, pp. 350–353.

[54] F. Hessar and S. Roy, "Capacity considerations for secondary networks in tv white space," *Mobile Computing, IEEE Transactions on*, vol. PP, no. 99, pp. 1–1, 2014.

[55] D. Cox and D. Reudink, "Dynamic Channel Assignment in Two-Dimensional Large-Scale Mobile Radio Systems," *The Bell Systems Technical Journal*, vol. 51, no. 7, pp. 1611–1629, 1972.

[56] L. Narayanan, *Handbook of wireless networks and mobile computing.* New York, NY, USA: John Wiley & Sons, Inc., 2002, ch. Channel assignment and graph multicoloring, pp. 71–94. [Online]. Available: http://dl.acm.org/citation.cfm?id=512321.512325

[57] W. Si, S. Selvakennedy, and A. Y. Zomaya, "An overview of Channel Assignment methods for multi-radio multi-channel wireless mesh networks," *J. Parallel Distrib. Comput.*, vol. 70, no. 5, pp. 505–524, May 2010. [Online]. Available: http://dx.doi.org/10.1016/j.jpdc.2009.09.011

[58] I. Katzela and M. Naghshineh, "Channel assignment schemes for cellular mobile telecommunication systems: a comprehensive survey," *Personal Communications, IEEE*, vol. 3, no. 3, pp. 10–31, 1996.

[59] D. Martinez, A. Andrade, and A. Martinez, "Interference-aware dynamic channel allocation scheme for cellular networks," in *Performance Evaluation of Computer and Telecommunication Systems (SPECTS), 2010 International Symposium on*, 2010, pp. 295–300.

[60] A. Mishra, S. Banerjee, and W. Arbaugh, "Weighted coloring based channel assignment for WLANs," *SIGMOBILE Mob. Comput. Commun. Rev.*, vol. 9, no. 3, pp. 19–31, Jul. 2005.

[61] C. Zhao and L. Gan, "Dynamic Channel Assignment for Large-Scale Cellular Networks Using Noisy Chaotic Neural Network," *Neural Networks, IEEE Transactions on*, vol. 22, no. 2, pp. 222–232, 2011.

[62] Y. Tam, R. Benkoczi, H. Hassanein, and S. Akl, "Channel Assignment for Multihop Cellular Networks: Minimum Delay," *Mobile Computing, IEEE Transactions on*, vol. 9, no. 7, pp. 1022–1034, 2010.

[63] J. Nasreddine, A. Achtzehn, J. Riihijarvi, and P. Mahonen, "Enabling Secondary Access through Robust Primary User Channel Assignment," in *Global Telecommunications Conference (GLOBECOM 2010), 2010 IEEE*, 2010, pp. 1–5.

[64] V. Chandrasekhar and J. Andrews, "Spectrum allocation in tiered cellular networks," *Communications, IEEE Transactions on*, vol. 57, no. 10, pp. 3059–3068, 2009.

[65] K. Doppler, S. Redana, M. Wódczak, P. Rost, and R. Wichman, "Dynamic resource assignment and cooperative relaying in cellular networks: concept and performance assessment," *EURASIP J. Wirel. Commun. Netw.*, vol. 2009, pp. 24:1–24:14, Jan. 2009.

[66] Q. Xin and J. Xiang, "Joint QoS-aware admission control, channel assignment, and power allocation for cognitive radio cellular networks," in *Mobile Adhoc and Sensor Systems, 2009. MASS '09. IEEE 6th International Conference on*, 2009, pp. 294–303.

[67] D. Li and J. Gross, "Distributed TV Spectrum Allocation for Cognitive Cellular Network under Game Theoretical Framework," in *Proc. IEEE International Symposium on Dynamic Spectrum Access Networks DYSPAN'12*, 2012, pp. 327–338.

[68] A. Subramanian, M. Al-Ayyoub, H. Gupta, S. Das, and M. Buddhikot, "Near-optimal dynamic spectrum allocation in cellular networks," in *New Frontiers in Dynamic Spectrum Access Networks, 2008. DySPAN 2008. 3rd IEEE Symposium on*, 2008, pp. 1–11.

[69] L. Cao, L. Yang, X. Zhou, Z. Zhang, and H. Zheng, "Optimus: Sinr-driven spectrum distribution via constraint transformation," in *New Frontiers in Dynamic Spectrum, 2010 IEEE Symposium on*, 2010, pp. 1–12.

[70] S. Im and H. Lee, "Dynamic spectrum allocation based on binary integer programming under interference graph," in *Personal Indoor and Mobile Radio Communications (PIMRC), 2012 IEEE 23rd International Symposium on*, 2012, pp. 226–231.

[71] M. Anuj and T. M. A., "A branch-and-price approach for graph multi-coloring," *Extending the Horizons: Advances in Computing, Optimization, and Decision Technologies*, p. 1529, 2007.

[72] M. Tercero, K. Sung, and J. Zander, "Exploiting temporal secondary access opportunities in radar spectrum," *Wireless Personal Communications*, vol. 72, no. 3, pp. 1663–1674, 2013.

[73] Strategic Technology Office, "Shared spectrum access for radar and communications (ssparc)," Broad Agency Announcement, February 2013.

[74] R. Saruthirathanaworakun, J. Peha, and L. Correia, "Opportunistic sharing between rotating radar and cellular," *Selected Areas in Communications, IEEE Journal on*, vol. 30, no. 10, pp. 1900–1910, 2012.

[75] R. Saruthirathanaworakun, "Gray-space spectrum sharing with cellular systems and radars, and policy implications," Ph.D. Thesis, Carnegie Mellon University, 2012.

[76] R. Saruthirathanaworakun, J. Peha, and L. Correia, "Gray-space spectrum sharing between multiple rotating radars and cellular network hotspots," in *Vehicular Technology Conference (VTC Spring), 2013 IEEE 77th*, June 2013, pp. 1–5.

[77] F. Paisana, J. Miranda, N. Marchetti, and L. DaSilva, "Database-aided sensing for radar bands," in *Dynamic Spectrum Access Networks (DYSPAN), 2014 IEEE International Symposium on*, April 2014, pp. 1–6.

[78] M. Tercero, K. W. Sung, and J. Zander, "Impact of aggregate interference on meteorological radar from secondary users," in *Wireless Communications and Networking Conference (WCNC), 2011 IEEE*, March 2011, pp. 2167–2172.

[79] H. Shajaiah, A. Khawar, A. Abdel-Hadi, and T. Clancy, "Resource allocation with carrier aggregation in lte advanced cellular system sharing spectrum with s-band radar," in *Dynamic Spectrum Access Networks (DYSPAN), 2014 IEEE International Symposium on*, April 2014, pp. 34–37.

[80] M. Rahman and J. Karlsson, "Feasibility evaluations for secondary lte usage in 2.7-2.9ghz radar bands," in *Personal Indoor and Mobile Radio Communications (PIMRC), 2011 IEEE 22nd International Symposium on*, Sept 2011, pp. 525–530.

[81] H. Deng and B. Himed, "Interference mitigation processing for spectrum-sharing between radar and wireless communications systems," *Aerospace and Electronic Systems, IEEE Transactions on*, vol. 49, no. 3, pp. 1911–1919, July 2013.

[82] "Presentation: spectrum with significant federal commitments, 225 mhz - 3.7 ghz," US National Telecommunications and Information Administration (NTIA), 2009.

[83] 3.5 GHz Spectrum Access System Workshop and Online Discussion. [Online]. Available: http://www.fcc.gov/blog/35-ghz-spectrum-access-system-workshop-and-online-discussion

[84] "Coexistence of S Band radar systems and adjacent future services," Ofcom, Tech. Rep., December 2009.

[85] F. H. Sanders, J. E. Carroll, G. A. Sanders, and R. L. Sole, "Effects of Radar Interference on LTE Base Station Receiver Performance," U.S. Derpatment Of Commerce, National Telecommunications and Information Administration, Tech. Rep. NTIA Report 14-499, December 2013.

[86] ITU, "Characteristics of radiolocation radars, and characteristics and protection criteria for sharing studies for aeronautical radionavigation and meteorological radars in the radiodetermination service operating in the frequency band 2700-2900 MHz," International Telecommunication Union, Tech. Rep., 2000-2003.

[87] "Characteristics of and protection criteria for sharing studies for radiolocation, aeronautical radionavigation and meteorological radars operating in the frequency bands between 5250 and 5850 MHz," ITU, Tech. Rep. Rec. ITU-R M.1638, 2003.

[88] F. H. Sanders, R. L. Sole, J. E. Carroll, G. S. Secrest, and T. L. Allmon, "Analysis and Resolution of RF Interference to Radars Operating in the Band 2700-2900 MHz from Broadband Communication Transmitters," U.S. Department Of Commerce, National Telecommunications and Information Administration, Tech. Rep., October 2012.

[89] E. F. Drocella, L. Brunson, and C. T. Glass, "Description of a model to compute the aggregate interference from radio local area networks employing dynamic frequency selection to radars operating in the 5 ghz frequency range," National Telecommunications and Information Administration (NTIA), Tech. Rep., May 2009.

[90] W. Alberhseim, "A closed-form approximation to robertson's detection characteristics," *Proceedings of the IEEE*, vol. 69, no. 7, pp. 839–839, July 1981.

[91] H. Ochiai and H. Imai, "On the distribution of the peak-to-average power ratio in ofdm signals," *Communications, IEEE Transactions on*, vol. 49, no. 2, pp. 282–289, Feb 2001.

[92] M. Haenggi and R. K. Ganti, "Interference in large wireless networks," *Found. Trends Netw.*, vol. 3, no. 2, pp. 127–248, Feb. 2009. [Online]. Available: http://dx.doi.org/10.1561/1300000015

[93] K. W. Sung, M. Tercero, and J. Zander, "Aggregate interference in secondary access with interference protection," *Communications Letters, IEEE*, vol. 15, no. 6, pp. 629–631, June 2011.

[94] R. Van Nee, V. Jones, G. Awater, A. Van Zelst, J. Gardner, and G. Steele, "The 802.11n MIMO-OFDM Standard for Wireless LAN and Beyond," *Wireless Personal Communications*, vol. 37, no. 3-4, pp. 445–453, 2006.

[95] D. C. Halperin, "Simplifying the Configuration of 802.11 Wireless Networks with Effective SNR," Ph.D. Thesis, University of Washington, 2012.

[96] D. Evans and M. D. Gallagher, "Potential Interference From Broadband Over Power Line (BPL) Systems To Federal Government Radiocommunications At 1.7 - 80 MHz," U.S. Department of Commerce, National Telecommunications and Information Administration, Tech. Rep. NTIA Report 04-413, April 2004, Section 4: Characterization Of Federal Government Radio Systems And Spectrum Usage.

[97] Walter H.W. Tuttlebee, *Software Defined Radio: Enabling Technologies* , 1st ed. England: John Wiley and Sons, 2002.

[98] W. Tuttlebee, "Software-defined radio: facets of a developing technology," *Personal Communications, IEEE*, vol. 6, no. 2, pp. 38–44, Apr 1999.

[99] F. K. Jondral, "Software-defined radio: Basics and evolution to cognitive radio," *EURASIP J. Wirel. Commun. Netw.*, vol. 2005, no. 3, pp. 275–283, Aug. 2005.

[100] "HackRF One: an open source SDR platform," http://greatscottgadgets.com/hackrf/.

[101] K. Tan, H. Liu, J. Zhang, Y. Zhang, J. Fang, and G. M. Voelker, "Sora: High-performance software radio using general-purpose multi-core processors," *Commun. ACM*, vol. 54, no. 1, pp. 99–107, Jan. 2011.

[102] "bladeRF - the USB 3.0 Superspeed Software Defined Radio," http://nuand.com/.

[103] Ettus Research, "Universal Software Radio Peripheral (USRP)," http://www.ettus.com/.

[104] Y. Yuan, P. Bahl, R. Chandra, P. Chou, J. Ferrell, T. Moscibroda, S. Narlanka, and Y. Wu, "Knows: Cognitive radio networks over white spaces," in *New Frontiers in Dynamic Spectrum Access Networks, 2007. DySPAN 2007. 2nd IEEE International Symposium on*, April 2007, pp. 416–427.

[105] S. Narlanka, R. Chandra, P. Bahl, and J. Ferrell, "A hardware platform for utilizing tv bands with a wi-fi radio," in *Local Metropolitan Area Networks, 2007. LANMAN 2007. 15th IEEE Workshop on*, June 2007, pp. 49–53.

[106] P. Bahl, R. Chandra, T. Moscibroda, R. Murty, and M. Welsh, "White space networking with wi-fi like connectivity," *SIGCOMM Comput. Commun. Rev.*, vol. 39, no. 4, pp. 27–38, Aug. 2009.

[107] R. Chandra, T. Moscibroda, P. Bahl, R. Murty, G. Nychis, and X. Wang, "A campus-wide testbed over the tv white spaces," *SIGMOBILE Mob. Comput. Commun. Rev.*, vol. 15, no. 3, pp. 2–9, Nov. 2011.

[108] R. Ahuja, R. Corke, and A. Bok, "Cognitive Radio System using IEEE 802.11a over UHF TVWS," in *New Frontiers in Dynamic Spectrum Access Networks, 2008. DySPAN 2008. 3rd IEEE Symposium on*, Oct 2008, pp. 1–9.

[109] P. Murphy, A. Sabharwal, and B. Aazhang, "Design of warp: A wireless open-access research platform," in *European Signal Processing Conference*, 2006.

[110] "Adaptrum TV White Space system," http://www.adaptrum.com/.

[111] C. Phillips, M. Ton, D. Sicker, and D. Grunwald, "Practical radio environment mapping with geostatistics," in *Dynamic Spectrum Access Networks (DYSPAN), 2012 IEEE International Symposium on*, Oct 2012, pp. 422–433.

[112] "Field Programmable RFIC by Lime Microsystems," http://www.limemicro.com/products/.

[113] James F. Kurose and Keith W. Ross, *Computer Networking: A Top-Down Approach*, 6th ed. Pearson, 2012.

[114] *IEEE Standard for Local and Metropolitan Area Networks: Overview and Architecture*, IEEE Computer Society Std. 802-2014, 2014.

[115] Altera Corporation, *Nios II Processor Reference Handbook.* , February 2014. [Online]. Available: http://www.altera.com/literature/lit-nio2.jsp

[116] *Information technology - Telecommunications and information exchange between systems - Local and metropolitan area networks - Specific requirements - Part 2: Logical Link Control*, IEEE Computer Society Std. 8802-2:1994, 1994.